RL-TR-96-207
Final Technical Report
December 1996

ADAPTIVE INTERFERENCE CANCELLATION AND SIGNAL SEPARATION TECHNIQUES FOR MULTIUSER SYSTEMS

New Jersey Institute of Technology

Y. Bar-Ness, A. Haimovich, H. Ge, N. Sezgin, and X. Wu

APPROVED FOR PUBLIC RELEASE; DISTRIBUTION UNLIMITED.

Rome Laboratory
Air Force Materiel Command
Rome, New York

This report has been reviewed by the Rome Laboratory Public Affairs Office (PA) and is releasable to the National Technical Information Service (NTIS). At NTIS it will be releasable to the general public, including foreign nations.

RL-TR-96-207 has been reviewed and is approved for publication.

APPROVED: Richard N. Smith
RICHARD N. SMITH
Project Engineer

FOR THE COMMANDER: John A. Graniero
JOHN A. GRANIERO
Chief Scientist
Command, Control, & Communications Directorate

If your address has changed or if you wish to be removed from the Rome Laboratory mailing list, or if the addressee is no longer employed by your organization, please notify RL/C3BA, 525 Brooks Road, Rome, NY 13441-4505. This will assist us in maintaining a current mailing list.

Do not return copies of this report unless contractual obligations or notices on a specific document require that it be returned.

REPORT DOCUMENTATION PAGE

Form Approved
OMB No. 0704-0188

1. AGENCY USE ONLY (Leave Blank)	2. REPORT DATE	3. REPORT TYPE AND DATES COVERED
	December 1996	Final Mar 94 - Sep 95

4. TITLE AND SUBTITLE

ADAPTIVE INTERFERENCE CANCELLATION AND SIGNAL SEPARATION TECHNIQUES FOR MULTIUSER SYSTEMS

5. FUNDING NUMBERS

C - F30602-94-C-0135
PE - 62702F
PR - 4519
TA - 63
WU - P6

6. AUTHOR(S)

Y. Bar-Ness, A. Haimovich, H. Ge, N. Sezgin, and X. Wu

7. PERFORMING ORGANIZATION NAME(S) AND ADDRESS(ES)

New Jersey Institute of Technology
Department of Electrical Engineering
Newark NJ 07102-1982

8. PERFORMING ORGANIZATION REPORT NUMBER

N/A

9. SPONSORING/MONITORING AGENCY NAME(S) AND ADDRESS(ES)

Rome Laboratory/C3BA
525 Brooks Road
Rome NY 13441-4505

10. SPONSORING/MONITORING AGENCY REPORT NUMBER

RL-TR-96-207

11. SUPPLEMENTARY NOTES

RL Project Engineer: Richard N. Smith/C3BA/(315) 330-7436

12a. DISTRIBUTION/AVAILABILITY STATEMENT

Approved for public release; distribution unlimited.

12b. DISTRIBUTION CODE

13. ABSTRACT (Maximum 200 words)

As a continuation of previous years' research on the Bootstrap algorithm, this year's research concentrates on using the F/F bootstrap with the signum function as a discriminator, when it is applied to separation of multiuser CDMA. The performance of this structure was studied and compared with other approaches of signal separation. In addition, research on two new topics was initiated. The first concerns using an adaptive array to improve separator performance. The second, term end "multi-shot separator", is a novel idea that can be implemented for an asynchronous multi-user channel which, in particular, can handle cases wherein the cross-correlation matrix is singular.

14. SUBJECT TERMS	15. NUMBER OF PAGES
Signal Processing, Adaptive Antennas	124
	16. PRICE CODE

17. SECURITY CLASSIFICATION OF REPORT	18. SECURITY CLASSIFICATION OF THIS PAGE	19. SECURITY CLASSIFICATION OF ABSTRACT	20. LIMITATION OF ABSTRACT
UNCLASSIFIED	UNCLASSIFIED	UNCLASSIFIED	UL

Abstract

As a continuation of previous years' research on the Bootstrap algorithm, this year's research concentrates on using the F/F bootstrap with the signum function as a discriminator, when it is applied to separation of multiuser CDMA. The performance of this structure was studied and compared with other approaches of signal separation. In addition, research on two new topics was initiated. The first concerns using an adaptive array to improve separator performance. The second, termand "multi-shot separator", is a novel idea that can be implemented for an asynchronous multi-user channel which, in particular, can handle cases wherein the cross-correlation matrix is singular.

Contents

I Introduction

Reported below are the results of a study carried out at the Center for Communication and Signal Processing Research at New Jersey Institute of Technology between July 1994 and December 1995. This research can be considered a continuation of previous research performed during 1991/92 [1] , 1992/1993 [2] and 1993/1994 [3]. Its aim is to further widen the investigation of methods for separation of multiuser signals. This can occur in satellite communication microwave terrestrial links or in wireless multiuser channels. Although some emphasis was placed on using code division multiple access (CDMA), this is not a requirement in the proposed approaches.

Historically the group at the Center has been involved in investigating algorithms for interference cancelation and signal separation. The algorithm termed "Bootstrap Algorithm" was first proposed by the principle investigator in 1981 [4], and later it was used for cancelling cross polarization in satellite communications [5] and in microwave terrestrial radio link [6, 7, 8].

During the 91/92 and 92/93 phases of this research, a thorough study of the "bootstrap algorithm" was performed. Three different structures were proposed in [1]; namely, the Backward/Backward (B/B), the Forward/Forward (F/F) and the Forward/Backward (F/B) structure. They are depicted in Figures 1, 2 and 3, as they applied to "dually polarized signals." The bootstrap separator of co-channel signals is principly composed of cancellers, each one using the outputs of the other cancellers to facilitate control of its adaptive weights. In fact such structures performs as a "signal separator" rather than an interference canceler. Since for its operation, there is no need for a reference signal (as in the LMS canceler), it is sometimes justifiably called a blind separator. Note that in the B/B algorithm, the weights are controlled by power minimization; in the F/F algorithm they are controlled by decorrelating the outputs; while in F/B by a combination of both. It was shown that for these algorithms to converge to a state of signal separation a signal distinguisher, termed discriminator (DIS), is needed. Such a discriminator uses some known, simple estimates of the signals themselves as in the case of the regular LMS noise canceler. In general the adaptive weights are controlled with recursive equations as follows:

for the case of the power criterion

$$w_{ij}^{n+1} = w_{ij}^{(n)} + \mu f\left[|Dz_i|^2\right] \qquad j \neq i \quad i,j = 1 \cdots K,$$

and for the decorrelator control

$$w_{ij}^{n+1} = w_{ij}^{(n)} + \mu f\left[|(Dz_i)z_j|^2\right] \qquad j \neq i \quad i,j = 1 \cdots K, \tag{1}$$

where $z_i \quad i = 1 \cdots K$ (K is the number of co-channels) is the output of the decorrelator, and D is the discriminator operator. In the work reported in [1] and [2] the discriminator was assumed heuristically as imposing a slightly different gain on the signal and interference at each output (also see published references [9, 10, 11, 12]). There it was possible to examine convergence behavior and error probability performance and compare it to other separators known in the literature. In [13] a third-order function was used as a discriminator. Some preliminary results were also obtained, which describe the 92/93 phase of the research, in applying these algorithms for separating co-channel CDMA signals, and blind channel equalization.

During 93/94 [3] further research was performed in two directions of application: separation of a multiuser CDMA signal and blind equalization of dispersive communication channels. For the first topic, we proposed a two stage canceler for synchronous multiuser CDMA [14]. The first stage is a decorrelating detector while the second is an adaptive interference canceler. To further improve the performance, a soft decision was used instead of the hard decision that precedes the second stage [15]. The slope of the soft decision was chosen heuristically based on measurements performanced on the output of the first stage. The bootstrap separator was also used as a second stage instead of a minimum power canceler. The work also extended to the asynchronous case. A one shot matched filter was used to model this case.

For blind equalization, we proposed a blind decision feedback equalizer base on the decorrelator [16], and we introduced a blind maximum likelihood sequence estimator [17], and a form of reduced complexity sequence estimator that uses state partitioning [18].

During this phase of research we concentrate on three main topics:

1. We perform a thorough study of the F/F bootstrap which uses the signum function as a discriminator. We examine its error performance when it is applied to multiuser CDMA, and we compare its

performance to what is known as a correlating detector on one the hand and to the MMSE detector on the other. We show that in contrast to the other detector, the bootstrap can perform better when the channel cross-correlation matrix is not accurately known. We further suggest a method for bit combining estimated data in an asynchronous channel, which results in an improvement in output error probability of the decorrelating detector. A method for signal separation that is closely related to the F/F bootstrap stage algorithm, termed gradient-based decorrelating algorithm, was also studied and used for multiuser CDMA. It is shown that such an approach depicts a smaller eigenvalue-spread than that of the corresponding method.

2. An adaptive array is also used for performance improvement in multiuser communication.

3. A new approach is suggested to handle multiuser signal separation in asynchronous CDMA. It can, in particular, handle singular cases.

II Technical Summary

II.1 The FF Bootstrap Algorithm With Signum Function Discriminator

For the general multi-user the equivalent low-pass signal, the input of the matched filter, is given by

$$r(t) = \sum_{k=1}^{K} \sum_{i} b_k(i) \sqrt{a_k(i)} s_k(t + iT - \tau_k) + n(t), \tag{2}$$

where K is the number of users, and a_k, b_k, s_k and τ_k are the signal amplitude, user bit, signature waveform, and relative delay of the k^{th} user. $n(t)$ is the zero mean AWGN, with a two-sided power spectral density of $N_0/2$.

For the synchronous channel encountered in down-link communication channels the τ_k are zero for all k. In the asynchronous up-link channels the τ_k are not necessarily equal. For the former case the output of the k^{th} matched filter is the composite of bit b_k and all interfering bits given by a linear combination through the cross-correlation factor ρ_{kj}. In matrix notation we can write

$$x(i) = PA\boldsymbol{b}(i) + \boldsymbol{n}(i), \tag{3}$$

where

$$P = \begin{bmatrix} 1 & \rho_{12} & \rho_{13} & \cdots & \rho_{1K} \\ \rho_{12} & 1 & \rho_{23} & \cdots & \rho_{2K} \\ \rho_{13} & \rho_{23} & \ddots & & \\ \vdots & \vdots & & & \rho_{K-1,K} \\ \rho_{1K} & \rho_{2K} & & \rho_{K-1,K} & 1 \end{bmatrix}, \tag{4}$$

and $A = diag\left(\sqrt{a_1}, \cdots, \sqrt{a_K}\right)$, $\boldsymbol{b}(i) = [b_1(i), \cdots, b_K(i)]$ and $\boldsymbol{n}(i)$ is a zero-mean Gaussian noise vector with covariance $R_n = P\sigma^2$. For the asynchronous case one may use the one-shot matched filter proposed by Verdú in [19] . In this case (3) will contain a linear combination of $b_k(i)$, $b_j(i)$ and $b_j(i-1)$ for $j = 1 \ldots K, j \neq k$. That is, the matrix P will be replaced by another square matrix with $1+2(K-1) = 2K-1$ dimensions. The output of this one shot matched filter $x_k(i)$ will contain a linear combination through this $(2K-1)\times(2K-1)$ cross-correlation matrix of $b_k(i)$ and bits i and $i-1$ of all other users. If the τ_k are known then all the elements of this matrix are known provided one knows the codes. Therefore, for both synchronous and asynchronous cases the output of the matched filters is given by (3), with the corresponding definition of $\boldsymbol{b}(i)$.

II.1.1 The principle bootstrap structure

Following the matched filter we have (see Fig. 4)

$$\boldsymbol{x} = V\boldsymbol{x} = V\,P\,A\boldsymbol{b} + V\boldsymbol{n} = V\,P\,A\boldsymbol{b} + \boldsymbol{\zeta}. \tag{5}$$

We use $V = I - W$ with

$$W^T = \begin{bmatrix} 0 & w_{12} & w_{13} & \cdots & w_{1K} \\ w_{21} & 0 & w_{23} & \cdots & w_{2K} \\ \vdots & & \ddots & & \vdots \\ \vdots & & & 0 & w_{K-1,K} \\ w_{K1} & \cdots & & w_{K,K-1} & 0 \end{bmatrix} \tag{6}$$

For the two-user case the principle structure using the signum discriminator in given in Fig. 5. That is, the weights are controlled by the recursion

$$\begin{aligned} w_{12}(n+1) &= w_{12}(n) - \mu z_1 \mathrm{sgn}(z_2) \\ w_{21}(n+1) &= w_{21}(n) - \mu z_2 \mathrm{sgn}(z_1). \end{aligned} \tag{7}$$

The mean steady state value of these weights are given by

$$\mathrm{E}(z_i \mathrm{sgn}(z_j)) = 0 \qquad i \neq j = 1, 2. \tag{8}$$

In Appendix A [20] it is shown that when z_j has a high SNIR then $\mathrm{sgn}(z_j) \sim b_j$ and the corresponding steady state weights equal the corresponding cross-coupling ($w_{12} = w_{21} = \rho$), in which case total cancellation of interference occurs. This is sometimes called near-far resistance, since the probability of error does not depend on the level of interference. For the general multiuser case we have

$$SNR_k = P_k^{-1} \boldsymbol{\rho}_k, \tag{9}$$

where the index k for a matrix or vector means the k-th row and column k are taken out of the matrix, or that the k-th element is taken out of the vector.

At this limiting condition or high SNIR we have for the signal-to-noise ratio

$$SNR_k = \frac{a_k \left(1 - \boldsymbol{\rho}_k^T \boldsymbol{P}_k^{-1} \boldsymbol{\rho}_k\right)}{\sigma^2}. \tag{10}$$

On the other hand when z_j does not have a large SNIR to justify $\text{sgn}(z_j) = b_j$ then (8) is not valid in steady state.

For the two-user case, let $\text{sgn}(z_1) = b_1$, however $\text{sgn}(z_2) \neq b_2$ then $\text{E}(z_1\text{sgn}(z_2)) = 0$ implies $w_{21} = \rho$. But $\text{E}(z_2\text{sgn}(z_1)) = 0$ will only imply $w_{12} = \rho + \delta$ $(w_{12} \neq \rho)$. Performing the required analysis in Appendix A,

$$\delta = \frac{-\rho}{1 + \sqrt{\frac{\pi}{2} LSNR} \frac{1}{(1-\rho^2)} \left(1 - 2Q\left(\sqrt{LSNR}\right)\right) e^{\frac{LSNR}{2}}}, \tag{11}$$

where $LSNR$ is the limiting-signal-to-noise ratio at the output:

$$LSNR = \frac{a_2\left(1-\rho^2\right)}{\sigma^2}. \tag{12}$$

From (11) we notice that δ has the opposite sign of ρ and that its absolute value $|\delta|$ decreases from $|\rho|$ to zero when the $LSNR$ increases from zero to infinity.

The corresponding probability of error

$$P_{e_1} = \frac{1}{2} Q\left(\frac{\sqrt{a_1}\left(1-\rho^2-\rho\delta\right) + \sqrt{a_2}\delta}{\sigma\sqrt{1-\rho^2+\delta^2}}\right) + \frac{1}{2} Q\left(\frac{\sqrt{a_1}\left(1-\rho^2-\rho\delta\right) - \sqrt{a_2}\delta}{\sigma\sqrt{1-\rho^2+\delta^2}}\right). \tag{13}$$

For small a_2, $\delta \to -\rho$. Then $P_{e_1} \to Q\left(\sqrt{a_1}/\sigma\right)$ the error corresponding to a simple BPSK signal. For large a_2, $\delta \to 0$, and $P_{e_1} \to Q\left(\sqrt{a_1}\sqrt{1-\rho^2}/\sigma\right)$, the error corresponding to the limiting case (Verdú's decorrelating detector), see Fig. 6.

Note that if one knows the matrix P, then instead of V, we may use P^{-1} (this is the Verdúdecorrelating detector) whose probability of error is constant and equals the limiting value. Hence we conclude that even if P is known the bootstrap separator outperforms Verdú's detector for almost all SNR. A thorough study of this bootstrap structure, including the multiuser case, is given in Appendix A.

II.1.2 Comparative Study of Linear Minimum Mean Square Error (LMMSE) and the F/F Bootstrap Algorithm with Signum Discriminator

The LMMSE multiuser detector decodes $\boldsymbol{b}$ based on

$$\hat{\boldsymbol{b}} = \text{sgn}\left(\hat{\boldsymbol{\theta}}_{LMMSE}\right), \tag{14}$$

where

$$\hat{\boldsymbol{\theta}}_{LMMSE} = \boldsymbol{W}\boldsymbol{x} = \underbrace{\left(\boldsymbol{P} + \sigma^2 \boldsymbol{A}^{-2}\right)^{-1}}_{\boldsymbol{W}} \cdot \boldsymbol{x}.$$

It's probability of error $P_e(k)$ has been derived [21], (see also appendix B):

$$P_e(k) = \frac{1}{2^K} \sum_{\boldsymbol{b}_k} \mathrm{Q}\left(\frac{\sqrt{a_k} - b_k \sigma^2 \boldsymbol{w}_k^T \boldsymbol{A}^{-1} \boldsymbol{b}_l}{\sigma_k} \right). \tag{15}$$

Under weak and strong interference conditions, the above error probability expression will reduce into the single-user BPSK limit or into that of the decorrelating detector, respectively.

$$P_e(k) = \begin{cases} \mathrm{Q}\left(\frac{\sqrt{a_k}}{\sigma}\right), & \text{weak interference} \\ \mathrm{Q}\left(\frac{\sqrt{a_k(1-\boldsymbol{\rho}_k^T \boldsymbol{P}_k^{-1} \boldsymbol{\rho}_k)}}{\sigma}\right), & \text{strong interference} \end{cases} \tag{16}$$

In Fig. 7 the performance of the LMMSE detector as compared to the bootstrap detector is shown.

II.1.3 The Bootstrap Algorithm for an Unknown Channel

In many applications (not necessarly CDMA) the matrix P is unknown. In CDMA applications the matrix P might not be accurately known, as a result of the unknown effect of the fading channel or as a result of errors in estimating the relative delays between users in the asynchronous uplink mobile communication channel.

To see the advantage of the bootstrap algorithm in these situations we first write (2) for the two-user case as

$$\begin{aligned} r(t) &= \sqrt{a_1} s_1(t) b_1(0) + \sqrt{a_2 \epsilon_2} \frac{1}{\sqrt{\epsilon_2}} s_2^L(t) b_2(-1) \\ &\quad + \sqrt{a_2(1-\epsilon_2)} \frac{1}{\sqrt{1-\epsilon_2}} s_2^R(t) b_2(0) + n(t), \end{aligned} \tag{17}$$

where $0 \le \tau_2 \le T$ is considered unknown or estimated with an error; and,

$$\begin{aligned} s_2^L(t) &= \begin{cases} s_2(t+T-\tau_2) & \text{if } 0 \le t \le \tau_2 \\ 0 & \text{if } \tau_2 < t \le T \end{cases} \\ s_2^R(t) &= \begin{cases} 0 & \text{if } 0 \le t \le \tau_2 \\ s_2(t-\tau_2) & \text{if } \tau_2 < t \le T \end{cases} \\ \epsilon_2 &= \int_0^{\tau_2} s_2^2(t+T-\tau_2) dt. \end{aligned} \tag{18}$$

As shown in Fig. 8, we apply $r(t)$ to a bank of filters by using as a second input $s_1(t), s_2^{L'}(t), s_2^{R'}(t)$, respectively, the signature function of Eq. (18) extended to τ_2' instead of τ_2, normalized by ϵ_2' instead of ϵ_2. As a result we have at the output of the matched filters for the zero-th bit

$$\mathbf{x}'(0) = \mathbf{P}^T \mathbf{A}\mathbf{b}(0) + \mathbf{n}(0), \tag{19}$$

where

$$\mathbf{P}^T = \begin{bmatrix} 1 & \rho_{21} & \rho_{12} \\ \rho_{21}' & \rho_{22}^{L'L} & \rho_{22}^{L'R} \\ \rho_{12}' & \rho_{22}^{R'L} & \rho_{22}^{R'R} \end{bmatrix}, \tag{20}$$

$\mathbf{A} = \text{diag}[\sqrt{a_1}, \sqrt{a_2\epsilon_2}, \sqrt{a_2(1-\epsilon_2)}]$ and

$\mathbf{b}(0) = [b_1(0), b_2(-1), b_2(0)]^T$. $\mathbf{n}(t)$ is zero-mean Gaussian vector with covariance

$$\mathbf{R}_n = \begin{bmatrix} 1 & \rho_{21}' & \rho_{12}' \\ \rho_{21}' & 1 & 0 \\ \rho_{12}' & 0 & 1 \end{bmatrix} \frac{N_0}{2}. \tag{21}$$

If the relative delay τ_2 is known then we choose $\tau_2' = \tau_2$, and as a result $\rho_{21}' = \rho_{21}, \rho_{12}' = \rho_{12}, \rho_{22}^{L'L} = \rho_{22}^{R'R} = 1$, $\rho_{22}^{R'L} = \rho_{22}^{L'R} = 0$ and $\epsilon_2' = \epsilon_2 = 1$. The matrix $\mathbf{P}_D$ is known. If $|\rho_{21}| + |\rho_{12}| < 1$ then $\mathbf{P}_D$ is invertible. A simple linear transformation by $\mathbf{P}_D^{-1}$ results in

$$\mathbf{z}(0) = \mathbf{A}\mathbf{b}(0) + \mathbf{P}_D^{-T}\mathbf{n}(0), \tag{22}$$

where $\mathbf{P}_D$ is the modified cross-coupling matrix. Since the components of $\mathbf{b}(0)$ are assumed uncorrelated then the components of $\mathbf{z}(0)$ are also so. A detailed analysis of applying partial codes corresponding to τ' instead of τ as given in Fig. 8 is in Appendix C. (see also [22]).

The results of using the bootstrap when $\tau_2' < \tau_2$ so that $\epsilon_2' = 0.35$ instead of $\epsilon_2 = .4$ is given in Fig. 9 and Fig. 10. Note that when using the conventional detector with P'^{-1} (instead of P^{-1}) the probability of error is approximately 0.5, while with the bootstrap bit error rate is adequate and almost equal to that when P is known.

II.1.4 Maximum Ratio Data Combining for Performance Improvement of One-shot Asynchronous Detectors

Using a one-shot matched filter followed by a decorrelating detector results in outputs corresponding to the main user and the left (earlier bit) and right (current bit) portion of the code of the other users. Due to reduced power, these outputs will result in a degradated probability of error. In Appendix D we propose a method of combining the data of the split code users. We suggest using a combining gain in proportion to the relative user delays. The resulting decorrelating detector always performs better than the split-output detector. For the two user asynchronous case, following the matched filter we have

$$\mathbf{x}(0) = \mathbf{PAb}(0) + \mathbf{n}(0), \tag{23}$$

where

$$\mathbf{P}^T = \begin{bmatrix} 1 & \rho_{12}^L & \rho_{12}^R \\ \rho_{21}^L & 1 & 0 \\ \rho_{21}^R & 0 & 1 \end{bmatrix}, \tag{24}$$

$\mathbf{A} = \text{diag}[\alpha_1, \alpha_2, \alpha_3] = \text{diag}[\sqrt{a_1},\ sqrta_2\epsilon_2, \sqrt{a_2(1-\epsilon_2)}]$ and $\mathbf{b}(0) = [b_1(0), b_2(-1), b_2(0)]^T$. The $\mathbf{n}(t)$ is a zero-mean Gaussian vector with covariance, $\mathbf{P}N_0/2$.

$$\begin{aligned} \rho_{12}^L &= \frac{1}{\sqrt{\epsilon_2}} \int_0^T s_2^L(t) s_1(t) dt \\ \rho_{12}^R &= \frac{1}{\sqrt{1-\epsilon_2}} \int_0^T s_2^R(t) s_1(t) dt. \end{aligned} \tag{25}$$

If we use the bootstrap with $\boldsymbol{V} = \boldsymbol{I} - \boldsymbol{W}$ then following the result of eq. (9) we have

$$\begin{aligned} z_1(0) &= \sqrt{a_1}(1 - \boldsymbol{\rho}_1^T \mathbf{P}_1^{-1} \boldsymbol{\rho}_1) b_1(0) + n_{D1}(0) \\ z_2(0) &= \sqrt{a_2\epsilon_2}(1 - \boldsymbol{\rho}_2^T \mathbf{P}_2^{-1} \boldsymbol{\rho}_2) b_2(-1) + n_{D2}(0) \\ z_3(0) &= \sqrt{a_2(1-\epsilon_2)}(1 - \boldsymbol{\rho}_3^T \mathbf{P}_3^{-1} \boldsymbol{\rho}_3) b_2(0) + n_{D3}(0), \end{aligned} \tag{26}$$

with the corresponding SNR

$$\text{SNR}_k = \frac{\alpha_k^2 (1 - \boldsymbol{\rho}_k^T \mathbf{P}_k^{-1} \boldsymbol{\rho}_k)}{N_0/2}, \quad k = 1, 2, 3. \tag{27}$$

We suggest combining the data at the output of the bootstrap as in Fig. 11.

$$z_{2C}(0) = z_2(0) + \gamma z_3(-1). \tag{28}$$

In Appendix D (see also [23]) it is shown that choosing $\gamma = \sqrt{\frac{1-\epsilon_2}{\epsilon_2}}$ will result in maximum SNR_{2C} It is also shown that such a choice will make SNR_{2C} greater than the uncombined SNR_2 or SNR_3 for any ϵ and any $\boldsymbol{P}$. As depicted in Fig. 12, combining data gives better error probability performance.

II.1.5 Adaptive Setting of Threshold for Soft Tentative Decision of a Multistage Canceler

In [3] we presented a multistage separator of a correlation detector (or bootstrap separator) followed by a hard limiter tentative decision followed by adaptive canceler. We also show that using a soft limiter instead, the performance would improve. The soft limiter used some heuristic threshold. In this phase of research (see Appendix E), we propse to adjust the threshold level so as to optimize the performance. The structure of two-stage (decorrelator/canceler) with adaptive soft-limiter is depicted in Fig. 13 with the adjustable threshold shown in Fig. 14. The optimal canceler weights and optimum threshold values were found analytically. In simulation the following two steepest descent algorithms were used.

$$\begin{aligned} w_{ij}^{(k+1)}(\lambda_{ij}^k) &= w_{ij}^k(\lambda_{ij}^k) + \mu \bigtriangledown_{w_{ij}} E\{y_i^2(\lambda_{ij}^k, w_{ij}^k)\} \\ \lambda_{ij}^{(k+1)}(w_{ij}^k) &= \lambda_{ij}^k(w_{ij}^k) + \mu \bigtriangledown_{\lambda_{ij}} E\{y_i^2(\lambda_{ij}^k, w_{ij}^k)\}. \end{aligned} \tag{29}$$

Comparing the performance when using a hard limiter, the heuristic threshold and the optimal threshold are given in Fig. 15.

II.1.6 Convergence of a Stochastic Gradient-Based Decorrelation Algorithm

We analyzed the performance of a stochastic gradient-based decorrelation algorithm for blind signal separation [25, 24] (see also Appendix F). The algorithm has a computational complexity comparable with the LMS algorithm, but is shown to be faster than the latter. The different speeds of convergence of the decorrelation algorithm and the LMS are shown to be a consequence of the different eigenvalue spreads associated with the implementation of the two algorithms. While the problem statement and proofs are quite general, the specific application considered is a synchronous multiuser multicarrier CDMA communication system in a fading environment. In this application the decorrelator is used as a multiuser detector. The convergence

speed of the two algorithms is illustrated in Fig. 16, which shows the average learning curves of the probability of error for SNR = 8 dB and SSR = -5 dB, where SSR is the ratio of the bit energy of the designated user to the user who serves as interference. The higher rate of convergence of the decorrelator is evident.

II.2 Adaptive Antenna for Performance Inprovement of Multiuser Communications

Antenna arrays provide diversity paths to combat multipath fading and are capable of suppressing spatial interference sources. Under consideration is a narrowband multiple access system such as TDMA. The channel is assumed to be flat fading. In [26] (see also Appendix G) we proposed an eigenanalysis-based filter, referred to as an *eigencanceler*, as an alternative to the Sample Matrix Inversion (SMI) method for small data sets. In the paper we develop analytical expressions for the average probability of error of the SMI and the eigencanceler methods for the case of single interference and a flat slowly fading Rayleigh channel. Consider the (I+N) correlation matrix $\boldsymbol{R}_n$. When the number of interferences L is less than N, the number of antennas in the array, the propagation vectors $\boldsymbol{u}_j$, $j = 1, \ldots, L$, are linearly independent (with probability one) and span a signal subspace, referred to as the *interference subspace*. Let $\lambda_1 \geq \ldots \geq \lambda_L \geq \lambda_{L+1} = \ldots = \lambda_N = \sigma^2$ be the eigenvalues of $\boldsymbol{R}_n$. The L largest λ_i are referred to as *principal eigenvalues* and their associated eigenvectors are referred to as *principal eigenvectors*. The interference subspace is spanned by the principal eigenvectors. The *noise subspace* is defined as the signal subspace associated with equal $(N-L+1)$ eigenvalues. Let $\boldsymbol{Q}_c$ and $\boldsymbol{Q}_v$ be matrices whose columns are the dominant and noise eigenvectors, respectively. Then in [26] the eigencanceler is defined as the optimal weight vector constrained to the noise subspace,

$$\begin{aligned} \boldsymbol{w}_e &= \boldsymbol{Q}_v \boldsymbol{Q}_v^H \boldsymbol{r}_{sx} \\ &= \left(\boldsymbol{I} - \boldsymbol{Q}_c \boldsymbol{Q}_c^H \right) \boldsymbol{r}_{sx} \end{aligned}, \tag{30}$$

where $\boldsymbol{r}_{sx}$ is the cross-correlation vector between the transmitted data and the received data.

The SNIR normalized with respect to the SNIR of the optimum combiner is given by

$$\rho = \frac{(\boldsymbol{u}_s^H \hat{\boldsymbol{R}}_n^{-1} \boldsymbol{u}_s)^2}{\boldsymbol{u}_s^H \hat{\boldsymbol{R}}_n^{-1} \boldsymbol{R}_n \hat{\boldsymbol{R}}_n^{-1} \boldsymbol{u}_s} \frac{1}{\boldsymbol{u}_s^H \boldsymbol{R}_n^{-1} \boldsymbol{u}_s}, \tag{31}$$

where $\boldsymbol{u}_s$ is the designated signal channel transfer vector and $\boldsymbol{R}_n$ is the interference+noise covariance matrix.

The random variable ρ is conditioned on both the channel and the covariance matrix estimate, and is bounded $0 \leq \rho \leq 1$. The normalized SNIR for the eigenanalysis-based method is given by the expression

$$\rho = \frac{(\boldsymbol{u}_s^H \hat{\boldsymbol{Q}}_v \hat{\boldsymbol{Q}}_v^H \boldsymbol{u}_s)^2}{\boldsymbol{u}_s^H \hat{\boldsymbol{Q}}_v \hat{\boldsymbol{Q}}_v^H \boldsymbol{R}_n \hat{\boldsymbol{Q}}_v \hat{\boldsymbol{Q}}_v^H \boldsymbol{u}_s} \frac{1}{\boldsymbol{u}_s^H \boldsymbol{R}_n^{-1} \boldsymbol{u}_s}. \tag{32}$$

The density of ρ for the eigenanalysis-based method is given by

$$f_\rho(\rho|\gamma) = \frac{K^L}{\Gamma(L)}(1-\rho)^{L-1}\rho^{-(L+1)}e^{-K(1-\rho)/\rho}, \tag{33}$$

where $\Gamma(.)$ is the standard gamma function. Since $\hat{\gamma} = \rho\gamma$ and $f_\gamma(\gamma)$ and $f_\rho(\rho)$ are known, the density of $\hat{\gamma}$ can be found from the expression

$$f_{\hat{\gamma}}(\hat{\gamma}) = \int_0^\infty \frac{1}{\gamma} f_\rho(\frac{\hat{\gamma}}{\gamma}|\gamma) f_\gamma(\gamma) d\gamma. \tag{34}$$

Combining eq. (34) and the conditioned probability of error $P_e(e \mid \gamma)$, the average probability of error for the SMI method can be written as

$$P_e = \int_0^\infty \frac{1}{\gamma} f_\gamma(\gamma)[\int_0^\gamma P_e(e \mid \gamma) f_\rho(\frac{\hat{\gamma}}{\gamma}|\gamma) d\gamma] d\gamma. \tag{35}$$

Then, the average probability of error for the eigenanalysis-based method can be found from expression (35), with $f_\rho(\frac{\hat{\gamma}}{\gamma}|\gamma) = f_\rho(\rho|\gamma)$ given by eq. (33).

The match between theory and simulations is illustrated by Figure 17. The curves shown represent the theoretical probability of error, and the probability of error based on simulations for $N = 9$, $K = 20$, and INR = 2 dB.

II.3 Multi-shot Approach for Separating Asynchronous Multiuser CDMA Signals

It has been noticed that the multiuser detector proposed in [22] to handle asynchronous transmission might run into the singularity problem in its enlarged "correlation" matrix for some relative delays between multiple access users. In order to mitigate the singularity problem, we proposed a new approach, termed multi-shot approach, to separate and detect multiuser signals in asynchronous CDMA Communication Systems. The multi-shot approach first explores the structure inherent in the matrix decomposition of the properly arranged

data, obtain from multi-shot matched filtering. Then we make a matrix approximation to make the tentative multiuser information bit estimation tractable and simple. After analyzing the cuase of bias introduced by matrix approximation, we further modified the filtering matrix and reduced the bias effect and improved the overall detection performance yet still minimized the computational complexity (linear to the number of users).

The system diagram is shown in figure 5 of Appendix G for the simpliest case which use the minimum number of consecutive symbols (N=3). Notice that all the matrix filterings involved in the system are only of dimenstion K (number of users). This simplification in system implementation is achieved by exploring the block-tridiagonal structure of the original matrix $\boldsymbol{P}$ of a larger dimension.

III Conclusions and Recommendations

During this period we made significant progress in applying the bootstrap algorithm to multiuser CDMA communications. In particular, we use the F/F structure and use the signum function as a discriminator. The simplicity and superiority of the algorithm was emphasized when we compared its performance to the MMSE on one hand and to Verdú's decorrelator on the other.

The adequacy of the algorithm to operate in an unknown channel was also demonstrated. Some ideas for improving error probability in the asynchronous channel were also suggested.

In addition, two new topics not directly related to the bootstrap, but important research initiatives, were studied. The first concerns with using adaptive arrays to improve separator performance. The second, termed multi-shot separator, is a novel idea that can be implemented for an asynchronous multiuser channel, and can in, particular, handle cases wherein the cross correlation matrix is singular.

In summary, during this period of research, we obtained an important result in applying the bootstrap algorithm for multiuser CDMA and initiated new work on other topics related to separation of signals.

A list of publications resulting from these results is given in section V. For further study we recommend the following:

- Continue examining the application of antenna arrays to improve separator performance.
- Further examine the performance of the multi-shot separator.
- Examine the effect of channel fading and multipath on separator performance.
- Examine the effect of uncertainty in relative delay on performance of the bootstrap algorithm.

IV References

[1] Y. Bar-Ness, A. Dinç and H. Messer-Yaron, "The Bootstrapped Algorithm: Fast Algorithm for Blind Signal Separation," Final Technical Report, RL-TR-93-24, April, 1993.

[2] Y. Bar-Ness, A. Dinç, H. Messer-Yaron, Z. Siveski, R. Kamel and R. Onn, "The bootstrapped Algorithm: A Fast Algorithm for Blind Signal Separation," Final Technical Report,RL-TR-93-236, Dec., 1993.

[3] Y. Bar-Ness, Z. Siveski, A. Haimovich, N. Ansari, R. Kamel and D. W. Chen, "Fast Algorithms for Blind Signal Separation and Channel Equalization," Final Technical Report, RL-TR-95-72, April 1995.

[4] Y. Bar-Ness and J. Rokah, "Cross-Coupled Bootstrapped Interference Canceler," Antenna and Propagation Symposium, Conference Proceedings, pp. 292-295, 1981.

[5] Y. Bar-Ness, J. Carlin and M. Steinberger, "Bootstrapping Adaptive Cross Pol Cancelers for Satellite Communication," Proc. of the IEEE International Conference on Communications (ICC), No. 4F5, Philadelphia, PA, June 1982

[6] W. Carlin, Y.Bar-Ness, S. Gross, M. Steinberger and W. Studdiford, "An IF Cross-Pol Canceler for Microwave Radio Systems," Journal on Selected Area in Communications - Advances in Digital Communication by Radio, Vol. SS AC-5, No. 3, pp. 502-514, April, 1987.

[7] Y. Bar-Ness and M. Steinberger, "Cross-Pol Canceler Architecture for Microwave Radio Applications," International Conference on Communications, Conference Proceedings paper, No. 52.5, Seattle WA, June 1987.

[8] Y. Bar-Ness, "Effect of Number of Taps on cross-Pol Canceler Performance for Digital Radio," The IEEE Global Communications Conference (GLOBECOM) 1987, paper No. 31.7.

[9] A. Dinç and Y. Bar-Ness, "Performance Comparison of LMS Diagonalizer and Bootstrapped Adaptive Cross-Pol Canceler over Non-Dispersive Channel," The 1990 Military Communications Conference, Monterey, CA, paper 3.7, Sept. 30-Oct. 3, 1990.

[10] A. Dinç and Y. Bar-Ness, "Error Probabilities of Bootstrapped Blind Adaptive Cross-Pol Canceler For M-ary QAM Signals over Non-dispersive Fading Channel," IEEE 1992 International Conference on Communications, Chicago. IL, paper 353.5 June 15, 1992.

[11] A. Dinç and Y. Bar-Ness, "Convergence and Performance Comparison of Three Different Structures of Bootstrap Blind Adaptive Algorithm for Multisignal Co-Channel Separation," MILCOM '92, San Diego, CA, pp. 913-918, Oct. 12, 1992.

[12] A. Dinç and Y. Bar-Ness, "A Forward/Backward Bootstrap Structure for Blind Separation of Signals in a Multi-Channel Dispersive Environment," ICASSP'93, Minneapolis MN, pp. III 376 - III 379, April 27-30, 1993

[13] A. Dinç and Y. Bar-Ness, "Bootstrap: A Fast Unsupervised Learning Algorithm," IEEE 1992 International Conference on Acoustics, Speech and Signal Processing, ICASSP'92, San Francisco, CA, paper 43.8, March 23, 1992.

[14] Z. Siveski, Y. Bar-Ness and D. W. Chen, "Error Performance of Synchronous Multiuser Code Division Multiple Access Detector with Multidimensional Adaptive Canceler," European Trans. on Telecommunications and Related Technologies, vol 5, no. 6, pp 719-724, Nov.-Dec. 1994.

[15] D. W. Chen, Z. Siveski and Y. Bar-Ness, "Synchronous Multiuser Detector with Soft Decision Adaptive Canceler," 28th Annual Conf. on Inf. Sci. and Sys., Princeton, NJ, March 1994.

[16] R. Kamel and Y. Bar-Ness, "Blind Decision Feedback Equalization Using Decorrelation Algorithm," Globecom '93 Comm. Theory Mini Conference, Houston, TX, pp. 87-91, Nov 1993.

[17] R. Kamel and Y. Bar-Ness, "Reduced State Sequence Estimation of Digital Sequences In Dispersive Channels Using State Partitioning," Electronic Letters, Vol. 30, pp. 14-17, January 6, 1994.

[18] R. Kamel and Y. Bar-Ness, "Blind Maximum Likelihood Sequence Estimation of Digital Sequences in the Presence of Intersymbol Interference," Electronic Letters, Vol. 30, no. 7, pp. 537-539, March 31, 1994.

[19] S. Verdú, "Recent Progress in Multiuser Detection," Advances in Communication and Signal Processing, Springer-Verlag, 1989.

[20] Y. Bar-Ness and J.B. Punt, "Adaptive Bootstrap CDMA Multiuser Detector," Wireless Personal Communications, an International Journal, special issue on "Signal Separation and Interference Cancellation for PIMRC," Forthcoming.

[21] H. Ge and Y. Bar-Ness, "Comparative Study of Linear Minum Mean Square Error (LMMSE Estimate-based and the Adaptive Bootstrap Multiuser Detector for CDMA Communications," ICC'96, Dallas, TX, vol , pp. , June 1996.

[22] Y. Bar-Ness and N. Sezgin, "Adaptive Multiuser Bootstrapped Decorrelating CDMA Detector for One Shot Asynchronous Unknown Channels," ICASSP'95, Detroit, MI, pp. 1733-1736, May 9-12, 1995.

[23] Y. Bar-Ness and N. Sezgin, "Maximum Signal-to-Noise Ratio Data Combining for One-Shot Asynchronous Multiuser CDMA Detector," PIMRC'95, Toronto, Canada, pp 188-192, Sept 27-29,1995.

[24] A. Haimovich, Y. Bar-Ness and R. Manzo, "A Stochastic Gradient-Based Decorrelation Algorithm with Applications to Multicarrier CDMA," Proceedings of the 1995 IEEE 45th Vehicular Technology Conference, Chicago, pp. 464-468.

[25] A. Haimovich and Y. Bar-Ness "On the Performance of a Stochastic Gradient-Based Decorrelation Algorithm for Multiuser Multicarrier CDMA," Wireless Personal Communications, Vol. 2, No. 4, 1995/1996, pp. 357-371.

[26] X. Wu and A.M. Haimovich, "Adaptive Arrays for Increased Performance in Mobile Communications," Proceedings of the Sixth International Symposium on Personal, Indoor and Mobile Communications (PIMRC'95), Toronto, Canada, pp. 653-657, Sept. 1995.

V List of Publications

V.1 Papers in Professional Journals

1. Messer, H. and Bar-Ness, Y., "Simultaneous Spatial Separation and Direction-of-Arrival Estimation of Wideband Sources Using Bootstrapped Algorithms," IEEE Trans. on Circuits and Systems, vol. 43, pp. 316-328, April 1996.

2. Y. Bar-Ness and J.B. Punt, "Adaptive Bootstrap CDMA Multiuser Detector," Wireless Personal Communications, an International Journal, special issue on "Signal Separation and Interference Cancellation for PIMRC," Forthcoming.

3. A. Haimovich and Y. Bar-Ness, "On the Performance of a Stochastic Gradient-Based Decorrelation Algorithm for Multiuser Multicarrier CDMA," Wireless Personal Communications, Vol. 2, No. 4, 1995/1996, pp. 357-371

V.2 Papers in Conference Proceedings

1. Y. Bar-Ness and N. Sezgin, "Adaptive Threshold Setting for Multiuser CDMA Signal Separator with Soft Tentative Decision," the 29th Annual Conference on Information Science and Systems, Johns Hopkins University Baltimore, MD, March 1995.

2. Y. Bar-Ness and N. Sezgin, "Adaptive Multiuser Bootstrapped Decorrelating CDMA Detector for One Shot Asynchronous Unknown Channels," ICASSP'95, Detroit, MI, pp. 1733-1736, May 9-12, 1995.

3. Haimovich A., Bar-Ness, Y., and Manzo, R., "A Stochastic Gradient-Based Decorrelation Algorithm with Applications to Multicarrier CDMA," 1995 IEEE Vehicular Technology Conference, Chicago, IL, vol. 1, pp. 464-468, July 1995.

4. Bar-Ness, Y., "The Bootstrap Decorrelating Algorithm: A Promising Tool for Adaptive Separation of Multiuser CDMA Signals," invited paper, 7th Tyrrhenian International Workshop on Digital Communication, Viareggio, Italy, September 10-14, 1995.

5. Bar-Ness, Y. and Punt, J.B., "An Improved Multiuser CDMA Decorrelating Detector," PIMRC'95, Toronto, Canada, pp. 975-979, September 27-29, 1995.

6. Bar-Ness, Y. and Sezgin N., "Maximum Signal-to-Noise Ratio Data Combining for One-Shot Asynchronous Multiuser CDMA Detector," PIMRC'95, Toronto, Canada, pp. 188-192, September 27-29, 1995.

7. Ge, H. and Bar-Ness, Y., "Bayesian Approach of Multiuser Separation of Interference Suppression in CDMA Systems," IEEE 29th Asilomar Conference on Signal Systems and Computers, October 1995.

8. Bar-Ness, Y., "Recent Results on Adaptive Multiuser Signal Separation in CDMA: Important Steps in Meeting the Needs of Third Generation Wireless Communication Systems," IEE International Conference on Personal Wireless Communications, New Delhi, India, February 19-21, 1996.

9. Ge, H. and Bar-Ness, Y., "Multi-Shot Approach to Multiuser Separation and Interference Suppression in Asynchronous CDMA," the 30th Annual Conference on Information Sciences and Systems," Princteton University, Princeton, NJ, March 20-22, 1996.

10. Ge, H. and Bar-Ness, Y., "Performance Analysis on Linear Minimum Mean Square Error (LMMSE) Estimator-Based Multiuser Detector," IEEE 8th Signal Processing Conference (SSAP-96), Greece, June 1996.

11. Ge, H. and Bar-Ness, Y., "Comparative Study of Linear Minimum Mean Square Error (LMMSE) and the Adaptive Bootstrap Multiuser Detectors for CDMA Communications," the International Conference on Communications, June 1996

12. Sezgin, N. and Bar-Ness, Y., "Adaptive Soft Limiter Bootstrap Separator CDMA Channel with Singular Partial Cross-Correlation Matrix," the International Conference on Communications, June 1996.

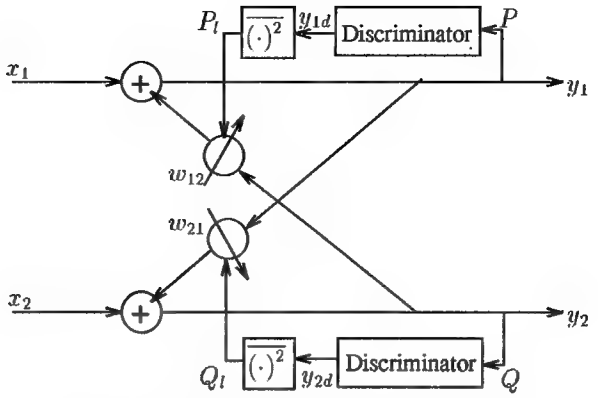

Figure 1: B/B dual polarization separator

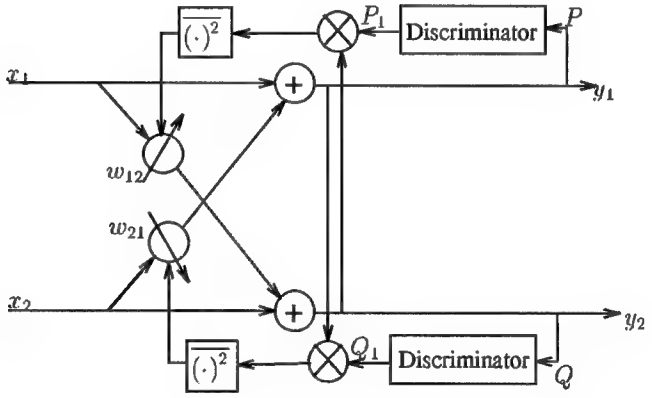

Figure 2: F/F dual polarization separator

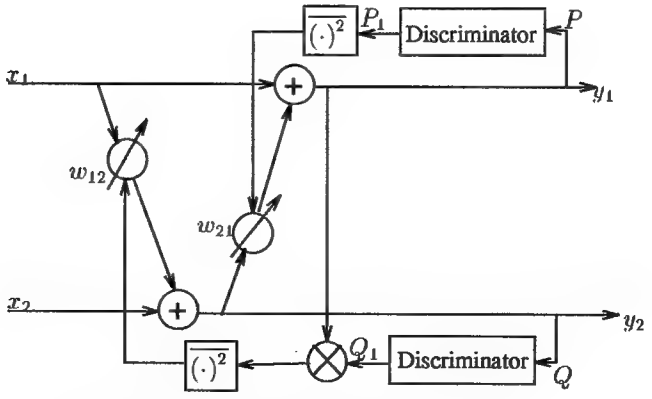

Figure 3: F/B dual polarization separator

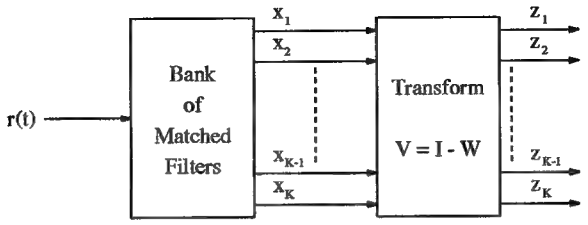

Figure 4: Transformation of matched filter outputs.

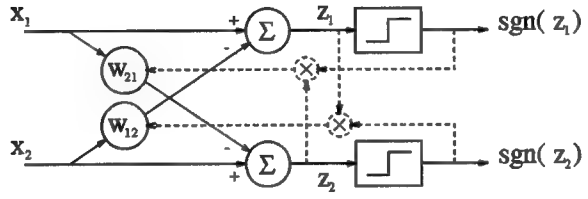

Figure 5: Decorrelator for two users.

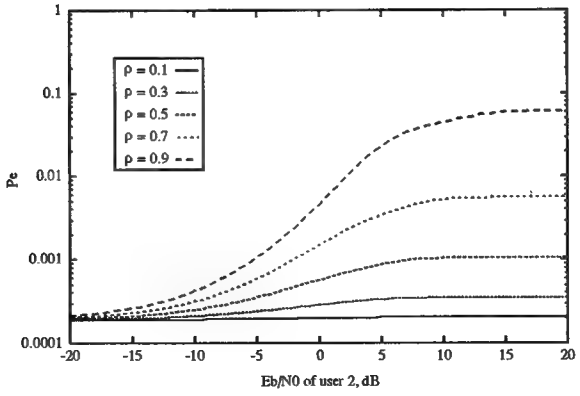

Figure 6: Theoretical error probability of user 1 as a function of the energy of user 2. $Eb/N0_1 = 8dB$.

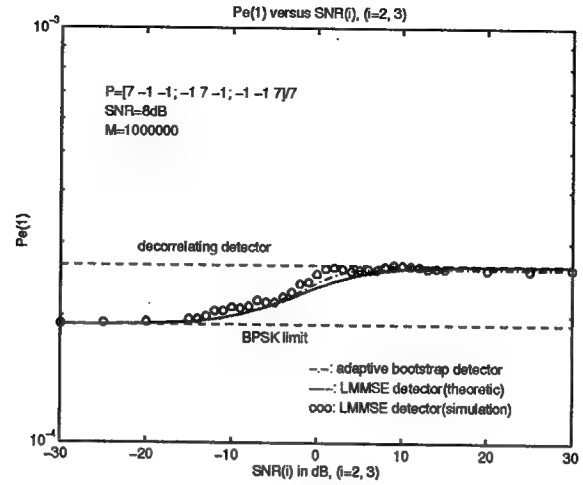

(a). High capacity case

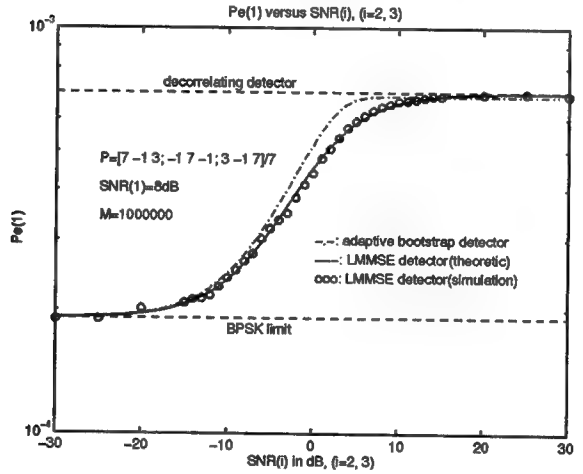

(b). Medium capacity case

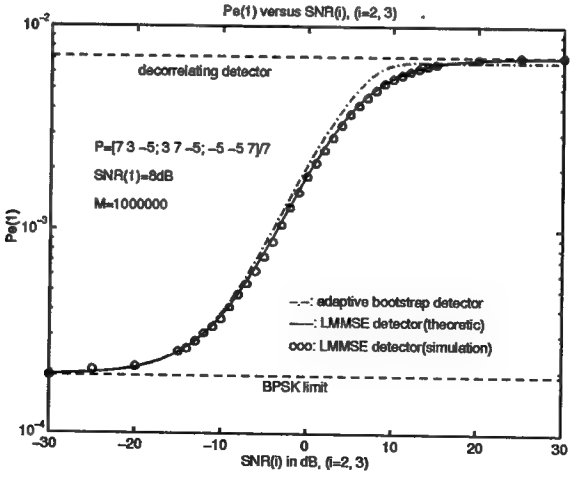

(c). Low capacity case1:w

Figure 7: Performance of the LMMSE detector and the adaptive bootstrap detector in a multi-user CDMA system. Also shown in the figures are the results of the decorrelating detector and the BPSK limit. Parameters used: $\mathrm{SNR}_1 = 8\mathrm{dB}$, $K = 3$, M= 1000000 independent trials.

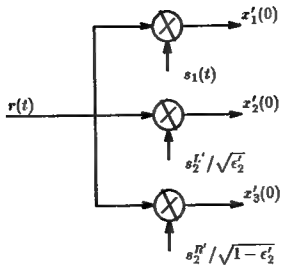

Figure 8:

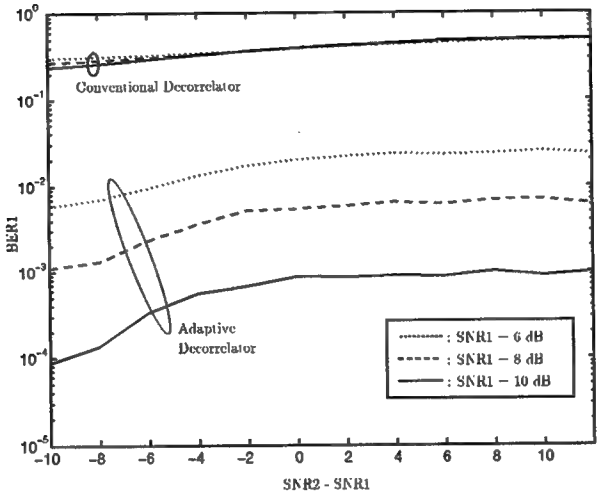

Figure 9: Performance Comparison of Adaptive and Conventional Detectors for fixed SNR1-variabe interference (Unknown-delay case)

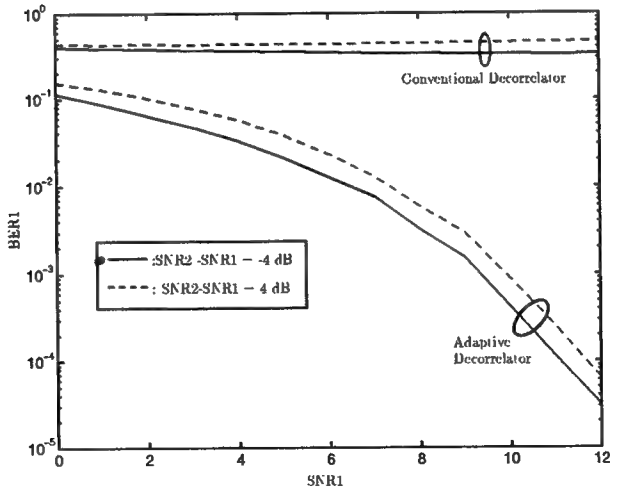

Figure 10: Performance Comparison of Adaptive and Conventional Detectors for fixed SNR1-variabe interference (Unknown-delay case)

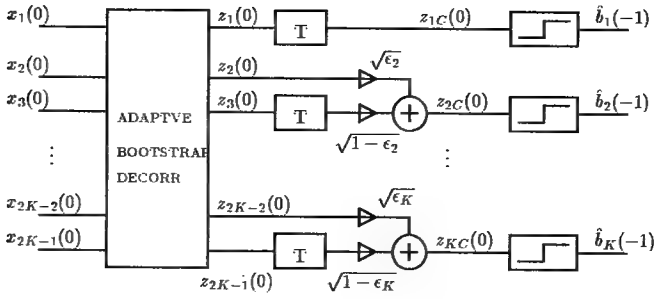

Figure 11: Asynchronous K-user Combining Scheme

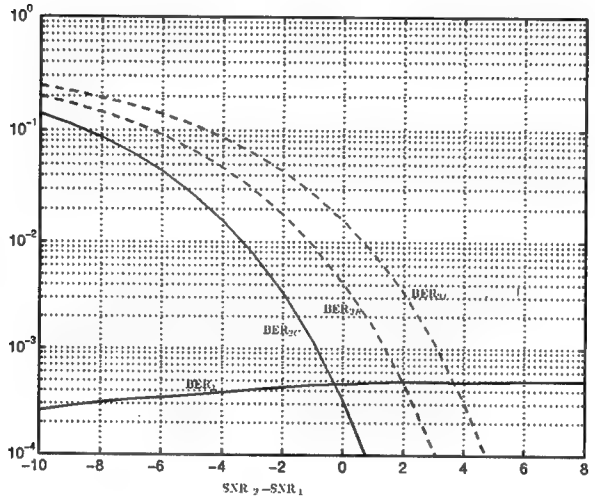

Figure 12: Performance of the Scheme in Fig. 11 for K=2, SNR_1=8 dB, $\epsilon_2 = 0.4$

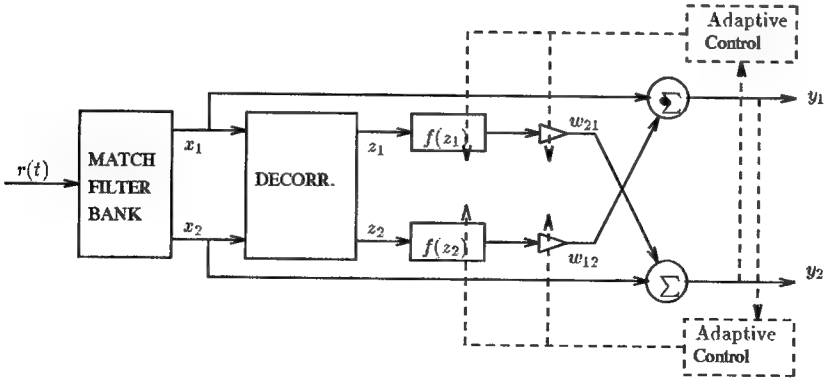

Figure 13: Two-stage (decorrelator/canceller) Detector with Adaptive Soft Limiter

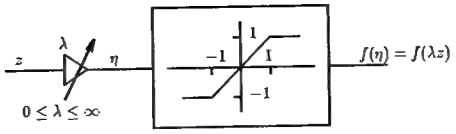

Figure 14: Soft Limiter with controlled threshold

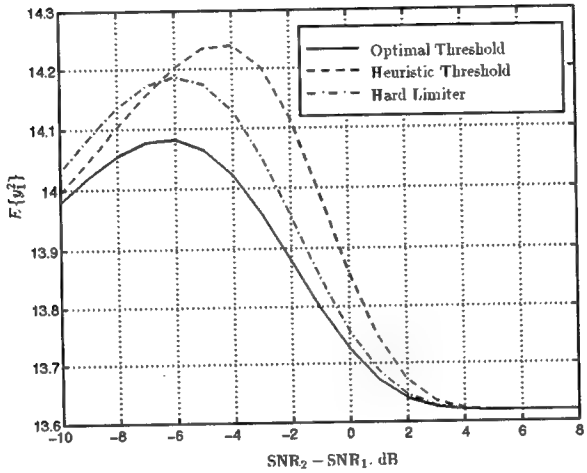

Figure 15: Output Energy of desired user, $\mathrm{E}\{y_1^2\}$ with Hard Limiter, Heuristic Threshold and Optimal Threshold; $\mathrm{SNR}_1 = 8$ dB, $\rho = 0.7$

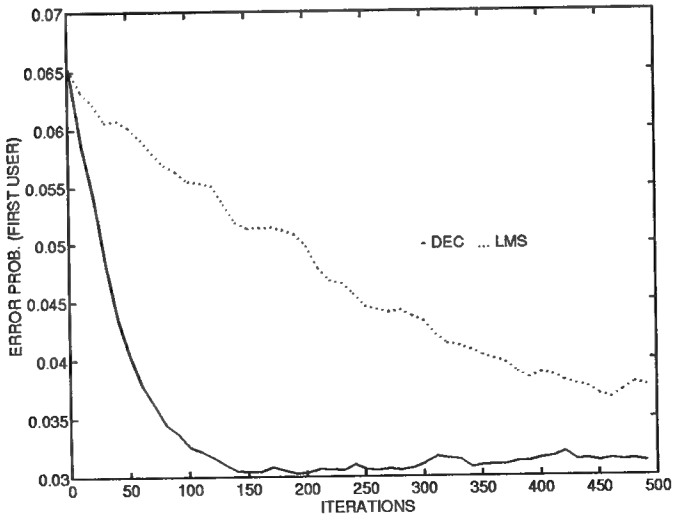

Figure 16: Learning curve of the probability of error of the first user for N=4 users, SNR=8dB, SSR=-5dB.

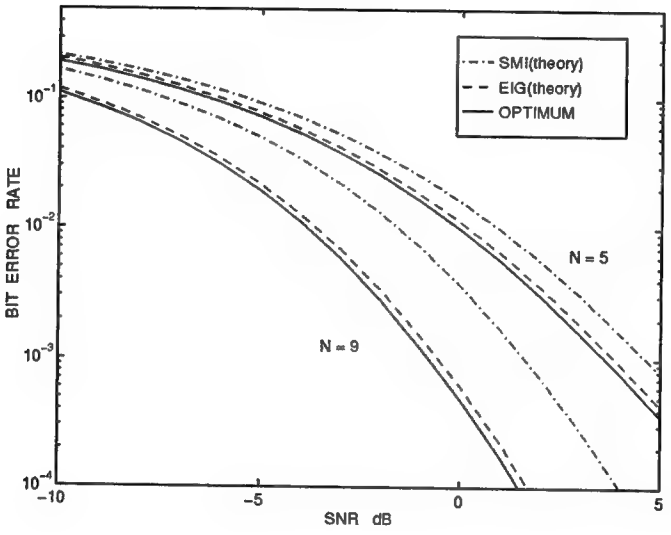

Figure 17: The average BER versus the average received SNR for adaptive array with one interference with K=20, INR=2dB. (analytical results)

Appendix A

An Improved Multi-User CDMA Decorrelating Detector

Y. Bar-Ness and J.B. Punt
Center for Communications and Signal Processing Research
Department of Electrical Engineering
New Jersey Institute of Technology
Newark, NJ 07102-1982, USA
e-mail: barness@hertz.njit.edu

Abstract

Decorrelating detectors were proposed as tools to combat the near-far problem in multi-user CDMA communication systems. They were also used as the first stage of many two-stage, multi-user signal separators to facilitate tentative decisions for the canceller stage. These decorrelators result in a complete separation of signals, but also in relatively high additive noise. An improved multi-user detector is proposed in this paper. It may not totally reject other signals, but it does result in a better error probability, particularly in regions where interference energies are low. The proposed improved decorrelators can be implemented by an adaptive algorithm and hence are better suited for a changing environment.

1 Introduction

A conventional single-user detector for the Code Division Multiple Access (CDMA) scheme consists of a bank of filters, each one matched to the signature sequence of a particular user. Besides the desired signal, the sampled output of each matched filter contains the residual interference from all other users. The presence of strong interference often makes it impossible to detect weak users, a condition referred to as the near-far problem. To eliminate this problem Verdú proposed a receiver [1] that is optimum in the multi-user environment. It is

optimum in the sense that it completely separates the signals from different users' signals. Achievement of performance with this optimal receiver comes at the expense of high computational complexity. A class of sub-optimum receivers that use decorrelating detectors and which are based on linear transformation of the sampled matched filters' output was considered in [2] and [3]. These decorrelating detectors were also used as a first stage of many two-stage, multi-user detectors to facilitate tentative decisions for the second (canceller) stage. This second stage can be a fixed canceller, assuming knowledge of signal energies ([4], [5]), an adaptive canceller assuming no knowledge of energies ([6]), an adaptive canceller with soft-decision ([7]) or a canceller with optimum soft-decision ([8]). Verdú's decorrelating detector uses the inverse of the cross-correlation matrix to separate signals from the different users. However, separation can be achieved whenever the transformation diagonalises the cross-correlation matrix. We will discuss a different transformation that will also separate the signals and show that the output *SNR* and hence the error probability remains unchanged.

However, we are mainly interested in a low error probability, not so much in total signal separation. Therefore, the resulting signal-to-interference-plus-noise ratio is the parameter that should be minimised. To do this we suggest a linear transformation that minimises the correlation between the different transform outputs and the hard limiter outputs. This transformation is shown to perform better than the optimal separation decorrelator, particularly for high signal-to-interference ratios.

2 Matched Filters

For the general multi-user the equivalent low-pass signal at the input of the matched filter is given by

$$r(t) = \sum_{k=1}^{K} \sum_{i} b_k(i) \sqrt{a_k(i)} s_k(t + iT - \tau_k) + n(t) \tag{1}$$

where K is the number of users, and a_k, b_k, s_k and τ_k are the signal amplitude, user bit, signature waveform and relative delay of the k^{th} user. $n(t)$ is the zero mean AWGN, with a two-sided power spectral density of $N_0/2$.

For the synchronous channel encountered in down-link communication channels the τ_k are zero for all k. In the asynchronous up-link channels the τ_k are not necessarily equal. For the former case the output of the k^{th} matched filter is the composite of bit b_k and all interfering bits given by a linear combination through the cross-correlation factor ρ_{kj}. In matrix notation we can write:

$$\boldsymbol{x}(i) = PA\boldsymbol{b}(i) + \boldsymbol{n}(i) \tag{2}$$

where

$$P = \begin{bmatrix} 1 & \rho_{12} & \rho_{13} & \cdots & \rho_{1K} \\ \rho_{12} & 1 & \rho_{23} & \cdots & \rho_{2K} \\ \rho_{13} & \rho_{23} & \ddots & & \\ \vdots & \vdots & & & \rho_{K-1,K} \\ \rho_{1K} & \rho_{2K} & & \rho_{K-1,K} & 1 \end{bmatrix} \tag{3}$$

and $A = diag\left(\sqrt{a_1}, \cdots, \sqrt{a_K}\right)$, $\boldsymbol{b}(i) = [b_1(i), \cdots, b_K(i)]$ and $\boldsymbol{n}(i)$ is a zero-mean Gaussian noise vector with covariance $R_n = P\sigma^2$. For the asynchronous case one may use the one-shot matched filter proposed by Verdú in [9] . In this case (1) will contain a linear combination of $b_k(i)$, $b_j(i)$ and $b_j(i-1)$ for $j = 1 \ldots K, j \neq k$. That is, the matrix P will be replaced by another square matrix with $1 + 2(K-1) = 2K-1$ dimensions. The output of this one shot matched filter $\boldsymbol{x}_k(i)$ will contain a linear combination through this $(2K-1) \times (2K-1)$ cross correlation matrix of $b_k(i)$ and bits i and $i-1$ of all other users. If the τ_k are known then all the elements of this matrix are known provided one knows the codes. Therefore, for both synchronous and asynchronous cases the output of the matched filters is given by (2) with the corresponding definition of $\boldsymbol{b}(i)$.

3 Multi-user Decorrelating Detectors

3.1 Verdú's approach

Lupas and Verdú used the inverse of the matrix P to separate the signals [2]. That is:

$$\boldsymbol{z} = P^{-1}\boldsymbol{x} = A\boldsymbol{b} + P^{-1}\boldsymbol{n} \tag{4}$$

$$= A\boldsymbol{b} + \boldsymbol{\xi} \tag{5}$$

where $\boldsymbol{z} = [z_1, \cdots, z_K]$, and without loss of generality we dropped the dependency on i. It follows that $E\left[\boldsymbol{\xi}\boldsymbol{\xi}^T\right] = P^{-1}\sigma^2$. Apart from noise, note that $\boldsymbol{z}$ contains data from only one user. Using a decision on the elements of $\boldsymbol{z}$, we get as output $\hat{\boldsymbol{b}} = \mathrm{sgn}(\boldsymbol{z})$. Clearly this detector is near-far resistant. The probability of error for $\hat{b_k}$ depends on the signal-to-noise ratio

$$SNR_k = \frac{a_i}{E\left[\xi_k^2\right]} = \frac{a_i}{\sigma^2}\frac{|P|}{|P_k|} \tag{6}$$

where $|P|$ is the determinant of P and $|P_k|$ is the kk^{th} co-factor of P.

The Verdú separator is only one of many possible separators. In fact any linear transformation that diagonalises matrix P will do. In the next section we present such a transformation and examine its properties and the performance of the corresponding multi-user detector.

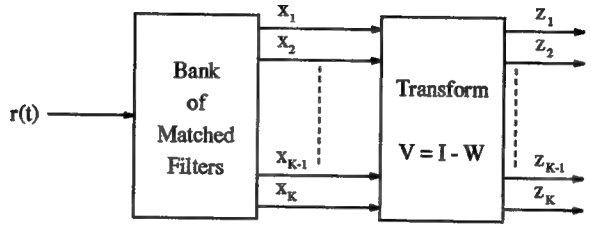

Figure 1: Transformation of matched filter outputs.

3.2 Different Decorrelating Detector

Let

$$\begin{aligned} \boldsymbol{z} = V\boldsymbol{x} &= VPA\boldsymbol{b} + V\boldsymbol{n} \\ &= VPA\boldsymbol{b} + \boldsymbol{\zeta} \end{aligned} \tag{7}$$

We will try to find $V \neq P^{-1}$ so that VP is a diagonal matrix. We propose to use $V = I - W$, where

$$W^T = \begin{bmatrix} 0 & w_{12} & w_{13} & \cdots & w_{1K} \\ w_{21} & 0 & w_{23} & \cdots & w_{2K} \\ \vdots & & \ddots & & \\ \vdots & & & 0 & w_{K-1,K} \\ w_{K1} & \cdots & & w_{K,K-1} & 0 \end{bmatrix} \tag{8}$$

as shown in Fig. 1

Note that W is not necessarily a symmetric matrix. The output of the detector is:

$$z_k = \boldsymbol{x}_k - \boldsymbol{w}_k^T \boldsymbol{x}_k + \zeta_k \tag{9}$$

where $\boldsymbol{w}_k$ is the k^{th} column of W without $w_k k$ and $\boldsymbol{x}_k$ is the vector $\boldsymbol{x}$ with $\boldsymbol{x}_k$ taken out. We propose to choose W so that

$$E\left[z_k \boldsymbol{b}_k\right] = 0 \tag{10}$$

where the k^{th} element is taken out of $\boldsymbol{b}$ to form $\boldsymbol{b}_k$.

If the signal-to-noise-plus-interference ratio for any of the $z_j, j \neq k$ is large, then $E\left[z_k \mathrm{sgn}\left(z_j\right)\right] = E\left[z_k b_j \left(1 - P_{e_j}\right)\right]$. Under this condition (10) is an approximation of

$$E\left[z_k \mathrm{sgn}\left(\boldsymbol{z}_k\right)\right] = 0 \quad \text{for } k = 1, 2, \ldots, K \tag{11}$$

where $\boldsymbol{z}_k$ is $\boldsymbol{z}$ without the k^{th} element. By using (9) we get for (10):

$$E\left[\left(\boldsymbol{x}_k - \boldsymbol{w}_k^T \boldsymbol{x}_k\right) \boldsymbol{b}_k\right] = 0 \quad \text{for } k = 1, 2, \ldots, K \tag{12}$$

One can show that

$$\boldsymbol{x}_k = P_k A_k \boldsymbol{b}_k + \sqrt{a_k} b_k \boldsymbol{\rho}_k + \boldsymbol{n}_k \tag{13}$$

where the index k for a matrix or vector means that rows and columns k are taken out of the matrix, or that element k is taken out of the vector. Note that

$$\begin{aligned} E\left[\boldsymbol{x}_k \boldsymbol{b}_k\right] &= E\left[\left(\sqrt{a_k} b_k + \boldsymbol{\rho}_k^T A_k \boldsymbol{b}_k + \boldsymbol{n}_k\right) \boldsymbol{b}_k\right] \\ &= A_k \boldsymbol{\rho}_k \end{aligned} \tag{14}$$

where we use the fact that the data of the different users are uncorrelated and independent of the noise. Also using (13) we have

$$\begin{aligned} E\left[\boldsymbol{b}_k \boldsymbol{x}_k^T\right] &= E\left[\boldsymbol{b}_k \left(\boldsymbol{b}_k^T A_k P_k + \sqrt{a_k} b_k \rho_k + \boldsymbol{n}_k^T\right)\right] \\ &= A_k P_k \end{aligned} \tag{15}$$

Therefore substituting (14) and (15) in (12) we get

$$\boldsymbol{w}_k = P_k^{-1} \boldsymbol{\rho}_k \tag{16}$$

Using these $\boldsymbol{w}_k$ the linear transformation V will diagonalise the correlation matrix P. From the definition of W, P_1 and $V = I - W$

$$VP = diag\left(1 - \boldsymbol{w}_1^T \boldsymbol{\rho}_1, \cdots, 1 - \boldsymbol{w}_K^T \boldsymbol{\rho}_K\right) \tag{17}$$

and for the noise covariance

$$E\left[\boldsymbol{\zeta}\boldsymbol{\zeta}^T\right] = E\left[V \boldsymbol{n}\boldsymbol{n}^T V^T\right] = \sigma^2 V P V^T \tag{18}$$

VP is diagonal and the diagonal terms of V are unity, hence

$$E\left[\zeta_k^2\right] = \sigma_{\zeta_k}^2 = \left(1 - \boldsymbol{w}_k^T \boldsymbol{\rho}_k\right) \sigma^2 \tag{19}$$

Therefore,

$$\begin{aligned} SNR_k &= \frac{a_i \left(1 - \boldsymbol{w}_k^T \boldsymbol{\rho}_k\right)}{\sigma^2} \\ &= \frac{a_i \left(1 - \boldsymbol{\rho}_k^T \left(P_k\right)^{-1} \boldsymbol{\rho}_k\right)}{\sigma^2} \end{aligned} \tag{20}$$

where we also used (16).

Using $E\left[\zeta_k^2\right] \geq 0$ and the fact that P_k is positive definite, we can show that

$$0 \leq 1 - \boldsymbol{\rho}_k^T \left(P_k\right)^{-1} \boldsymbol{\rho}_k \leq 1 \tag{21}$$

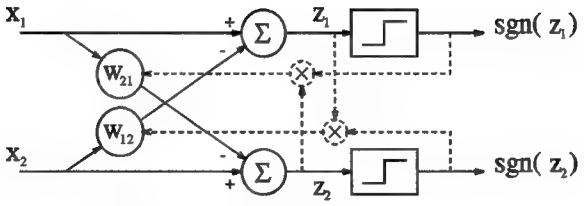

Figure 2: Decorrelator for two users.

Furthermore, it can be shown that

$$1 - \boldsymbol{\rho}_k^T \left(P_k\right)^{-1} \boldsymbol{\rho}_k = \frac{|P|}{|P_k|} \tag{22}$$

Now comparing (20) with (6) we conclude that if we use $E\left[z_k \boldsymbol{b}_k\right] = 0$ as a diagonalising transformation, then the SNR at the output (and hence also the error probability at the decorrelator output) is equal to that of the Verdú transformation.

3.3 An Improved Decorrelating Detector

Using (11) directly will result in a linear transformation that will not separate the signals totally, but will leave some interference residue in the output. The additive noise, however, will be smaller so that the output signal-to-noise-plus-interference ratio will be better (or at least as good) than the total separation signal-to-noise ratio. This gives us improved performance in the low interference region. Solving (11) analytically without using the high signal-to-noise assumption is rather difficult due to the correlated noise. However, using numerical solutions we find that particularly in the region where interference power is low, the output SNR is better and so is the probability of error. To show this without relying solely on numerical methods we use the two-user case. Extending the proof to a multi-user case is possible following similar reasoning. From Fig. 2:

$$\begin{aligned} x_1 &= \sqrt{a_1} b_1 + \rho \sqrt{a_2} b_2 + n_1 \\ x_2 &= \sqrt{a_2} b_2 + \rho \sqrt{a_1} b_1 + n_2 \end{aligned} \tag{23}$$

with $E\left[n_1^2\right] = E\left[n_2^2\right] = \sigma^2$ and $E\left[n_1 n_2\right] = \rho\sigma^2$. Also

$$\begin{aligned} z_1 &= x_1 - w_{12} x_2 \\ &= \sqrt{a_1}\left(1 - w_{12}\rho\right) b_1 + \sqrt{a_2}\left(\rho - w_{12}\right) b_2 + \\ &\quad n_1 - w_{12} n_2 \end{aligned} \tag{24}$$

and

$$\begin{aligned} z_2 &= \cdot\ x_2 - w_{21}x_1 \\ &= \sqrt{a_2}\left(1 - w_{21}\rho\right)b_2 + \sqrt{a_1}\left(\rho - w_{21}\right)b_1 + \\ &\quad n_2 - w_{21}n_1 \end{aligned} \tag{25}$$

The variance of the noise in output z_1 is:

$$\sigma^2_{noise\ z_1} = \sigma^2\left(1 - 2w_{12}\rho + w_{12}^2\right) \tag{26}$$

and the signal-to-noise plus interference at this output is:

$$SNIR_{z_1} = \frac{a_1\left(1 - w_{12}\rho\right)^2}{\sigma^2\left(1 - 2w_{12}\rho + w_{12}^2\right) + a_2\left(\rho - w_{12}\right)^2} \tag{27}$$

If $a_1 \gg a_2$ and $a_1 \gg \sigma^2$ then $SNIR_{z_1} \gg 1$ provided that w_{12} is of the same order as ρ. Under these conditions $\mathrm{sgn}\left(z_1\right) \simeq b_1$, and hence $E\left[z_2\mathrm{sgn}\left(z_1\right)\right] = 0$ will lead to $w_{21} = \rho$. When these conditions are met, let

$$w_{12} = \rho + \delta \tag{28}$$

To find δ we must equate

$$\begin{aligned} &E\left[z_1\mathrm{sgn}\left(z_2\right)\right] \\ &= E\left[\left(\sqrt{a_1}\left(1 - \rho^2 - \rho\delta\right)b_1 - \delta\sqrt{a_2}b_2 + \zeta_1'\right)\cdot\right. \\ &\qquad \left.\left(\mathrm{sgn}\left(\sqrt{a_2}\left(1 - \rho^2\right)b_2 + \zeta_2\right)\right)\right] \end{aligned} \tag{29}$$

to zero, where we used (24) and (25) together with $w_{21} = \rho$ and $w_{12} = \rho + \delta$, and we also defined

$$\begin{aligned} \zeta_1' &= n_1 - w_{12}n_2 &&= n_1 - \left(\rho + \delta\right)n_2 \\ \zeta_2 &= n_2 - w_{21}n_1 &&= n_2 - \rho n_1 \end{aligned} \tag{30}$$

(29) can be separated into

$$\begin{aligned} &E\left[\left(\sqrt{a_1}\left(1 - \rho^2 - \rho\delta\right)b_1 - \delta\sqrt{a_2}b_2\right)\cdot\right. \\ &\qquad \left.\mathrm{sgn}\left(\sqrt{a_2}\left(1 - \rho^2\right)b_2 + \zeta_2\right)\right] + \\ &E\left[\zeta_1'\mathrm{sgn}\left(\sqrt{a_2}\left(1 - \rho^2\right)b_2 + \zeta_2\right)\right] \end{aligned} \tag{31}$$

By performing the expectation it can be shown that

$$\delta = \frac{-\rho}{1 + \sqrt{\frac{\pi}{2}LSNR}\frac{1}{\left(1-\rho^2\right)}\left(1 - 2Q\left(\sqrt{LSNR}\right)\right)e^{\frac{LSNR}{2}}} \tag{32}$$

where $LSNR$ is the limiting-signal-to-noise ratio at the output:

$$LSNR = \frac{a_2\left(1 - \rho^2\right)}{\sigma^2} \tag{33}$$

From (32) we notice that δ has the opposite sign of ρ and that its absolute value $|\delta|$ decreases from $|\rho|$ to zero when $LSNR$ increases from zero to infinity.

We now calculate the error probability at z_1. Using w_{12} given by (28), and (24) we have

$$z_1 = \sqrt{a_1}\left(1-\rho^2-\rho\delta\right)b_1 + \sqrt{a_2}\delta b_2 + \zeta_1' \tag{34}$$

where ζ_1' is given by (30). The probability of error can be found to be

$$\begin{aligned} P_{e_1} &= \frac{1}{2}Q\left(\frac{\sqrt{a_1}\left(1-\rho^2+\sqrt{a_2}\delta\right)}{\sigma\sqrt{1-\rho^2+\delta^2}}\right) + \\ &\quad \frac{1}{2}Q\left(\frac{\sqrt{a_1}\left(1-\rho^2-\sqrt{a_2}\delta\right)}{\sigma\sqrt{1-\rho^2+\delta^2}}\right) \end{aligned} \tag{35}$$

For small a_2, $\delta \to -\rho$. Then $P_{e_1} \to Q\left(\sqrt{a_1}/\sigma\right)$, the error corresponding to a simple BPSK signal. When a_2 is large, $\delta \to 0$, and $P_{e_1} \to Q\left(\sqrt{a_1}\sqrt{1-\rho^2}/\sigma\right)$, the error corresponding to Verdú's decorrelating detector.

3.4 An Adaptive Version of the Improved Decorrelating Detector

The transformation which corresponds to the solution of (11) can be obtained as a steady state of the following adaptive algorithm, previously referred to in the literature as the "bootstrap algorithm" [10]:

$$\begin{aligned} &\boldsymbol{w}_k(i+1) = \boldsymbol{w}_k(i) + \mu z_k \mathrm{sgn}(\boldsymbol{z}_k) \\ &\quad \text{for } k = 1, 2, \ldots, K \end{aligned} \tag{36}$$

With this algorithm the steady state output error probability is upper-bounded by a value equal to that obtained by Verdú's decorrelator. This value is reached only when the interference-to-noise ratios for all the other users are large in comparison to the desired-signal-to-noise ratio.

4 Numerical Results

Although only the derivation for the two-user case is presented, a similar analysis can be carried out for the multi-user case. Results for both the two-user and the multi-user cases are presented.

For two users, Fig. 3 shows the dependence of δ on $LSNR$ for different values of ρ. The corresponding probability of error is given in Fig. 4. It can be seen from these graphs that the improved decorrelator acts at least as good as the total signal separator, going asymptotically to the results of the separator, for high interference power.

Results for multi-user systems are shown in figs. 5 to 7. For a system with high cross-correlation, Fig. 5 shows δ_{12} and δ_{13}. The error probability for user 1 in this system is given in Fig. 6. It varies between the error probability for a single user BPSK system for low interference and Verdú's error probability for high interference.

A simulation was run for a system with cross-correlation $-1/7$ for all users. In Fig. 7 the results are compared to the theoretical curve, which confirms the outcome. Again, the total signal separator error and the BPSK error are shown to bound the improved decorrelator.

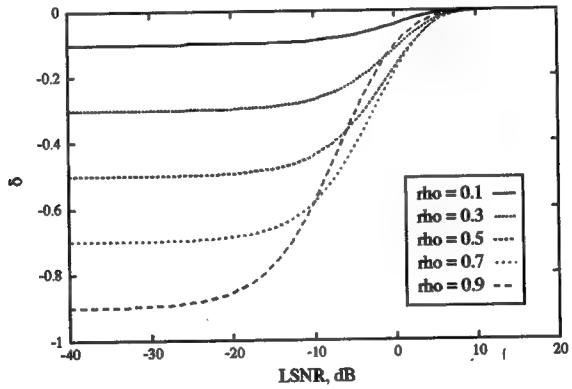

Figure 3: δ as a function of $LSNR$ for different values of ρ. $Eb/N0_1 = 8dB$.

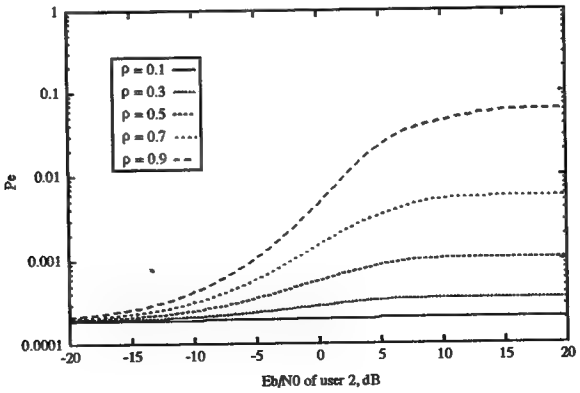

Figure 4: Theoretical error probability of user 1 as a function of the energy of user 2. $Eb/N0_1 = 8dB$.

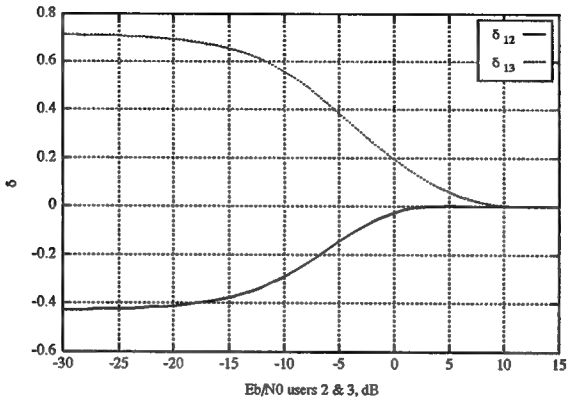

Figure 5: δ_{12} and δ_{13} as a function of the energy of users 2 and 3. $Eb/N0_1 = 8dB$, $\rho_1 3 = \rho_{23} = -5/7$, $\rho_{12} = 3/7$.

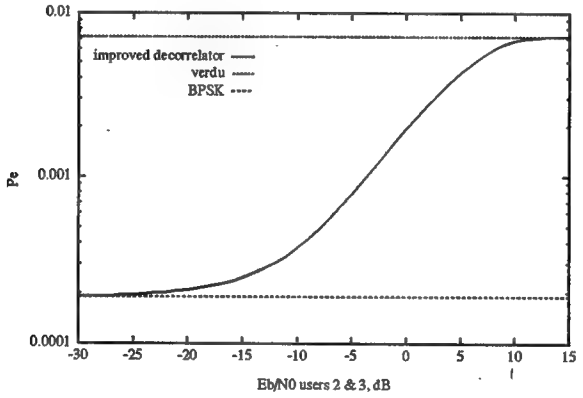

Figure 6: Theoretical error probability of user 1 as a function of the energy of users 2 and 3. $Eb/N0_1 = 8dB$, $\rho_{13} = \rho_{23} = -5/7$, $\rho_{12} = 3/7$.

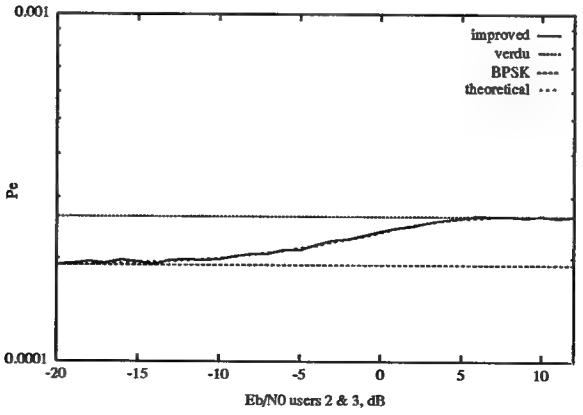

Figure 7: Simulated error probability of user 1 as a function of the energy of users 2 and 3. $Eb/N0_1 = 8dB$. $\rho = -1/7$.

References

[1] S. Verdú, "Minimum probability of error for asynchronous Gaussian multiple access channels," *IEEE Transactions on Information Theory*, Vol. IT-32, No. 1, Jan. 1986, pp. 85-96.

[2] R. Lupas and S. Verdú, "Linear multiuser detector for synchronous code division multiple access channels," *IEEE Transactions on Information Theory*, Vol. IT-35, No. 1, Jan. 1989, pp. 123-136.

[3] R. Lupas and S. Verdú, "Near-far resistance of multiuser detectors in asynchronous channels," *IEEE Transactions on Communications*, Vol. COM-38, No. 4, Apr. 1990, pp. 496-508.

[4] M.K. Varanasi and B. Aazhang, "Multi stage detector in asynchronous code division multiple access communications," *IEEE Transactions on Communications*, Vol. COM-38, No. 4, Apr. 1990, pp. 509-519.

[5] M.K. Varanasi and B. Aazhang, "Near-optimum detector in synchronous code division multiple-access systems," *IEEE Transactions on Communications*, Vol. COM-39, No. 5, May 1991, pp. 725-736.

[6] Z. Siveski, Y. Bar-Ness and D.W. Chen, "Error performance of a synchronous multiuser code division multiple access detector with a multi dimensional adaptive canceler," *The European Transactions on Telecommunications and Related Technologies*, Vol. 5, No. 6, Nov.-Dec. 1994.

[7] D.W. Chen, Z. Siveski and Y. Bar-Ness, "Synchronous multiuser CDMA detector with a soft decision adaptive canceler," *The 28th Annual Conference on Information Sciences and Systems*, Princeton, NJ, Mar. 1994.

[8] Y Bar-Ness and N. Sezgin, "Adaptive Threshold Setting for Multi-User CDMA Signal Separators with Soft Tentative Decision," *The 29th Annual Conference on Information Sciences and Systems*, Baltimore, MD, Mar. 1995.

[9] S. Verdú, "Recent progress in multiuser detection," *Advances in Communication and Signal Processing*, Springer Verlag, 1989.

[10] A. Dinc and Y. Bar-Ness, "Bootstrap: a fast unsupervised learning algorithm," *IEEE 1992 International Conference on Acoustics, Speech and Signal Processing*, ICASSP '92, San Francisco, CA, Mar. 23 1992, paper 43.8.

Appendix B

Comparative Study of the Linear Minimum Mean Squared Error (LMMSE) and the Adaptive Bootstrap Multiuser Detectors for CDMA Communications *

Hongya Ge and Yeheskel Bar-Ness
Center of Communications and Signal Processing Research,
Dept. of Elec. & Comp. Engg.
New Jersey Institute of Technology,
University Heights, Newark, NJ 07102

Abstract

In this work, we analyze the performance of *linear* minimum mean squared error (LMMSE) estimate-based multiuser detector for CDMA Communication Systems. Through numerical evaluation and computer simulations, we also compare the performance of the LMMSE detector [1] and the adaptive bootstrap multiuser detector [2]. Our analysis and simulations show that even though these two detectors were proposed based on different optimization criteria, they exhibit approximately equal performance in multiuser CDMA communications applications.

1 Introduction

Multiuser separation and interference suppression is an active research topic in CDMA communications area. Various detectors have been proposed to balance the computational simplicity and reliable detection performance [1 – 7]. Most of the proposed detectors treat the multiuser signal vector as a deterministic vector, and work only on the *conditional* probability density function (PDF) of the data, given the multiuser signal vector. We notice that the information bit of multiuser is actually a *random* vector. Therefore the optimal approach of separating the information bits of multiuser and suppressing the interference is equivalent to estimating *each realization* of the multiuser information bits with

*This work was supported in part by the Office of Sponsored Research, NJIT, and Rome Air Force Lab under contract F30602-94-C-0135

minimum probability of error. By incorporating a prior knowledge (in a statistical sense) of the multiuser signal vector, one can always improve the overall detection performance. The availability of the a prior knowledge depends on the specific communication systems. Under the linearity constraint, we investigated the *linear* minimum mean squared error (LMMSE) estimate-based multiuser detector, analyzed its detection performance, and compared with the performance of the adaptive bootstrap multiuser detector [2]. It should be pointed out that the LMMSE detector was proposed in [1] and was termed as MMSE detector. Based on statistical signal processing concept, the MMSE estimate is obtained by finding the conditional mean of the posterior PDF of the multiuser information bit, given the received data. And this MMSE estimate-based detector is, in general, a *nonlinear* detector. If we constrain our detector to be in the linear class, we can find, as proposed in [1] and not accurately termed as MMSE detector, the *sub-optimal* **linear** MMSE (LMMSE) estimate-based detector. In this paper, we further analyze the performance of the LMMSE detector in detail and verify our results through numerical evaluation and computer simulation. Comparative study of performances of the linear class of decorrelating detector, LMMSE detector, and adaptive bootstrap multiuser detector is provided in this work.

2 Description of the Problem

Due to the multiple access (MA) scheme used in CDMA systems, the available baseband data $r(t)$ at the receiver is actually a mixture of multiuser data embedded in additive noise. That is,

$$r(t) = \sum_{i} \sum_{k=1}^{K} \sqrt{a_k(i)}\, b_k(i)\, s_k(t - iT - \tau_k) + n(t)\,, \tag{1}$$

where K is the number of users, $a_k(i)$, $b_k(i)$, $s_k(t)$, and τ_k are the bit energy, information bit, signature waveform, and transmission delay of the kth user in the ith symbol interval (of duration T), respectively. $n(t)$ is a white Gaussian process, with two-sided power spectral density of σ^2.

In this work, we only consider the case when $\tau_k = 0$ $(k = 1, \ldots, K)$, which corresponds to the synchronous channel. The synchronous channel model is valid for down-link channel (from base station to mobiles). Note that once the channel is synchronized, all the information bits of the multiusers in the ith symbol interval are completely contained in the data $r(t)$ within the ith symbol interval. Therefore, we can concentrate on solving multiuser separation problem within a specific symbol interval (say $i = 0$ th interval) without lose of generality.

Let us consider a specific bit interval, say $i = 0$. After ignoring index i, we

have,

$$r(t) = \left[\ s_1(t)\ \ s_2(t)\ \ \cdots\ \ s_K(t)\ \right] \cdot \mathbf{A} \cdot \mathbf{b} + n(t)\,, \qquad 0 \le t \le T\,, \qquad (2)$$

with $\mathbf{A} = \mathrm{diag}\{\sqrt{a_1}, \sqrt{a_2}, \cdots, \sqrt{a_K}\}$, and $\mathbf{b} = \begin{bmatrix} b_1 \\ b_2 \\ \vdots \\ b_K \end{bmatrix}$

We then filter $r(t)$ with a bank of matched filters, whose impulse responses are given by,

$$h_k(t) = s_k(T-t)\,, \qquad k = 1, 2, \ldots, K.$$

Columnize the sampled outputs of the bank of matched filters at $t = T$, we get the following matrix notation,

$$\mathbf{x} = \mathbf{P} \cdot \mathbf{A} \cdot \mathbf{b} + \mathbf{n}\,, \qquad (3)$$

where $\mathbf{x} = \left[\ x_1(T)\ \ x_2(T)\ \ \cdots\ \ x_K(T)\ \right]^T$, with $x_k(T) = r(t) * h_k(t)\,|_{t=T}$ being the kth matched filter output sampled at time instant $t = T$; and $\mathbf{n} \sim \mathcal{N}(\mathbf{0}, \sigma^2\,\mathbf{P})$ being the *colored* Gaussian noise due to the matched filtering. Note that the model in (3) is also valid for asynchronous channel, except for a larger dimension. Since for asynchronous channel, by introducing the partioned signature waveforms $s_1(t)$, $s_2^L(t)$, $s_2^R(t)$, $\cdots$, $s_K^L(t)$, and $s_K^R(t)$ as in [3], the resultant matrix $\mathbf{P}$ in (3) is of a dimension $(2K-1) \times (2K-1)$. If the matrix $\mathbf{P}$ is nonsingular, one may use the one-shot method of [3]. For more general asynchronous channel, we also proposed a multi-shot approach in [7] to handle the possible singularity problem. In the sequel, we only consider the synchronous channel for notational simplicity.

Note that matrix $\mathbf{P}$ in (3) is the cross-correlation matrix of the signature waveforms. $\mathbf{P}$ is symmetric, positive definite and nonsingular, and its elements are given by,

$$P[i, j] = \int_0^T s_i(t)\, s_j(t)\, dt \triangleq \rho_{ij}\,. \qquad \begin{matrix} i = 1, 2, \ldots, K; \\ j = 1, 2, \ldots, K. \end{matrix}$$

In practice, due to the finite bandwidth constraint and the existence of a large number of users, the signature waveforms are not idealy orthonormal. Therefore the matrix $\mathbf{P}$ will not be an identity matrix in general. The non-diagonal nature of the $\mathbf{P}$ matrix will cause the multiple access interference (MAI). In order to remove the MAI, various detectors have been proposed [1 – 7]. One major effort of proposing various detectors is trying to balance the computational simplicity and reliable detection performance. In the following sections, we first summarize various *linear* multiuser detectors, and propose new approaches to analyze their performances from statistical signal processing and parameter estimation point of view. we then compare their performances through numerical evaluations and computer simulations.

3 Linear Class of Multiuser Detectors

In this section, we review some recently proposed *linear* multiuser detectors from statistical signal processing point of view, analyze their performances, and make a comparative study of the decorrelating detector, the LMMSE detector, and the adaptive bootstrap multiuser detector.

3.1 Simple Decorrelating Detector

The simple decorrelating detector [5] is originated by finding a *linear* conditional maximum likelihood estimate (MLE) of the signal vector $\boldsymbol{\theta} = \mathbf{A} \cdot \mathbf{b}$ from the *conditional* PDF $p(\mathbf{x}|\boldsymbol{\theta})$ obtained from (3). It then detects the multiuser information bit $\mathbf{b}$ by directly making decision on the *linear* conditional MLE $\hat{\boldsymbol{\theta}} = \mathbf{P}^{-1} \cdot \mathbf{x}$, which is simply a linear matrix inverse filtering operation on the data $\mathbf{x}$. The outputs of the multiuser decorrelator can be written as,

$$\mathbf{z} = \mathbf{P}^{-1} \cdot \mathbf{x} = \mathbf{A} \cdot \mathbf{b} + \mathbf{v}\,, \tag{4}$$

with $\mathbf{v} \sim \mathcal{N}(\mathbf{0}, \sigma^2 \mathbf{P}^{-1})$ being the colored Gaussian noise with a *different* covariance matrix.

From (4) we can see that the signal bits are separated. The detector then makes decision from,

$$\hat{\mathbf{b}} = \text{sign}(\mathbf{z})\,. \tag{5}$$

This detector has the advantage of structural simplicity. It is also near-far resistant. But a potential problem associated with this detector is that noise is enhanced by the $\mathbf{P}^{-1}$ inverse filtering. We show that this detector has its limited performance from the following simple analysis. Content-Length: 19623 X-Lines: 461 Status: O

Assume that we are interested in getting the probability of error expression of the kth user of the decorrelating detector in (5), where vector $\mathbf{z}$ is defined in (4) and $\mathbf{A}\,\mathbf{b}$ is assumed fixed. We can then re-arrange the order of the components of data vector $\mathbf{z}$ in (4) as following,

$$\mathbf{z} \triangleq \begin{bmatrix} z_k \\ \underline{\mathbf{z}}_k \end{bmatrix} = \begin{bmatrix} \sqrt{a_k}\, b_k \\ \mathbf{A}_k\, \underline{\mathbf{b}}_k \end{bmatrix} + \begin{bmatrix} v_k \\ \underline{\mathbf{v}}_k \end{bmatrix}, \tag{6}$$

where $\underline{\mathbf{b}}_k$ is a $(K-1)$ dimensional vector constructured from the *original* K dimensional vector $\mathbf{b}$ with its kth component removed; $\mathbf{A}_k$ is a $(K-1)\times(K-1)$ matrix constructured from the *original* $K \times K$ dimensional matrix $\mathbf{A}$ with row and column associated with the kth user removed. Similar notations also apply to $\underline{\mathbf{z}}_k$, $\underline{\mathbf{v}}_k$, $\underline{\boldsymbol{\rho}}_k$, and $\mathbf{P}_k$ used in the later sections. When $\mathbf{A}\,\mathbf{b}$ is given and fixed, we have,

$$\begin{bmatrix} z_k \\ \underline{\mathbf{z}}_k \end{bmatrix} \sim \mathcal{N}\left(\begin{bmatrix} \sqrt{a_k}\, b_k \\ \mathbf{A}_k\, \underline{\mathbf{b}}_k \end{bmatrix}, \sigma^2 \mathbf{P}^{-1} \right). \tag{7}$$

Note the fact that

$$\mathbf{P}^{-1} = \begin{bmatrix} 1 & \underline{\rho}_k^T \\ \underline{\rho}_k & \mathbf{P}_k \end{bmatrix}^{-1}$$

$$= \begin{bmatrix} \frac{1}{1-\mathbf{P}_k^{-1}\underline{\rho}_k} & -\frac{\underline{\rho}_k^T \mathbf{P}_k^{-1}}{1-\underline{\rho}_k^T \mathbf{P}_k^{-1}\underline{\rho}_k} \\ \underline{\rho}_k^T)^{-1}\underline{\rho}_k & (\mathbf{P}_k - \underline{\rho}_k \underline{\rho}_k^T)^{-1} \end{bmatrix}$$

Hence, for a given $\mathbf{A}\,\mathbf{b}$, $z_k \sim \mathcal{N}\left(\sqrt{a_k}\,b_k,\ \frac{\sigma^2}{1-\underline{\rho}_k^T \mathbf{P}_k^{-1}\underline{\rho}_k}\right)$, probability of error of the kth user can be easily found as,

$$\begin{aligned} P_e(k) &= P\{z_k > 0 \,|\, b_k = -1\}\ P\{b_k = -1\} + \\ &\quad P\{z_k < 0 \,|\, b_k = -+\}\ P\{b_k = +1\} \\ &= \sqrt{\frac{a_k\,(1-\underline{\rho}_k^T \mathbf{P}_k^{-1}\underline{\rho}_k)}{\sigma^2}} \leq Q\left(\sqrt{\frac{a_k}{\sigma^2}}\right), \end{aligned} \tag{8}$$

where $Q(x) = \int_x^\infty \frac{1}{\sqrt{2\,\pi}} e^{-t^2/2}\,dt$, and we assume that $P\{b_k = +1\} = P\{b_k = -1\} = 1/2$.

Note that in (8), the matrix $\mathbf{P}_k$ is a $(K-1)\times(K-1)$ matrix, constructed from $\mathbf{P}$ matrix after removing the contribution of the kth user. Matrix $\mathbf{P}_k$ is positive definite, since it is a sub-matrix of the positive definite matrix $\mathbf{P}$. Therefore the inequality $0 < (1-\underline{\rho}_k^T \mathbf{P}_k^{-1}\underline{\rho}_k) \leq 1$ will always hold, with the equality holds if and only if $\mathbf{P}$ is a diagonal matrix. This corresponds to the case of using a set of perfect orthonormal signature waveforms. Hence, the performance of the decorrelating detector in (5) will always worse than the BPSK limit, as shown in the inequality in (8). The near-far resistance of the decorrelating detector can be easily seen from its $P_e(k)$ expression in (8), since $P_e(k)$ is invariant to $\mathbf{A}_k$.

We further notice the following fact that the above decorrelating detector is also a linear estimate-based detector. Part of its limited performance is due to the fact that linear estimate $\hat{\boldsymbol{\theta}} = \mathbf{P}^{-1}\mathbf{x}$ is based on the *conditional* PDF $p(\mathbf{x}|\boldsymbol{\theta})$. Therefore, we can expect to further improve its detection performance and maintain its linear feature, by incorporating the joint statistics of both $\boldsymbol{\theta}$ and $\mathbf{x}$ into the estimate as demonstrated in the following linear minimum mean squared error (LMMSE) estimate-based detector.

3.2 Linear Minimum Mean Square Error (LMMSE) Estimate-based Multiuser Detector

It is well known that among the linear class of estimates, LMMSE estimate exhibits the minimum mean squared estimation error. Therefore we can improve the detection performance of the above *linear* decorrelating detector by deriving a LMMSE estimate-based multiuser detector. Specifically, let us rewrite the matched filter outputs in (3) as,

$$\mathbf{x} = \mathbf{P}\,\mathbf{A}\,\mathbf{b} + \mathbf{n} = \mathbf{P}\,\boldsymbol{\theta} + \mathbf{n}\,. \tag{9}$$

We assume that all the components of the random multiuser information bit $\mathbf{b}$ are independent and identically distributed (i.i.d.) with zero mean and unit variance. Even further, the random vector $\boldsymbol{\theta}$ and noise vector $\mathbf{n}$ are statistically independent. For most communication applications, these assumptions are reasonable ones. We then define a new random vector as follows,

$$\mathbf{y} \triangleq \begin{bmatrix} \boldsymbol{\theta} \\ \mathbf{x} \end{bmatrix} = \begin{bmatrix} \mathbf{A}\,\mathbf{b} \\ \mathbf{x} \end{bmatrix} = \underbrace{\begin{bmatrix} \mathbf{A} & \mathbf{0} \\ \mathbf{P}\,\mathbf{A} & \mathbf{I} \end{bmatrix}}_{\mathbf{H}} \cdot \begin{bmatrix} \mathbf{b} \\ \mathbf{n} \end{bmatrix}.$$

The expectation and covariance matrix of the new vector $\mathbf{y}$ can be found as,

$$\begin{aligned} & E(\mathbf{y}) = \mathbf{0}\,, \\ & \operatorname{cov}(\mathbf{y}) \;= \mathbf{H}\,\operatorname{cov}\left(\begin{bmatrix} \mathbf{b} \\ \mathbf{n} \end{bmatrix}\right)\mathbf{H}^T \\ & \qquad\quad = \begin{bmatrix} \mathbf{A}^2 & \mathbf{A}^2\mathbf{P} \\ \mathbf{P}\,\mathbf{A}^2 & \mathbf{P}\,\mathbf{A}^2\mathbf{P} + \sigma^2\mathbf{P} \end{bmatrix} \\ & \qquad\quad \triangleq \begin{bmatrix} \sum_{\boldsymbol{\theta}\boldsymbol{\theta}} & \sum_{\boldsymbol{\theta}\mathbf{x}} \\ \sum_{\mathbf{x}\boldsymbol{\theta}} & \sum_{\mathbf{x}\mathbf{x}} \end{bmatrix}. \end{aligned}$$

Then LMMSE estimate of $\boldsymbol{\theta}$ can be formed from the following [8, 9],

$$\begin{aligned} \hat{\boldsymbol{\theta}}_{LMMSE} \;&= E(\boldsymbol{\theta}) + \sum_{\boldsymbol{\theta}\mathbf{x}} \sum_{\mathbf{x}\mathbf{x}}^{-1} (\mathbf{x} - E(\mathbf{x})) \\ &= \sum_{\boldsymbol{\theta}\mathbf{x}} \sum_{\mathbf{x}\mathbf{x}}^{-1} \cdot \mathbf{x} \\ &= \underbrace{\left(\mathbf{P} + \sigma^2\,\mathbf{A}^{-2}\right)^{-1}}_{\mathbf{W}} \cdot \mathbf{x}\,. \end{aligned} \tag{10}$$

The LMMSE estimate-bsaed multiuser detector makes its decision based on the decision rule,

$$\hat{\mathbf{b}} = \operatorname{sign}\left(\hat{\boldsymbol{\theta}}_{LMMSE}\right). \tag{11}$$

Note that the diagonal matrix $\sigma^2 \mathbf{A}^{-2}$ involved in $\mathbf{W}$ of (10) is actually the inverse SNR matrix, i. e.

$$\sigma^2 \mathbf{A}^{-2} = \begin{bmatrix} a_1/\sigma^2 & 0 & \cdots & 0 \\ 0 & a_2/\sigma^2 & \cdots & 0 \\ \vdots & \vdots & \ddots & \vdots \\ 0 & 0 & \cdots & a_K/\sigma^2 \end{bmatrix}^{-1} \tag{12}$$

When the interferences of other users are small compared to the noise level, $\mathbf{W}$ reduces into a *diagonal* matrix, or $\mathbf{W} = (\mathbf{P} + \sigma^2 \mathbf{A}^{-2})^{-1} \approx (\mathbf{I} + \sigma^2 \mathbf{A}^{-2})^{-1}$. In this case, LMMSE detector has the same performance as that of the single user detector, which is the BPSK limit. When the interference levels are very large compared to the noise level, then $\mathbf{W} = (\mathbf{P} + \sigma^2 \mathbf{A}^{-2})^{-1} \approx \mathbf{P}^{-1}$, LMMSE detector's performance is compariable to that of the decorrelating detector. Therefore, the overall performance of LMMSE detector is better than that of the decorrelating detector. Even further, we can calculate the probability of error of the kth user based on the following observation.

We arrange the order of all the users such that $\boldsymbol{\theta}^T = [\ \theta_k \quad \underline{\boldsymbol{\theta}}_k^T\ ]$. We then decompose the above derived $\hat{\boldsymbol{\theta}}_{LMMSE}$ as follows,

$$\begin{aligned} \hat{\boldsymbol{\theta}}_{LMMSE} &= \mathbf{W}\,\mathbf{x} = (\mathbf{P} + \sigma^2 \mathbf{A}^{-2})^{-1}\,\mathbf{x} \\ &= (\mathbf{P}\,\sigma^2 \mathbf{A}^{-2})^{-1} \cdot (\mathbf{P}\,\mathbf{A}\,\mathbf{b} + \mathbf{n}) \\ &= \boldsymbol{\theta} - \sigma^2 \mathbf{W}\,\mathbf{A}^{-1}\,\mathbf{b} + \mathbf{W}\,\mathbf{n} \\ &= \boldsymbol{\theta} + \mathbf{e} \end{aligned} \tag{13}$$

where the estimation error, $\mathbf{e} = -\sigma^2 \mathbf{W}\,\mathbf{A}^{-1}\,\mathbf{b} + \mathbf{W}\,\mathbf{n}$, contains both *bias* and noise components. We will notice later that the improved performance of the LMMSE detector is achieved by trade-off a little bias for less noise variance, which finally results in less overall mean squared error (MSE).

For a given information bit $\mathbf{b}$, LMMSE detector of (10) makes an errorous decision on the kth user's information bit b_k whenever,

$$\text{OR} \begin{matrix} e_k < -\sqrt{a_k};\ \text{when } b_k = +1, \\ e_k > +\sqrt{a_k};\ \text{when } b_k = -1. \end{matrix}$$

Therefore, the probability of error for the kth user can be expressed as,

$$\begin{aligned}
P_e(k) = \; & P_e\left(k \,|\, b_k, \underline{\mathbf{b}}_k\right) P(b_k)\, P\left(\underline{\mathbf{b}}_k\right) \\
= \; & P(e_k > +\sqrt{a_k} \,|\, b_k = -1, \underline{\mathbf{b}}_k)\, P(b_k = -1) + \\
& P(e_k < -\sqrt{a_k} \,|\, b_k = +1, \underline{\mathbf{b}}_k)\, P(b_k = +1)\, P\left(\underline{\mathbf{b}}_k\right) \\
= \; & \tfrac{1}{2}\left\{P(e_k > +\sqrt{a_k} \,|\, b_k = -1, \underline{\mathbf{b}}_k) + \right. \\
& \left. P(e_k < -\sqrt{a_k} \,|\, b_k = +1, \underline{\mathbf{b}}_k)\right\} \cdot P\left(\underline{\mathbf{b}}_k\right) \\
= \; & \tfrac{1}{2^K} \sum_{\underline{\mathbf{b}}_k} \left[Q\left(\tfrac{\sqrt{a_k} - R_k(b_k=-1, \underline{\mathbf{b}}_k)}{\sigma_k} \right) + Q\left(\tfrac{\sqrt{a_k} + R_k(b_k=+1, \underline{\mathbf{b}}_k)}{\sigma_k} \right) \right],
\end{aligned} \tag{14}$$

where $R_k(\cdot) = -\sigma^2\, \mathbf{w}_k^T\, \mathbf{A}^{-1}\, \mathbf{b}$, $\sigma_k^2 = \sigma^2\, \mathbf{w}_k^T\, \mathbf{P}\, \mathbf{w}_k$, and $\mathbf{w}_k^T$ is the kth row of $\mathbf{W}$ matrix. Or,

$$\mathbf{w}_k^T = \frac{\left[\; 1 \quad -\underline{\boldsymbol{\rho}}_k^T \left(\mathbf{P}_k + \sigma^2\, \mathbf{A}_k^{-2}\right)^{-1} \;\right]}{1 + \sigma^2/a_k - \underline{\boldsymbol{\rho}}_k^T \left(\mathbf{P}_k + \sigma^2\, \mathbf{A}_k^{-2}\right)^{-1} \underline{\boldsymbol{\rho}}_k}.$$

We also verified the fact that under weak and strong interference conditions, the above error probability expression will reduce either into the single user BPSK limit or into that of the decorrelating detector as follows,

$$P_e(k) = \begin{cases} Q\left(\dfrac{\sqrt{a_k}}{\sigma}\right), & \text{small interferences} \\ Q\left(\dfrac{\sqrt{a_k\left(1 - \underline{\boldsymbol{\rho}}_k^T\, \mathbf{P}_k^{-1}\, \underline{\boldsymbol{\rho}}_k\right)}}{\sigma}\right), & \text{strong interferences} \end{cases}$$

For the case of $K = 2$, the above expression can be simplified as,

$$P_e(1) = \frac{1}{2}\left\{ Q\left(\frac{\sqrt{a_1} - R_1(-1,+1)}{\sigma_1}\right) + \left(\frac{\sqrt{a_1} + R_1(-1,-1)}{\sigma_1}\right)\right\}, \tag{15}$$

with

$$R_1(-1,+1) = \sigma^2\, \frac{\left(1 + \sigma^2/a_2\right)/\sqrt{a_1} + \rho/\sqrt{a_2}}{(1 + \sigma^2/a_1)(1 + \sigma^2/a_2) - \rho^2},$$

$$R_1(-1,-1) = \sigma^2\, \frac{\left(1 + \sigma^2/a_2\right)/\sqrt{a_1} - \rho/\sqrt{a_2}}{(1 + \sigma^2/a_1)(1 + \sigma^2/a_2) - \rho^2},$$

$$\sigma_1 = \sigma\, \frac{\sqrt{\left((1 + \sigma^2/a_2) - \rho^2\right)^2 + \rho^2\left(1 - \rho^2\right)}}{(1 + \sigma^2/a_1)(1 + \sigma^2/a_2) - \rho^2}.$$

We can also easily verify that the following facts,

$$\lim_{\frac{a_2}{\sigma^2} \ll 1} P_e(1) = Q\left(\frac{\sqrt{a_1}}{\sigma}\right), \qquad \text{BPSK limit}$$

$$\lim_{\frac{a_2}{\sigma^2} \gg 1} P_e(1) = Q\left(\frac{\sqrt{a_1\,(1-\rho^2)}}{\sigma}\right), \text{ decorrelating detector}$$

3.3 Adaptive Bootstrap Multiuser Detector

In [2], an adaptive bootstrap multiuser detector was proposed by minimizing the correlation between the canceler output of the desired user, say z_k, and the hard-limiter decision on the canceler output of other users, say $\text{sign}(\underline{\mathbf{z}}_k)$. That is, the matrix $\mathbf{W}$, with its diagonal elements being zeros, is adaptively chosen such that

$$E\{\, z_k \,\text{sign}(\underline{\mathbf{z}}_k)\,\} = \mathbf{0}\,, \qquad k = 1, 2, \ldots, K\,, \tag{16}$$

where $\mathbf{z} = \left[\; z_k \quad \underline{\mathbf{z}}_k^T \;\right]^T = (\mathbf{I} - \mathbf{W})\,\mathbf{x}$. The adaptive version of the alogrithm updates the kth column of $\mathbf{W}$ with its kth zero-element removed, say $\underline{\mathbf{w}}_k$, as follows,

$$\underline{\mathbf{w}}_k(i+1) = \underline{\mathbf{w}}_k(i) + \mu\, z_k\, \text{sign}(\underline{\mathbf{z}}_k)\,, \quad k = 1, 2, \ldots, K\,. \tag{17}$$

Once matrix $\mathbf{W}$ is obtained adaptively, the bootstrap detector makes its decision based on the decision rule

$$\hat{\mathbf{b}} = \text{sign}\,(\,(\mathbf{I} - \mathbf{W})\,\mathbf{x}\,)\,.$$

The probability of error of the kth user, using an adaptive bootstrap multiuser detector, was calculated in [2] as,

$$P_e(k) = \frac{1}{2^{K-1}} \sum_{\underline{\mathbf{b}}_k} Q\,(\,\xi_k\,)\,, \tag{18}$$

with $\xi_k = \dfrac{\sqrt{a_k}\,(1 - \underline{\boldsymbol{\rho}}_k^T\,\mathbf{P}_k^{-1}\,\underline{\boldsymbol{\rho}}_k - \underline{\boldsymbol{\delta}}_k^T\,\mathbf{P}_k^{-1}\,\underline{\boldsymbol{\rho}}_k\,) + \underline{\boldsymbol{\delta}}_k^T\,\mathbf{A}_k\,\underline{\mathbf{b}}_k}{\sigma\sqrt{1 - \underline{\boldsymbol{\rho}}_k^T\,\mathbf{P}_k^{-1}\,\underline{\boldsymbol{\rho}}_k + \underline{\boldsymbol{\delta}}_k^T\,\mathbf{P}_k^{-1}\,\underline{\boldsymbol{\rho}}_k}}$

4 Numerical evaluations and computer simulations

Numerical evaluation and computer simulation results in this section further confirm our above derivations. Note that implementation of the LMMSE detector needs information on matrix $\mathbf{P}$ and SNR matrix of (11), but the adaptive bootstrap multiuser detector developed by BarNess et. al. [2] can achieve the same performance as that of the LMMSE detector without these information.

In the following figures, we show the performance comparison of the decorrelating detector, the LMMSE detector, and the adaptive bootstrap multiuser detector for high, medium, and low capacity cases. We also plot the BPSK limit as a reference lower bound on the performance. It can be seen that there is an equivalence between the LMMSE detector and the adaptive bootstrap multiuser detector. The improved performances of both the LMMSE and the adaptive bootstrap multiuser detectors are obtained by the idea of trade-off a little bias for less noise variance, which finally results in an overall less mean squared error (MSE). And the adaptive bootstrap multiuser detector provides a practical implementation of the LMMSE detector.

5 Conclusions

We investigate the performance of the *linear* minimum mean squared error (LMMSE) estimate-based detector and the adaptive bootstrap multiuser detector. Numerical evaluation and computer simulations verify our detailed analysis on the performance of the LMMSE detector. The theoretic analysis and computer simulations also confirm the inherent relationship between the LMMSE and adaptive bootstrap detectors. For the consideration of practical implementation, the adaptive bootstrap multiuser detector, which does not need the knowledge of the multiusers' signal-to-noise (SNR) matrix, is preferred for CDMA communications applications.

References

[1] U. Madhow, and M. L. Honig, "MMSE Interference Suppression for Direct-Sequence Spread-Spectrum CDMA," *IEEE Trans. on Comm.*, vol. 42, no. 12, Dec. 1994.

[2] Y. Bar-Ness, and J. Punt, "Adaptive Bootstrap CDMA Multiuser Detector," to appear in special issue of *Signal Separation and Interference Cancellation for Personal, Indoor and Mobile Radio Communication,* Wireless Personal Communications, An International Journal, Kluwer Academic Publishers.

[3] Y. Bar-Ness, and N. Sezgin, "Adaptive multiuser bootstrapped decorrelating CDMA detector for one-shot asynchronous unknown channel," In proceedings of ICASSP-95.

[4] S. Verdú, "Minimum Probability of Error for Asynchronous Gaussian Multiple-Access Channel," *IEEE Trans. on Information Theory,* vol. IT-32, no. 1, pp. 85–96, Jan. 1986.

[5] R. Lupas and S. Verdú, "Linear Multiuser Detector for synchronous code division multiple access channels," *IEEE Trans. on Information Theory,* vol. IT-35, no. 1, pp. 123-136, Jan. 1989.

[6] M. K. Varanasi and B. Aazhang, "Near-Optimum Detection in Synchronous Code-Division Multiple-Access Systems," *IEEE Trans. on Commun.*, vol. 39, no. 5, pp. 725–736, May. 1991.

[7] H. Ge, and Y. Bar-Ness, "Multi-shot Multiuser Detector for Asynchronous CDMA Channel," Proc. of the 30th Annual Conf. on Information Sciences and Systems, Princeton, New Jersey, Mar., 1996.

[8] P. J. Bickel, and K. J. Doksum, *Mathematical Statistics: Basic Ideas and Selected Topics,* Prentice Hall, Englewood Cliffs, New Jersey, 1977.

[9] L. L. Scharf, *Statistical Signal Processing: Detection, Estimation, and Time Series Analysis,* Addison-Wesley Publishing Company, 1990.

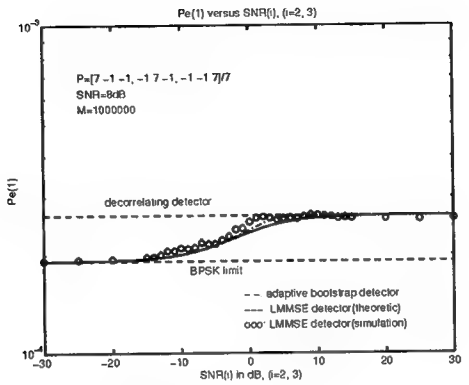

(a). High capacity case

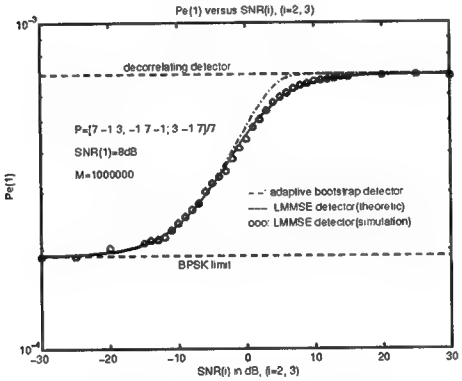

(b). Medium capacity case

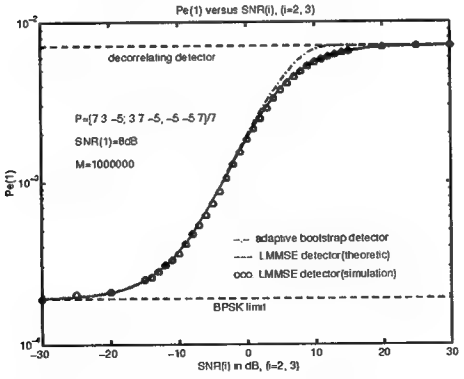

(c). Low capacity case.

Figure 1: Performance of the LMMSE detector and the adaptive bootstrap detector in multi-user CDMA system. Also shown in figure are the results of the decorrelating detector and the BPSK limit. Parameters used: $SNR_1 = 8\ dB$, $K = 3$, $M = 1000000$ independent trials.

Appendix C

Adaptive Multiuser Bootstrapped Decorrelating CDMA Detector for One-shot Asynchronous Unknown Channels *

Yeheskel Bar-Ness Nadir Sezgin

Abstract

Vast research was recently performed on signal detection of multiuser Code Division Multiple Access (CDMA). Particularly for uplink (users to base station) the signals are asynchronous and the near-far problem is an important issue to deal with. All near-far resistant detectors, adaptive or non-adaptive, assume knowledge of the relative delays of the different users' signals. Among these are the one-shot detectors suggested by Verdu. In this paper we suggest an adaptive algorithm to decorrelate the outputs of the one shot matched filters that assumes no knowledge of the relative delay. The performance of this approach is shown to be better than the non-adaptive "zero-forcing" method previously used and which implements linear transformation via the inverse of matched filters' output cross-correlation. For simplicity a two-user case is presented. Extension to a higher number of users is relatively simple.

I. INTRODUCTION

CDMA is considered to be a promising multiplexing method for multiuser personal, mobile and indoor communications. One of the problems a designer of such a system is faced with is the so called "near-far problem," resulting from excessive Multiple Access Interference (MAI) energy from nearby users, compared with the desired user's signal energy. Power control, that is, adjustment of transmitter power, depending on its location and the signal energies of the other users, has been suggested as a solution to this problem. But it requires a significant reduction in the signal energies of the strong users in order for the weaker users to achieve reliable communication. This results in an overall reduction in communication ranges.

An optimum near-far resistant multiuser detector, without a need for power control has been proposed by Verdu[1]. Its complexity, however, is exponen-

*This work was partially supported by a grant from Rome Air Force Lab (AFSC, Griffss Air Force Base) under the contract F30602-94-C-0135

tial in terms of the number of users, which makes it unsuitable for practical situations. Later, a sub-optimum detector whose complexity is linear was proposed[2]. However this detector, like Verdu's optimum detector, needs the knowledge of user signal energies.

Adaptive near-far resistant CDMA detectors that do not need the knowledge of the received signal energies have been developed at NJIT in recent years[3–6]. All these detectors assume a non-fading multiuser environment.

All asynchronous detectors (except [6]), adaptive or non-adaptive, assume knowledge of the different users signals' relative delays.

In this paper we propose to use the decorrelation algorithm for separation of the user signals obtained at the outputs of Verdu's one-shot bank of matched filters. For this we do not require knowledge of the relative delays.

In the next section we present the system model and drive the relation between the matched filters' output and the users data. Since the delays are not known, the cross-coupling matrix is considered unknown. The decorrelating algorithm and the decorrelator's steady-state weights and outputs are given in Section III. In Section IV. we discuss performance evaluation and in Section V. we present an example and results.

II. SYSTEM MODEL

For the asynchronous multiuser, the equivalent low-pass signal at the input of the matched filter bank is given by,

$$r(t) = \sum_{k=1}^{K} \sum_{i} b_k(i) \sqrt{a_k(i)} s_k(t + T - \tau_k) + n(t), \tag{1}$$

where K is the number of users, $\alpha_k, \theta_k, b_k, s_k$ and τ_k are the signal amplitude, carrier phase shift, user bit, signature waveform and the relative delay of the kth user. $n(t)$ is the zero mean AWGN, with a two-sided power spectral density of $N_0/2$.

For the sake of simplicity we will restrict ourselves to two users only. Extension to a higher number is relatively simple.

Representing the signal of Eq. (1) in one-shot of the ith bit of user one, and without loss of generality, letting $i = 0$, we write,

$$\begin{aligned} r(t) &= \sqrt{a_1} s_1(t) b_1(0) + \sqrt{a_2 \epsilon_2} \frac{1}{\sqrt{\epsilon_2}} s_2^L(t) b_2(-1) \\ &\quad + \sqrt{a_2(1-\epsilon_2)} \frac{1}{\sqrt{1-\epsilon_2}} s_2^R(t) b_2(0) + n(t), \end{aligned} \tag{2}$$

where $0 \leq \tau_2 \leq T$ is considered unknown or estimated with an error, and;

$$s_2^L(t) = \begin{cases} s_2(t + T - \tau_2) & \text{if } 0 \leq t \leq \tau_2 \\ 0 & \text{if } \tau_2 < t \leq T \end{cases}$$

$$s_2^R(t) = \begin{cases} 0 & \text{if } 0 \le t \le \tau_2 \\ s_2(t-\tau_2) & \text{if } \tau_2 < t \le T \end{cases}$$

$$\epsilon_2 = \int_0^{\tau_2} s_2^2(t+T-\tau_2)dt. \tag{3}$$

As shown in Fig. 1, we apply $r(t)$ to a bank of filters by using as a second input $s_1(t), s_2^{L'}(t), s_2^{R'}(t)$, respectively, the signature function of Eq. (3) extended to τ_2' instead of τ_2, normalized by ϵ_2' instead of ϵ_2.

The output of the first filter,

$$x_1'(0) = \sqrt{a_1}b_1(0) + \sqrt{a_2\epsilon_2}\rho_{12}b_2(0) + n_1(0), \tag{4}$$

where $n_1(0) = \int_0^T n(t)s_1(t)dt$ is a zero-mean Gaussian variable with variance of $N_0/2$, and

$$\rho_{21} = \frac{1}{\sqrt{\epsilon_2}}\int_0^T s_1(t)s_2(t+T-\tau_2)dt$$

$$\rho_{12} = \frac{1}{\sqrt{1-\epsilon_2}}\int_0^T s_1(t)s_2(t-\tau_2)dt. \tag{5}$$

The subscript in $x'(0)$ indicates that we are using zero bit of user one in our one-shot.

The output of the second filter is given by,

$$\begin{aligned} x_2'(0) &= \frac{1}{\sqrt{\epsilon_2'}}\int_0^T r(t)s_2^{L'}(t)dt \\ &= \sqrt{a_1}\rho_{21}^{L'}b_1(0) + \sqrt{a_2\epsilon_2}\rho_{22}^{L'L}b_2(-1) \\ &\quad + \sqrt{a_2(1-\epsilon_2)}\rho_{22}^{L'R}b_2(0) + n_2(0), \end{aligned} \tag{6}$$

where

$$\rho_{21}' = \frac{1}{\sqrt{\epsilon_2'}}\int_0^T s_1(t)s_2(t+T-\tau_2')dt$$

$$\rho_{22}^{L'L} = \frac{1}{\sqrt{\epsilon_2'\epsilon_2}}\int_0^T s_2(t+T-\tau_2)s_2(t+T-\tau_2')dt$$

$$\rho_{22}^{L'R} = \frac{1}{\sqrt{\epsilon_2'(1-\epsilon_2)}}\int_0^T s_2(t-\tau_2)s_2(t+T-\tau_2')dt$$

and

$$n_2(0) = \frac{1}{\sqrt{\epsilon_2'}}\int_0^T n(t)s_2(t+T-\tau_2')dt. \tag{7}$$

The output of the third filter is given by,

$$\begin{aligned} x_3'(0) &= \frac{1}{\sqrt{1-\epsilon_2'}} \int_0^T r(t) s_2^{R'}(t) dt \\ &= \sqrt{a_1}\rho_{12}' b_1(0) + \sqrt{a_2\epsilon_2}\rho_{22}^{R'L} b_2(-1) \\ &\quad + \sqrt{a_2(1-\epsilon_2)}\rho_{22}^{R'R} b_2(0) + n_3(0), \end{aligned} \tag{8}$$

where

$$\begin{aligned} \rho_{12}' &= \frac{1}{\sqrt{1-\epsilon_2'}} \int_0^T s_1(t) s_2(t-\tau_2') dt \\ \rho_{22}^{R'L} &= \frac{1}{\sqrt{(1-\epsilon_2')\epsilon_2}} \int_0^T s_2(t+T-\tau_2) s_2(t-\tau_2') dt \\ \rho_{22}^{R'R} &= \frac{1}{\sqrt{(1-\epsilon_2')(1-\epsilon_2)}} \int_0^T s_2(t-\tau_2) s_2(t-\tau_2') dt \end{aligned}$$

and

$$n_3(0) = \frac{1}{\sqrt{1-\epsilon_2'}} \int_0^T n(t) s_2(t-\tau_2') dt. \tag{9}$$

Combining, Eqs. (4), (6) and (8) in matrix form,

$$\mathbf{x}'(0) = \mathbf{P}^T \mathbf{A} \mathbf{b}(0) + \mathbf{n}(0), \tag{10}$$

where

$$\mathbf{P}^T = \begin{bmatrix} 1 & \rho_{21} & \rho_{12} \\ \rho_{21}' & \rho_{22}^{L'L} & \rho_{22}^{L'R} \\ \rho_{12}' & \rho_{22}^{R'L} & \rho_{22}^{R'R} \end{bmatrix}, \tag{11}$$

$\mathbf{A} = \text{diag}[\sqrt{a_1}, \sqrt{a_2\epsilon_2}, \sqrt{a_2(1-\epsilon_2)}]$ and
$\mathbf{b}(0) = [b_1(0), b_2(-1), b_2(0)]^T$. $\mathbf{n}(t)$ is zero-mean Gaussian vector with covariance,

$$\mathbf{R}_n = \begin{bmatrix} 1 & \rho_{21}' & \rho_{12}' \\ \rho_{21}' & 1 & 0 \\ \rho_{12}' & 0 & 1 \end{bmatrix} \frac{N_0}{2}. \tag{12}$$

2.1. Known Delay

If the relative delay τ_2 is known then we choose $\tau_2' = \tau_2$, and as a result $\rho_{21}' = \rho_{21}, \rho_{12}' = \rho_{12}, \rho_{22}^{L'L} = \rho_{22}^{R'R} = 1$, $\rho_{22}^{R'L} = \rho_{22}^{L'R} = 0$ and $\epsilon_2' = \epsilon_2 = 1$. The matrix $\mathbf{P}_D$ is known. If $|\rho_{21}| + |\rho_{12}| < 1$ then $\mathbf{P}_D$ is invertible. A simple linear transformation by $\mathbf{P}_D^{-1}$ results in,

$$\mathbf{z}(0) = \mathbf{A}\mathbf{b}(0) + \mathbf{P}_D^{-T}\mathbf{n}(0), \tag{13}$$

where $\mathbf{P}_D$ is the modified cross-coupling matrix. Since the components of $\mathbf{b}(0)$ are assumed uncorrelated then the components of $\mathbf{z}(0)$ are also so.

III. THE DECORRELATING ALGORITHM

3.1. Unknown Delay

For this case the matrix $\mathbf{P}$ is unknown. We propose to use an adaptive algorithm to decorrelate the outputs of bank of matched filters (see Fig. 2). From this figure we have

$$\mathbf{z}'(0) = \mathbf{x}'(0) - \mathbf{W}^T\mathbf{x}'(0), \tag{14}$$

where

$$\mathbf{W} = \begin{bmatrix} 0 & w_{12} & w_{13} \\ w_{21} & 0 & w_{23} \\ w_{31} & w_{32} & 0 \end{bmatrix}. \tag{15}$$

The kth output of the decorrelator can be expressed as,

$$z_k = x_k - \mathbf{w}_k^T\mathbf{x}_k \tag{16}$$

where $\mathbf{w}_k$ is the kth column of $\mathbf{W}$ with the element w_{kk} deleted and $\mathbf{x}_k$ is the vector obtained from $\mathbf{x}$ by deleting x_k.

The multidimensional decorrelator is the same as that frequently used in neural networks and other applications of signal separation[7–8].

For controlling the weights, we use the steepest descent algorithm which simultaneously reduces the absolute value of the correlation between the outputs of the decorrelator and the decision on all other outputs. That is, the weight, w_{lk} is controlled by the recursion,

$$w_{ml} \leftarrow w_{ml} - \mu(z_l\mathrm{sgn}(z_m)), \quad 1 \le l, m < 3, \quad l \ne m. \tag{17}$$

Recursion in Eq. (17), reaches steady-state in the mean when $E\{z_l\mathrm{sgn}(z_m)\} = 0$. Note that w_{21}, for example, is used to cancel residue of $b_2(-1)$ at the output of z_1. It will settle down only when that residue (being correlated with $\hat{b}_2(-1)$) is zero. But any reduction of $b_2(-1)$ at z_1 will improve $b_1(0)$ (smaller error) and hence, will be more effective in reducing the residue of $b_1(0)$ at z_2 and z_3 through the control weights w_{12} and w_{13}. Therefore, the process of residue cancellation is enhanced successively which justify, using the name "bootstrap" in the past.

In the notation of Eq. (16), we write Eq. (17) in vector form,

$$\mathbf{w}_k \leftarrow \mathbf{w}_k - \mu(z_k\mathrm{sgn}(\mathbf{z}_k)), \tag{18}$$

where again $\mathbf{z}_k$ is obtained from the column of $\mathbf{z}$ by deleting z_k. The steady state is reached if $E\{z_k\mathrm{sgn}(\mathbf{z}_k) = \mathbf{0}$ for $k = 1, 2, 3$.

Now, $\mathrm{sgn}(\mathbf{z}_k) = \hat{\mathbf{b}}_k$, and if we assume the SNR's are large enough such that the main contribution to the decorrelator output error is the multiuser interference, then $E\{z_k\hat{\mathbf{b}}_k\}$ can be approximated by,

$$\begin{aligned} E\{z_k\hat{\mathbf{b}}_k\} &= E\{z_k\hat{\mathbf{b}}_k\}(\mathbf{I} - 2\mathrm{Pr}(\hat{\mathbf{b}}_k \text{ in error})) \\ &= E\{z_k\hat{\mathbf{b}}_k\}(\mathbf{I} - 2P_{ek}). \end{aligned} \tag{19}$$

Equating (19) to zero and using (16) together with (10) we get,

$$E\{z_k\hat{\mathbf{b}}_k\} = E\{\rho_{kk}a_{kk}b_k + \boldsymbol{\rho}_k^T\mathbf{A}_k\mathbf{b}_k + n_k - \mathbf{w}_k^T\mathbf{x}_k\}\mathbf{b}_k = 0, \tag{20}$$

where ρ_{kk} is the kth term at the diagonal of $\mathbf{P}$, a_{kk} is the kth diagonal of $\mathbf{A}$, $\boldsymbol{\rho}_k$ is the kth column of $\mathbf{P}$ with its kth element deleted and so is $\mathbf{A}_k$.

3.2. Steady-State Weights and Decorrelator Output

Solving Eq. (20), we show in the Appendix that $E\{\mathbf{w}_k^T\mathbf{x}_k\mathbf{b}_k\} = \mathbf{A}_k\boldsymbol{\rho}_k$ We also show that, $E\{\mathbf{w}_k^T\mathbf{x}_k\mathbf{b}_k\} = \mathbf{A}_k\mathbf{P}_k\mathbf{W}_k$. Therefore, the steady-state weight resulting from the decorrelating algorithm is given by,

$$\mathbf{w}_k = \mathbf{P}_k^{-1}\boldsymbol{\rho}_k, \tag{21}$$

Substituting Eq. (21) in (16) with (A-2), we drive in the Appendix; Eq. (A-4), the decorrelator's steady-state outputs,

$$z_k = a_{kk}(\rho_{kk} - \boldsymbol{\rho}_k^T\mathbf{P}_k^{-T}\mathbf{r}_k)b_k + n_k - \boldsymbol{\rho}_k^T\mathbf{P}_k^{-T}\mathbf{n}_k. \tag{22}$$

where $\mathbf{P}_k$ is obtained from $\mathbf{P}$ by deleting the kth row and column, while $\mathbf{r}_k^T$ is the kth row without its kth element.

IV. PERFORMANCE EVALUATION

From Eq. (22) for user one, after combining the noise terms, we have,

$$z_1 = \sqrt{a_1}(1 - \boldsymbol{\rho}_1^T\mathbf{P}_1^{-T}\mathbf{r}_1)b_1 + \begin{bmatrix} 1 & \boldsymbol{\rho}_1^T \end{bmatrix}\begin{bmatrix} 1 & 0 \\ 0 & -\mathbf{P}_1^{-T} \end{bmatrix}\mathbf{n}. \tag{23}$$

Note that the decorrelating detector perfectly cancels the interfering signal energy. On the other hand, the desired user bit energy is modified by $(1 - \boldsymbol{\rho}_1^T\mathbf{P}_1^{-T}\mathbf{r}_1)$, and the noise variance is given by

$$\sigma_N^2 = \boldsymbol{\rho}_\epsilon^T\mathbf{R}^{-T}\mathbf{R}_n\mathbf{R}^{-1}\boldsymbol{\rho}_\epsilon\frac{N_0}{2}, \tag{24}$$

where $\boldsymbol{\rho}_\epsilon = \begin{bmatrix} 1 & \boldsymbol{\rho}_1^T \end{bmatrix}^T, \mathbf{R}^{-1} = \begin{bmatrix} 1 & 0 \\ 0 & -\mathbf{P}_1^{-T} \end{bmatrix}$ and $\mathbf{R}_n$ is the noise covariance matrix given in Eq. (12).

Let,

$$\gamma_1 = \frac{(1 - \boldsymbol{\rho}_1^T\mathbf{P}_1^{-1}\mathbf{r}_1)^2 a_1}{\sigma_N^2}. \tag{25}$$

The BER for binary PSK as a function of SNR is given by $Q(2\gamma_1)$, where $Q(x) = \frac{1}{\sqrt{2\pi}}\int_x^\infty e^{-t^2/2}dt$.

V. EXAMPLE AND RESULTS

In our numerical calculation and simulation, we assume $\epsilon_2 = 0.4, \rho_{21} = 0.2/\sqrt{0.4}, \rho_{12} = 0.6/\sqrt{0.6}$. If $\tau_2' < \tau_2$, then $\epsilon_2' < \epsilon_2$ (assumed 0.35) and hence the overlap of $s_2^{R'}$ with s_1 is larger than that of s_2^R. Therefore we take $\rho_{12}' = 0.25/\sqrt{0.35}$. With the same argument, $\rho_{21}' = 0.55/\sqrt{0.35}r, \rho_{22}^{L'L} = \sqrt{\epsilon_2'/\epsilon_2} = \sqrt{0.35/0.4}$ and $\rho_{22}^{R'R} = \sqrt{(1-\epsilon_2)/(1-\epsilon_2')} = \sqrt{0.6/0.65}$. Finally, $\rho_{22}^{R'L} = 0.05/\sqrt{(0.65)0.4}$. In summary,

$$\mathbf{P}^T = \begin{bmatrix} 1 & 0.3162 & 0.7746 \\ 0.3101 & 0.9354 & 0 \\ 0.9297 & 0.0981 & 0.9608 \end{bmatrix}. \tag{26}$$

Using matrix (26) the BER performance of both conventional and adaptive one-shot detectors is depicted in Figs. (3) and (4) for fixed interference, variable desired user energy and variable interference, fixed desired user energy respectively. In both figures, it can be observed that especially for high interfering energy the adaptive decorrelator, outperforms the conventional one.

Appendix

It is easy to show that, $E\{b_k\mathbf{b}_k\} = 0$,
$E\{(\boldsymbol{\rho}_k^T\mathbf{A}_k\mathbf{b}_k)\mathbf{b}_k\} = \mathbf{A}_k\boldsymbol{\rho}_k, E\{n_k\mathbf{b}_k\} = 0$, so that

$$E\{(\mathbf{w}_k^T\mathbf{x}_k)\mathbf{b}_k\} = \mathbf{A}_k\boldsymbol{\rho}_k. \tag{A-1}$$

From (10)

$$\begin{aligned} \mathbf{x}_k &= \begin{bmatrix} \mathbf{P}^T & \mathbf{r}_k \end{bmatrix} \begin{bmatrix} \mathbf{A}_k & 0 \\ 0 & a_{kk} \end{bmatrix} \begin{bmatrix} \mathbf{b} \\ b_k \end{bmatrix} + \mathbf{n}_k \quad (A-2) \\ &= \mathbf{P}_k^T\mathbf{A}_k\mathbf{b}_k + \mathbf{r}_k a_{kk} b_k + \mathbf{n}_k, \end{aligned}$$

Therefore,

$$E\{\mathbf{w}_k^T\mathbf{x}_k\mathbf{b}_k\} = \mathbf{A}_k\mathbf{P}_k\mathbf{w}_k. \tag{A-3}$$

From Eq. (16) together with Eq. (21),

$$\begin{aligned} z_k &= \rho_{kk}a_{kk}b_k + \boldsymbol{\rho}_k^T\mathbf{A}_k\mathbf{b}_k + n_k \\ &\quad -\boldsymbol{\rho}_k^T\mathbf{P}_k^{-T}(\mathbf{P}_k^T\mathbf{A}_k\mathbf{b}_k + \mathbf{r}_k a_{kk}b_k + \mathbf{n}_k) \qquad (A-4) \\ &= a_{kk}(\rho_{kk} - \boldsymbol{\rho}_k^T\mathbf{P}_k^{-T}\mathbf{r}_k)b_k + n_k - \boldsymbol{\rho}_k^T\mathbf{P}_k^{-T}\mathbf{n}_k. \end{aligned}$$

References

[1] S. Verdu, "Minimum Probability of Error for Asyncronous Gaussian Multiple Access Channels," IEEE Trans. on Inf. Theory, vol. IT-32, no. 1, pp. 85–96, Jan. 1986.

[2] M. K. Varanasi and B. Aazhang, "Near-optimum Detector in Synchronous Code Division Multiple Access Communications," IEEE Trans. on Comm., vol. COM-39, no. 5, pp. 725–736, May 1991.

[3] Z. Siveski, Y. Bar-Ness and D. W. Chen, "Adaptive Multiuser Detector for Synchronous CDMA Applications," 1994 Int'l Zurich Seminar on Digital Comm., ETH Zurich, Switzerland, May 1994.

[4] Y. Bar-Ness, Z. Siveski and D. W. Chen, "Bootstrapped Decorrelating Algorithm for Adaptive Interference Cancellation in Synchronous CDMA Systems," IEEE 3rd Int'l Symposium on Spread Spectrum Tech. and Appl., Ouly, Finland, July 1994.

[5] D. W. Chen, Z. Siveski and Y. Bar-Ness, "Synchronous Multiuser Detector with Soft Decision Adaptive Canceller," 28th Annual Conf. on Inf. Sci. and Sys., Princeton, NJ, March 1994.

[6] Y. Bar-Ness, D. W. Chen and Z. Siveski, "Adaptive Multiuser Bootstrapped Decorrelating CDMA Detector in Asynchronous Unknown Channels," Accepted to IEEE PIMRC'94, Delft, The Netherlands, Sept. 1994.

[7] A. Dinc and Y. Bar-Ness, "Convergence and Performance of three Different Structures of Bootsrapped Adaptive Algorithm for Multisignal Co-Channel Separation," Milcom '92, pp. 913–918, Oct. 92, San-Diego, CA.

[8] R. Kamel and Y. Bar-Ness, "Blind Decision Feedback Equalization Using Decorrelation Algorithm," Globecom '93 / Comm. Theory Mini Conference,

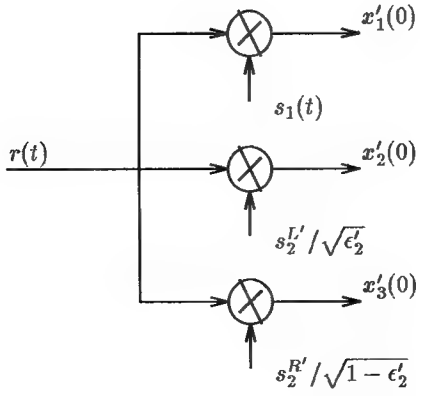

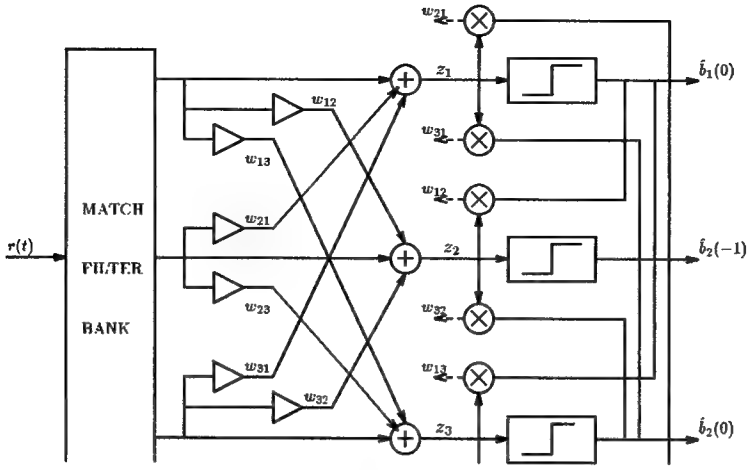

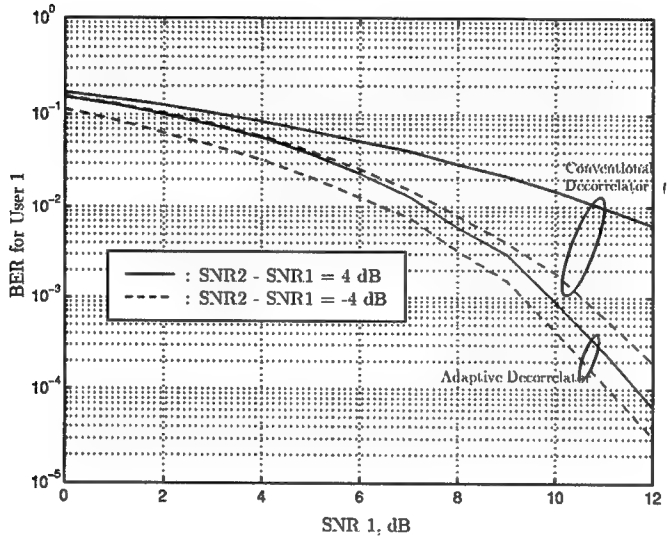

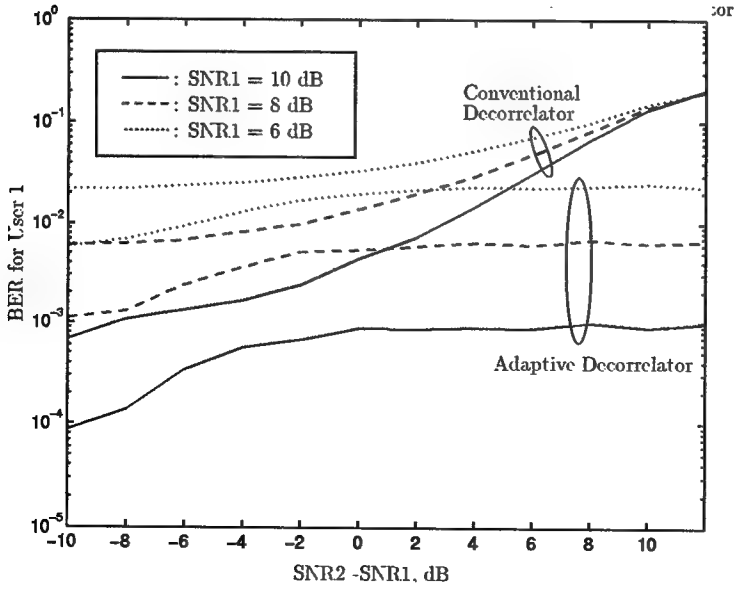

Fig. 4: Performance Comparison of Adaptive and Conventional Decorrelator for fixed SNR1 and variable Interference values.

Appendix D

Maximum Signal-to-noise Ratio Data Combining for One-shot Asynchronous Multiuser CDMA Detector *

Yeheskel Bar-Ness Nadir Sezgin

Abstract

Using a one-shot matched filter followed by a decorrelating detector, results in outputs corresponding to the main user and the left (earlier bit) and right (current bit) portion of the code of the other users. Due to reduced power, these outputs will result in a degradated probability of error. The purpose of this paper is to propose a method of combining for the data of the split code users. We suggest to use combining gain in proportion to the relative user delays. The resulting decorrelating detector always performs better than the split-output detector. Such diversity data combining eliminates the need for the multiple one-shot filters, one for each user.

I. INTRODUCTION

CDMA is considered to be a promising multiplexing method for multiuser personal, mobile and indoor communications. One of the problems a designer of such a system is faced with is the so called "near-far problem," resulting from excessive Multiple Access Interference (MAI) energy from nearby users, compared with the desired user's signal energy. Power control, that is, adjustment of transmitter power, depending on its location and the signal energies of the other users, has been suggested as a solution to this problem. But it requires a significant reduction in the signal energies of the strong users in order for the weaker users to achieve reliable communication. This results in an overall reduction in communication ranges.

An optimum near-far resistant multiuser detector, which does not need power control, has been proposed by Verdu[1]. Its complexity, however, is exponential in terms of the number of users, which makes it unsuitable for practical situations. Sub-optimum decorrelating detectors which are based on linear transformation of the sampled match filter outputs were considered in [2]

*This work was partially supported by a grant from Rome Air Force Lab (AFSC, Griffss Air Force Base, NY) under the contract F30602-94-C-0118

for the synchronous channel. For the asynchronous case, Verdu suggested to use a one-shot version of his decorrelating detector, in which $1+2(K-1)=2K-1$ (K is the number of users) filters are matched to one full code of a specific user (without loss of generality, called the first user) and two filters matched to the each other user. One filter matched to the left part of its code, corresponding to times between zero and τ_j (the delay of user j with respect to the first user) and to the right part of the code, corresponding to times between τ_j and T. The decorrelating detectors were also proposed as a first stage in a two-stage multiuser CDMA signal separator to facilitate tentative decision in a fixed canceller stage[4–5] assuming knowledge of signal energies, and in an adaptive canceller stage assuming no knowledge of energies[6–7]. One may easily conclude (see [7] for example) that with the one-shot decorrelator/adaptive-canceller we can obtain the data of the specific user to which the one-shot is matched. To obtain the other users' data we must repeat the one-shot matching arrangement to the other users. Otherwise, relying on the left or right portion of code of these users will result in reduced performance.

In this paper, we propose proportional ratio diversity data combining of the left and right portions to improve performance, instead of using one one-shot arrangement for each user.

II. SYSTEM MODEL

For the asynchronous multiuser, the equivalent low-pass signal at the input of the matched filter bank is given by,

$$r(t)=\sum_{k=1}^{K}\sum_{i}b_k(i)\sqrt{a_k(i)}s_k(t+iT-\tau_k)+n(t), \tag{1}$$

where K is the number of users, a_k, b_k, s_k and τ_k are the signal amplitude, user bit, signature waveform and the relative delay of kth user respectively. $n(t)$ is the zero mean AWGN, with a two-sided power spectral density of $N_0/2$.

For the sake of simplicity we will restrict ourselves to two users only. Extension to a higher number is relatively simple.

Representing the signal of Eq. (1) in one-shot of the ith bit of user one, and without loss of generality, letting $i=0$, we write,

$$\begin{aligned} r(t) &= \sqrt{a_1}s_1(t)b_1(0)+\sqrt{a_2\epsilon_2}\frac{1}{\sqrt{\epsilon_2}}s_2^L(t)b_2(-1) \\ &\quad +\sqrt{a_2(1-\epsilon_2)}\frac{1}{\sqrt{1-\epsilon_2}}s_2^R(t)b_2(0)+n(t), \end{aligned} \tag{2}$$

where $0\le\tau_2\le T$ is considered unknown or estimated with an error, and

$$s_2^L(t) \;=\; \begin{cases} s_2(t+T-\tau_2) & \text{if } 0\le t\le\tau_2 \\ 0 & \text{if } \tau_2<t\le T \end{cases}$$

$$s_2^R(t) = \begin{cases} 0 & \text{if } 0 \le t \le \tau_2 \\ s_2(t-\tau_2) & \text{if } \tau_2 < t \le T \end{cases}$$

$$\epsilon_2 = \int_0^{\tau_2} s_2^2(t+T-\tau_2)dt. \tag{3}$$

As shown in Fig. 1, we apply $r(t)$ to a bank of filters by using as a second input $s_1(t), s_2^L(t), s_2^R(t)$, respectively. Note that we have assumed the knowledge of τ_2. The result of this paper can be applied to the case where τ_2 is unknown or has been estimated with error (see [8]). Therefore, without loss of generality, τ_2 is considered to be known.

The output of the first filter,

$$\begin{aligned} x_1(0) &= \sqrt{a_1}b_1(0) + \sqrt{a_2\epsilon_2}\rho_{12}^L b_2(-1) \\ &\quad + \sqrt{a_2(1-\epsilon_2)}\rho_{12}^R b_2(0) + n_1(0), \end{aligned} \tag{4}$$

where $n_1(0) = \int_0^T n(t)s_1(t)dt$ is a zero-mean Gaussian variable with variance of $N_0/2$, and

$$\begin{aligned} \rho_{12}^L &= \frac{1}{\sqrt{\epsilon_2}} \int_0^T s_2^L(t)s_1(t)dt \\ \rho_{12}^R &= \frac{1}{\sqrt{1-\epsilon_2}} \int_0^T s_2^R(t)s_1(t)dt. \end{aligned} \tag{5}$$

The output of the second filter is given by,

$$\begin{aligned} x_2(0) &= \frac{1}{\sqrt{\epsilon_2}} \int_0^T r(t)s_2^L(t)dt \\ &= \sqrt{a_1}\rho_{21}^L b_1(0) + \sqrt{a_2\epsilon_2}\rho_{22}^{LL} b_2(-1) \\ &\quad + \sqrt{a_2(1-\epsilon_2)}\rho_{22}^{LR} b_2(0) + n_2(0), \end{aligned} \tag{6}$$

where

$$\begin{aligned} \rho_{21}^L &= \frac{1}{\sqrt{\epsilon_2}} \int_0^T s_1(t)s_2^L(t)dt = \rho_{12}^L \\ \rho_{22}^{LL} &= \frac{1}{\epsilon_2} \int_0^T (s_2^L(t))^2 dt = 1 \\ \rho_{22}^{LR} &= \frac{1}{\sqrt{\epsilon_2(1-\epsilon_2)}} \int_0^T s_2^R(t)s_2^L(t)dt = 0 \end{aligned}$$

and

$$n_2(0) = \frac{1}{\sqrt{\epsilon_2}} \int_0^T n(t)s_2^L dt. \tag{7}$$

The output of the third filter is given by,

$$\begin{aligned} x_3(0) &= \frac{1}{\sqrt{1-\epsilon_2}} \int_0^T r(t) s_2^R(t) dt \\ &= \sqrt{a_1}\rho_{21}^R b_1(0) + \sqrt{a_2\epsilon_2}\rho_{22}^{RL} b_2(-1) \\ &\quad + \sqrt{a_2(1-\epsilon_2)}\rho_{22}^{RR} b_2(0) + n_3(0), \end{aligned} \tag{8}$$

where

$$\begin{aligned} \rho_{21}^R &= \frac{1}{\sqrt{1-\epsilon_2}} \int_0^T s_1(t) s_2^R(t) dt = \rho_{12}^R \\ \rho_{22}^{RL} &= \frac{1}{\sqrt{(1-\epsilon_2)\epsilon_2}} \int_0^T s_2^L(t) s_2^R(t) dt = 0 \\ \rho_{22}^{RR} &= \frac{1}{1-\epsilon_2} \int_0^T (s_2^R(t))^2 dt = 1 \end{aligned}$$

and

$$n_3(0) = \frac{1}{\sqrt{1-\epsilon_2}} \int_0^T n(t) s_2^R(t) dt. \tag{9}$$

Combining, Eqs. (3), (5) and (7) in matrix form,

$$\mathbf{x}(0) = \mathbf{PAb}(0) + \mathbf{n}(0), \tag{10}$$

where

$$\mathbf{P}^T = \begin{bmatrix} 1 & \rho_{12}^L & \rho_{12}^R \\ \rho_{21}^L & 1 & 0 \\ \rho_{21}^R & 0 & 1 \end{bmatrix}, \tag{11}$$

$\mathbf{A} = \mathrm{diag}[\alpha_1, \alpha_2, \alpha_3] = \mathrm{diag}[\sqrt{a_1}, \sqrt{a_2\epsilon_2}, \sqrt{a_2(1-\epsilon_2)}]$ and $\mathbf{b}(0) = [b_1(0), b_2(-1), b_2(0)]^T$. The $\mathbf{n}(t)$ is a zero-mean Gaussian vector with covariance, $\mathbf{P}N_0/2$.

III. DECORRELATING DETECTOR

In an accompanied paper[9] we suggest to use linear transformation,

$$\mathbf{z}(0) = \mathbf{VPAb}(0) + \mathbf{Vn}(0) \tag{12}$$

$\mathbf{V}, (\mathbf{V} \neq \mathbf{P}^{-1})$ is chosen such that $\mathbf{VP}$ is a diagonal matrix, and $\mathbf{V} = \mathbf{I} - \mathbf{W}$, where

$$\mathbf{W}^T = \begin{bmatrix} 0 & w_{12} & w_{13} \\ w_{21} & 0 & w_{23} \\ w_{31} & w_{32} & 0 \end{bmatrix}. \tag{13}$$

The kth output of the decorrelator (see Fig. 2) can be expressed as,

$$z_k = x_k - \mathbf{w}_k^T \mathbf{x}_k, \tag{14}$$

where $\mathbf{w}_k$ is the kth column of $\mathbf{W}$ with the element w_{kk} deleted and $\mathbf{x}_k$ is the vector obtained from $\mathbf{x}$ by deleting x_k. In [9] it was shown that such $\mathbf{W}$ can be obtained by solving

$$E\{z_k \mathbf{b}_k\} = 0, \qquad k = 1, 2, 3; \tag{15}$$

where $\mathbf{b}_k$ is $\mathbf{b}$ without b_k. One can easily show that if the signal-to-noise-plus-interference ratio at any z_j is large, then $E\{z_k \text{sgn}(z_j)\} \approx E\{z_k b_j\}(1 - P_{ej})$ is a high SNR approximation of

$$E\{z_k \text{sgn}(\mathbf{z}_k)\} = 0, \qquad k = 1, 2, 3. \tag{16}$$

The solution of Eq. (14) can be obtained by adaptively controlling the weights w_{ml} by the steepest descent algorithm, which simultaneously reduces the absolute value of the correlation between the outputs of the decorrelator and the decision on all other outputs. That is, the weight, w_{lk} is controlled by the recursion,

$$w_{ml} \leftarrow w_{ml} - \mu(z_l \text{sgn}(z_m)), \quad 1 \leq l, m < 3, \quad l \neq m. \tag{17}$$

In [8] it is shown that the solution of Eqn. (13) is given by,

$$\mathbf{w}_k = \mathbf{P}_k^{-1} \boldsymbol{\rho}_k, \tag{18}$$

where $\boldsymbol{\rho}_k$ is the kth column of $\mathbf{P}$ without ρ_{kk}, and $\mathbf{P}_k$ is the matrix $\mathbf{P}$ without the kth row and column. Substituting in Eq. (11) we get,

$$\begin{aligned} z_1(0) &= \sqrt{a_1}(1 - \boldsymbol{\rho}_1^T \mathbf{P}_1^{-1} \boldsymbol{\rho}_1) b_1(0) + n_{D1}(0) \\ z_2(0) &= \sqrt{a_2 \epsilon_2}(1 - \boldsymbol{\rho}_2^T \mathbf{P}_2^{-1} \boldsymbol{\rho}_2) b_2(-1) + n_{D2}(0) \\ z_3(0) &= \sqrt{a_2(1 - \epsilon_2)}(1 - \boldsymbol{\rho}_3^T \mathbf{P}_3^{-1} \boldsymbol{\rho}_3) b_2(0) + n_{D3}(0), \end{aligned} \tag{19}$$

where $\mathbf{n}_D = [n_{D1}(0), n_{D2}(0), n_{D3}(0)]^T = \mathbf{V}\mathbf{n}(0)$ is the noise vector at the decorrelator output.

From Eq. (11) we notice that the covariance matrix of $\mathbf{n}_D(0)$ is given by,

$$\begin{aligned} \mathbf{C}_{\mathbf{n}_D} &= \mathbf{V} E\{\mathbf{n}(0)\mathbf{n}^T(0)\}\mathbf{V} \\ &= \mathbf{V}\mathbf{P}\mathbf{V}^T N_0/2. \end{aligned} \tag{20}$$

Hence the noise variance for the kth fictitious user (corresponding to the left or the right part of user 2) at the decorrelator output,

$$\sigma_{Dk} = (1 - \boldsymbol{\rho}_k^T \mathbf{P}_k^{-1} \boldsymbol{\rho}_k) \frac{N_0}{2} \qquad k = 1, 2, 3; \tag{21}$$

where we used the fact that $\mathbf{VP}$ is a diagonal matrix with the diagonal entries $(1 - \boldsymbol{\rho}_k^T \mathbf{P}_k^{-1} \boldsymbol{\rho}_k)$, $k = 1, 2, 3$; (see Eq.(12). Therefore,

$$\text{SNR}_k = \frac{\alpha_k^2 (1 - \boldsymbol{\rho}_k^T \mathbf{P}_k^{-1} \boldsymbol{\rho}_k)}{N_0/2}, \qquad k = 1, 2, 3; \tag{22}$$

where α_k is the kth diagonal element of the fictitious users' signal amplitude matrix, $\mathbf{A}$.

3.1. Decorrelating Output Data Combining

If we use ratio combining of a delayed version of $z_3(0)$ with $z_2(0)$ we get (see Fig. 2),

$$\begin{aligned} z_{2C}(0) &= z_2(0) + \gamma\sqrt{1-\epsilon_2}\, z_3(-1) \\ &= \sqrt{a_2\epsilon_2}(1-\boldsymbol{\rho}_2^T\mathbf{P}_2^{-1}\boldsymbol{\rho}_2)b_2(-1) \\ &\quad + \gamma\sqrt{a_2(1-\epsilon_2)}(1-\boldsymbol{\rho}_3^T\mathbf{P}_3^{-1}\boldsymbol{\rho}_3)b_2(-1) \\ &\quad + n_{D2}(0) + \gamma n_{D3}(-1). \end{aligned} \tag{23}$$

The noises $n_{D2}(0)$ and $n_{D3}(-1)$ are independent, as they are obtained from different time periods. Therefore, by using Eqs. (21) and (23) we get the combined output,

$$\mathrm{SNR}_{2C} = \frac{a_2\epsilon_2(1-\boldsymbol{\rho}_2^T\mathbf{P}^{-1}\boldsymbol{\rho}_2)[1+\gamma\sqrt{\frac{1-\epsilon_2}{\epsilon_2}}\frac{1-\boldsymbol{\rho}_3^T\mathbf{P}_3^{-1}\boldsymbol{\rho}_3}{1-\boldsymbol{\rho}_2^T\mathbf{P}_2^{-1}\boldsymbol{\rho}_2}]^2}{[1+\gamma^2\frac{1-\boldsymbol{\rho}_3^T\mathbf{P}_3^{-1}\boldsymbol{\rho}_3}{1-\boldsymbol{\rho}_2^T\mathbf{P}_2^{-1}\boldsymbol{\rho}_2}]N_0/2}. \tag{24}$$

One can show that $\gamma = \sqrt{\frac{1-\epsilon_2}{\epsilon_2}}$ will result in maximum SNR_{2C}, (see Fig. 2). With this value we get in relation to uncombined SNR_2,

$$\mathrm{SNR}_{2C} = (1+\frac{1-\epsilon_2}{\epsilon_2}\frac{1-\boldsymbol{\rho}_3^T\mathbf{P}_3^{-1}\boldsymbol{\rho}_3}{1-\boldsymbol{\rho}_2^T\mathbf{P}_2^{-1}\boldsymbol{\rho}_2})\mathrm{SNR}_2. \tag{25}$$

In relation to SNR_3,

$$\mathrm{SNR}_{2C} = (1+\frac{\epsilon_2}{1-\epsilon_2}\frac{1-\boldsymbol{\rho}_2^T\mathbf{P}_2^{-1}\boldsymbol{\rho}_2}{1-\boldsymbol{\rho}_3^T\mathbf{P}_3^{-1}\boldsymbol{\rho}_3})\mathrm{SNR}_3. \tag{26}$$

It has been shown in [9] that,

$$0 \le 1-\boldsymbol{\rho}_i^T\mathbf{P}_i^{-1}\boldsymbol{\rho}_i = \frac{|\mathbf{P}|}{|\mathbf{P}_i|} \le 1, \tag{27}$$

where $|\mathbf{P}|$ is the determinant of the cross-correlation matrix, and $\mathbf{P}$ and $|\mathbf{P}_i|$ is the iith co-factor of $\mathbf{P}$. Since $0 \le \epsilon \le 1$, it can easily be concluded that SNR_{2C} is greater than both uncombined results, for any ϵ and any correlation matrix P.

It is important to note that examining equal gain data combining resulted in an improvement only for certain values of ϵ.

IV. RESULTS

Using the linear transformation $\mathbf{V}$ which results from Eq. (15), then applying (22) for the uncombined output we presented in Fig. 3, the probability of error as a function of $\mathrm{SNR}_2 - \mathrm{SNR}_1$, with $\mathrm{SNR}_1 = 8$ dB and $\tau_2 = 0.4T$. The Gold code of length 7 is used as the signature sequences. In Fig. 4, we repeat Fig. 3 by simulating the algorithm of (17) instead of (15). In Fig. 5, we compare the results of the combined data for the second user obtained with (15), versus simulation with (17). We notice from these figures that the probability of error of the combined data is always better. Also noticeable is the fact that using the bootstrap algorithm of (17) we obtain better results, particularly at low SNR's.

Finally, in Fig. 6 we compare the result of the combined data (asynchronous) with the results when the channel is synchronous.

References

[1] S. Verdu, "Minimum Probability of Error for Asynchronous Gaussian Multiple Access Channels," IEEE Trans. on Info. Theory, vol. IT-32, no. 1, pp. 85–96, Jan. 1986.

[2] R. Lupas and S. Verdu, "Linear Multiuser Detector for Synchronous Code Division Multiple Access Channels," IEEE Trans. on Info. Theory, vol. IT-35, no. 1, pp. 123–136, Jan. 1989.

[3] S. Verdu, "Recent Progress in Multiuser Detection," Advances in Communication and Signal Processing, Springer-Verlag, 1989.

[4] M. K. Varanasi and B. Aazhang, "Multistage Detector in Asynchronous Code Division Multiple Acess Communications," IEEE Trans. on Comm., vol. COM-38, no. 4, pp. 507–515, April 1990.

[5] M. K. Varanasi and B. Aazhang, "Near-optimum Detector in Synchronous Code Division Multiple Access Communications," IEEE Trans. on Comm., vol. COM-39, no. 5, pp. 725–736, May 1991.

[6] Z. Siveski, Y. Bar-Ness and D. W. Chen, "Error Performance of Synchronous Multiuser Code Division Multiple Access Detector with Multidimensional Adaptive Canceller," The European Trans. on Telecom. and Related Tech., vol. 5, no. 6, Nov.–Dec. 1994.

[7] Z. Siveski, L. Zhong and Y. Bar-Ness, "Adaptive Multiuser CDMA Detector for Asynchronous AWGN Channels," PIMRC '94, The Hague, The Netherlands, pp. 416–419, Sept. 1994.

[8] Y. Bar-Ness and N. Sezgin, "Adaptive Multiuser Bootstrapped Decorrelating CDMA Detector for One-Shot Asyncronous Unknown Channels," ICASSP '95, Detroit, MI, pp. 1733–1736, May 1995.

[9] Y. Bar-Ness and J. Punt, "An Improved Multiuser CDMA Decorrelating Detector," PIMRC '95 companion paper.

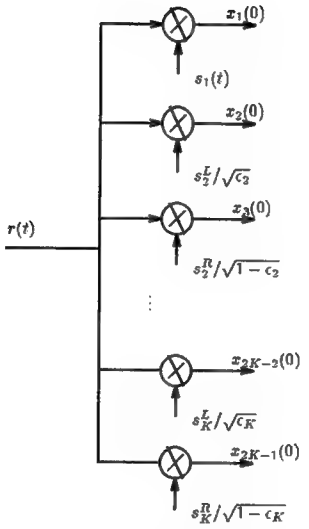

Fig. 1: Match Filter Bank for K Asynchronous Users.

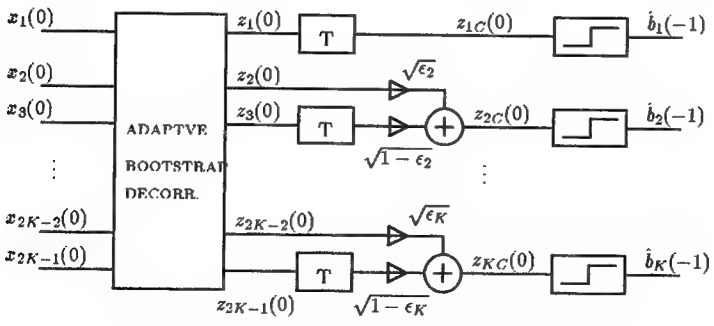

Fig. 2: Proposed Combining Scheme for Asynchronous K Users at bit interval, $i = 0$.

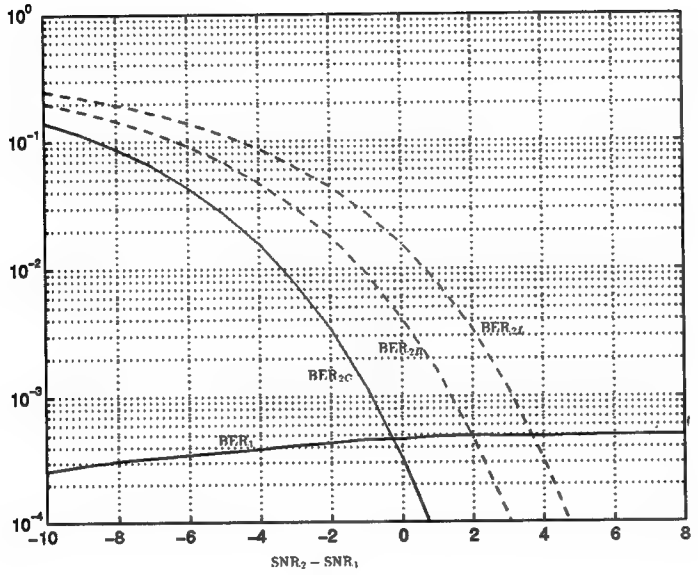

Fig. 3: BER Performance of the Proposed Scheme for $K = 2$; $SNR_1 = 8$ dB. $\epsilon_2 = 0.1$.

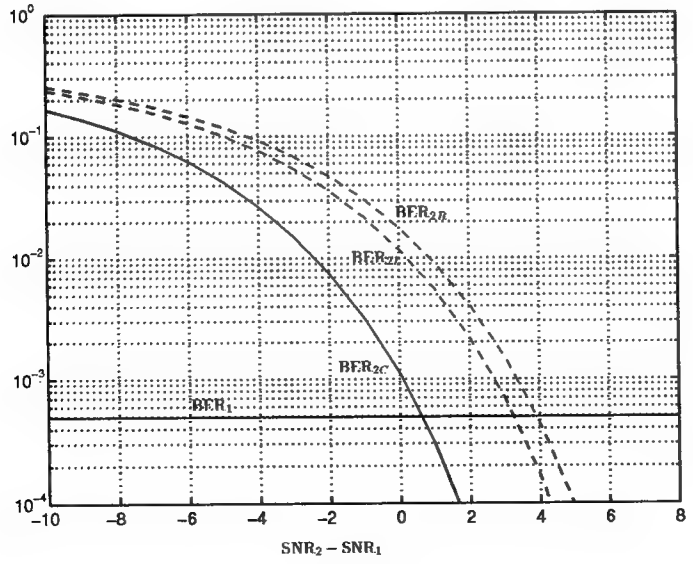

Fig. 4: Upper Bound of BER Performance Measure for $K = 2$; $SNR_1 = 8$ dB. $\epsilon_2 = 0.4$.

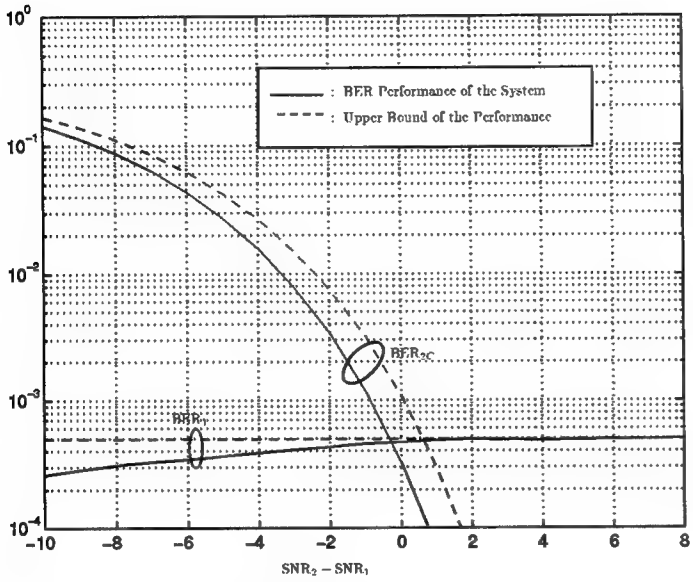

Fig. 5: BER Performance of the System, in comparison with the Upper Bound, for $K = 2$; $SNR_1 = 8$ dB, $c_2 = 0.4$.

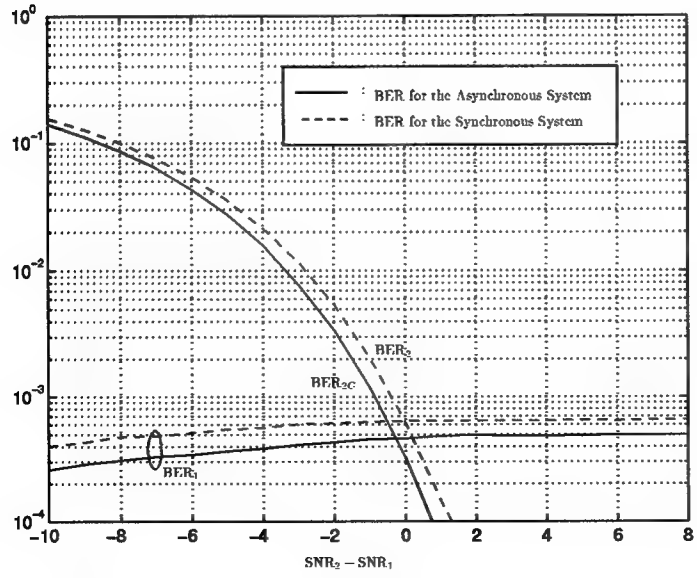

Fig.6: BER Performance of the System, in Comparison with the Synchronous Case for $K = 2$; $SNR_1 = 8$ dB.

Appendix E

Adaptive Threshold Setting For Multi-user CDMA Signal Separators with Soft Tentative Decision *

Yeheskel Bar-Ness Nadir Sezgin

Abstract

It was recently shown that in a two stage decorrelator-canceller for multiuser CDMA separation, soft tentative decision can help to improve performance, particularly when interference levels are moderate to low. The threshold points of the soft limiter were chosen heuristically and required continuous measurements of energies of all signals at the output of the decorrelator. In this paper we propose setting these thresholds adaptively by using minimum energy at the outputs of the canceller, and hence disposing of the need for measurement. The resulting decorrelator-canceller employs two algorithms; one for the canceller weights and the other for setting the threshold points.

I. INTRODUCTION

A synchronous multi-user CDMA receiver that employs a combination of a decorrelator [1] and an interference canceller, and whose weights are adaptively controlled, was presented in [2]. This scheme did not require the knowledge of the received signal energies, but performs as well as the fixed weight counterpart, described in [3]. Both used a hard decision on the decorrelator output to obtain a tentative data bit estimate. The performance of this two-stage decorrelator-canceller performs very well when the interferer's signal-to-noise ratios are high in comparison to those of the desired signal. The performance degrades when the former becomes the same level or lower than the latter. When eliminating the hard limiter, this cascaded two-stage detector performs better than that with the limiter at a low interference-to-noise ratio, but reaches the level of the decorrelator performance at high level of interference (see Fig. 1). This motivates the use of a soft limiter in which a tentative decision is made only at high interference energy. Such a decorrelator-canceller with a soft limiter was proposed in [4] for the synchronous case. In [5] the idea was extended to the

*This work was partially supported by a grant from Rome Air Force Lab (AFSC, Griffss Air Force Base, NY) under the contract F30602-94-C-0118

asynchronous case, wherein the one-shot decorrelator of Verdú[6] was used as a first stage. Zhang and Brady[7] also used soft decision tentative statistics in their multiuser asynchronous detector.

The question that remained is where the threshold point of the soft limiter should be located. In all the aforementioned references the threshold value was determined heuristically from the observed values of the decorrelator outputs. If, for example,

$$f(z) = \begin{cases} z/t & \text{if } |z| < t \\ \text{sgn}(z) & \text{otherwise} , \end{cases} \tag{1}$$

where t is the threshold point of the soft tentative decision that follows the decorrelator. In [4], t was chosen such that,

$$t_{lk} = \rho_{lk} \frac{[E\{|z_k|\}]^2}{E\{|z_l|\}}, \tag{2}$$

where z_k is the output of the decorrelator corresponding to the desired user and z_l corresponds to the interfering lth user. ρ_{lk} is the cross-correlation between the code sequences of users l and k. A similar choice was used in [5], for the asynchronous case. Notice that for setting the threshold a continual measure of energy at the output of the decorrelator is needed.

In this paper we propose an adaptive setting of this threshold, which minimizes the detector output energy. This will obviously require no measurements.

II. SYSTEM MODEL

For the general multi-user the equivalent low-pass signal at the input of the matched filter is given by

$$r(t) = \sum_{k=1}^{K} \sum_{i} b_k(i) \sqrt{a_k(i)} s_k(t + iT - \tau_k) + n(t), \tag{3}$$

where K is the number of users, a_k, b_k, s_k and τ_k are the signal amplitude, user bit, signature waveform and relative delay of the kth user. $n(t)$ is the zero mean AWGN, with a variance, σ^2.

For the synchronous channel encountered in down-link communication channels the τ_k are zero for all k. In the asynchronous up-link channels the τ_k are not necessarily equal to zero. For the former case the output of the kth matched filter is the composite of bit b_k and all interfering bits given by a linear combination through the cross-correlation factor ρ_{kj}. In matrix notation we can write:

$$\boldsymbol{x}(i) = \boldsymbol{P}\boldsymbol{A}\boldsymbol{b}(i) + \boldsymbol{n}(i), \tag{4}$$

where

$$\boldsymbol{P} = \begin{bmatrix} 1 & \rho_{12} & \cdots & \rho_{1K} \\ \rho_{12} & 1 & \cdots & \rho_{2K} \\ \vdots & \vdots & \ddots & \vdots \\ \rho_{1K} & \rho_{2K} & \cdots & 1 \end{bmatrix}, \tag{5}$$

and $\boldsymbol{A} = \text{diag}(\sqrt{a_1}, \cdots, \sqrt{a_K})$, $\boldsymbol{b}(i) = [b_1(i), \cdots, b_K(i)]^T$, and $\boldsymbol{n}(i)$ is a zero-mean Gaussian noise vector with covariance $\boldsymbol{R}_n = \boldsymbol{P}\sigma$. For the asynchronous case one may use the one-shot matched filter proposed by Verdú in [6]. In this case Eq. (3) will contain a linear combination of $b_k(i)$, $b_j(i)$ and $b_j(i-1)$ for $j = 1 \ldots K, j \neq k$. That is, the matrix $\boldsymbol{P}$ will be replaced by another square matrix, with $1 + 2(K-1) = 2K-1$ dimensions. The output of this one-shot matched filter $\boldsymbol{x}_k(i)$ will contain a linear combination through this $(2K-1) \times (2K-1)$ cross-correlation matrix of $\boldsymbol{b}_k(i)$ and bits i and $i-1$ of all other users. If the τ_ks are known then all the elements of this matrix are known provided one knows the codes. Therefore, for both synchronous and asynchronous cases the output of the matched filters is given by Eq. (4) with the corresponding definition of $\boldsymbol{b}(i)$.

For simplicity we will consider the two-user case. Extension to the multiuser case is possible.

Fig. 2 shows a block diagram of the proposed two stage (decorrelator-canceller) detection with soft decision defined in Eq. (1). Let $\lambda = 1/t$, then

$$f(z) = \begin{cases} 1 & \text{if } \lambda z > 1 \\ \lambda z & \text{if } -1 \leq \lambda z < 1 \\ -1 & \text{if } \lambda z < -1. \end{cases} \tag{6}$$

This function can be implemented with a gain whose value is λ followed by a 45° soft limiter (see Fig. 3).

III. DETECTOR'S OPTIMAL PARAMETERS AND ADAPTIVE CONTROL ALGORITHM

3.1 Optimal Canceller Weights

Following [1] we use $\boldsymbol{P}^{-1}$ as the linear transformation for the decorrelator to obtain

$$\boldsymbol{z} = \boldsymbol{A}\boldsymbol{b} + \boldsymbol{\xi}, \tag{7}$$

where $\boldsymbol{\xi} = [\xi_1, \xi_2]^T$ is a Gaussian vector with $E\{\boldsymbol{\xi}\boldsymbol{\xi}^T\} = \boldsymbol{P}^{-1}\sigma^2$

To find the optimal weight for the canceller stage, we write

$$y_1 = x_1 - w_{12} f(\lambda_2 z_2). \tag{8}$$

Equating the derivative of $E\{y_1^2\}$ with respect to w_{12} to zero we find,

$$w_{12,\text{opt}}(\lambda_2) = \frac{E\{x_1 f(\lambda_2 z_2)\}}{E\{f^2(\lambda_2 z_2)\}}. \tag{9}$$

Note that Eq. (9) describes the optimal weight in terms of the threshold, $1/\lambda_2$, and other system parameters. Using (A-1), (A-3) and (A-6) in the Appendix,

we get

$$w_{12,\text{opt}}(\lambda_2) = \frac{\rho\sqrt{a_2}\{G_1(\alpha_1,\alpha_2)+\lambda_2\sqrt{a_2}G_3(\alpha_1,\alpha_2)+Q(\alpha_1)-Q(\alpha_2)\}}{G_2(\alpha_0,\alpha_1,\alpha_2)+\sigma_{\eta_2}^2(1+\alpha_0^2)G_3(\alpha_1,\alpha_2)+Q(\alpha_1)+Q(\alpha_2)}, \tag{10}$$

where

$$\begin{aligned}
G_1(\alpha_1,\alpha_2) &= \sigma_{\eta_2}/\sqrt{2\pi}(e^{-\alpha_2^2/2}-e^{-\alpha_1^2/2}),\\
G_2(\alpha_0,\alpha_1,\alpha_2) &= \sigma_{\eta_2}^2/\sqrt{2\pi}((2\alpha_0-\alpha_2)e^{-\alpha_2^2/2}\\
&\quad -(2\alpha_0+\alpha_1)e^{\alpha_1^2/2}),\\
G_3(\alpha_1,\alpha_2) &= 1-Q(\alpha_1)-Q(\alpha_2),\\
\alpha_0 &= \lambda_2\sqrt{a_2}/\sigma_{\eta_2},\\
\alpha_1 &= (1-\lambda_2\sqrt{a_2})/\sigma_{\eta_2},\\
\alpha_2 &= (1+\lambda_2\sqrt{a_2})/\sigma_{\eta_2},
\end{aligned}$$

and $Q(\alpha)=\frac{1}{\sqrt{2\pi}}\int_\alpha^\infty e^{-x^2/2}dx$.

The hard limiter case can be obtained from Eq. (10) by letting λ_2 go to infinity. The first terms in the numerator and denominator clearly go to zero. The second term can be shown to go to zero by applying L' Hopital. Thus we are left with

$$\begin{aligned}
\lim_{\lambda_2\to\infty} w_{12,\text{opt}}(\lambda_2) &= \rho\sqrt{a_2}\lim_{\lambda_2\to\infty}\frac{Q(\alpha_1)-Q(\alpha_2)}{Q(\alpha_1)+Q(\alpha_2)}\\
&= \rho\sqrt{a_2}[1-2Q(\sqrt{\tfrac{a_2(1-\rho^2)}{\sigma}})],
\end{aligned} \tag{11}$$

the same result obtained in [2].

3.2 Optimal Threshold Level

To find the optimal threshold, by using Eq. (8) we get

$$\begin{aligned}
\frac{\partial E\{y_1^2\}}{\partial\lambda_2} &= 2w_{12}^2E\{f(\lambda_2z_2)\frac{df(\lambda_2z_2)}{d\lambda_2}\}\\
&\quad -2w_{12}E\{x_1\frac{df(\lambda_2z_2)}{d\lambda_2}\}=0.
\end{aligned} \tag{12}$$

For $w_{12}\neq 0$

$$w_{12}(\lambda_{2,\text{opt}}) = \frac{E\{x_1df(\lambda_2z_2)/d\lambda_2\}}{E\{f(\lambda_2z_2)df(\lambda_2z_2)/d\lambda_2\}}. \tag{13}$$

Note that Eq. (13) describes implicitly, λ_{opt} as a function of the weight w_{12}.

Using Eqs. (A-9) and (A-11) of the Appendix we get

$$w_{12}(\lambda_{2,\text{opt}}) = \frac{\rho\sqrt{a_2}[G_1(\alpha_1,\alpha_2)+\lambda_2\sqrt{a_2}G_3(\alpha_1,\alpha_2)]}{G_2(\alpha_0,\alpha_1,\alpha_2)+\sigma_{\eta_2}^2(1+\alpha_0^2)G_3(\alpha_1,\alpha_2)}. \tag{14}$$

Clearly, for this definition of α_0, α_1 and α_2 in Eq. (14), we must use $\lambda_{2,\text{opt}}$.

3.3 Optimal Threshold Setting for Optimal Detector

If we define the terms in the numerator of Eq. (14) as A and those in the denominator as B, then using $w_{12,\text{opt}}$ and $\lambda_{2,\text{opt}}$ in both, we write Eqs. (10) and (14) as

$$\begin{aligned} w_{12,\text{opt}}(\lambda_2) &= \frac{A+\rho\sqrt{a_2}[Q(\alpha_1)-Q(\alpha_2)]}{B+Q(\alpha_1)+Q(\alpha_2)} \\ w_{12}(\lambda_{2,\text{opt}}) &= \frac{A}{B}. \end{aligned} \tag{15}$$

To obtain both optimal weight, $w_{12,\text{opt}}$, and $\lambda_{2,\text{opt}}$ we must equate the two equations in (15), giving

$$\begin{aligned} w_{12,\text{opt}}(\lambda_{2,\text{opt}}) &= \frac{\rho\sqrt{a_2}[Q(\alpha_1)-Q(\alpha_2)]}{Q(\alpha_1)+Q(\alpha_2)} = \frac{A}{B} \\ &= \frac{\rho\sqrt{a_2}[G_1(\alpha_1,\alpha_2)+\lambda_2\sqrt{a_2}G_3(\alpha_1,\alpha_2)]}{G_2(\alpha_0,\alpha_1,\alpha_2)+\sigma_{\eta_2}^2(1+\alpha_0^2)G_3(\alpha_1,\alpha_2)}. \end{aligned} \tag{16}$$

Solving (16) will give us the optimal threshold setting $\lambda_{2,\text{opt}}$. With this value,

$$w_{12,\text{opt}}(\lambda_{2,\text{opt}}) = \frac{\rho\sqrt{a_2}[Q(\alpha_{1,\text{opt}})-Q(\alpha_{2,\text{opt}})]}{Q(\alpha_{1,\text{opt}})+Q(\alpha_{2,\text{opt}})}, \tag{17}$$

where

$$\begin{aligned} \alpha_{1,\text{opt}} &= (1-\lambda_{2,\text{opt}}\sqrt{a_2})/\sigma_{\eta_2}, \\ \alpha_{2,\text{opt}} &= (1+\lambda_{2,\text{opt}}\sqrt{a_2})/\sigma_{\eta_2}, \end{aligned}$$

and $\sigma_{\eta_2} = \lambda_2\sigma/\sqrt{1-\rho^2}$.

From Eq. (15), after some algebraic manipulation we can get the value of the optimal threshold $t_2 = 1/\lambda_2$:

$$\begin{aligned} t_{2,\text{opt}} &= \frac{\sigma}{\sqrt{1-\rho^2}}(Q(\alpha_1)-Q(\alpha_2)) \\ &\cdot \frac{(1+SNR_{2,\rho})G_3(\alpha_1,\alpha_2)-\frac{1}{\sqrt{2\pi}}\sqrt{SNR_{2,\rho}}G_1(\alpha_1,\alpha_2)}{\sqrt{\frac{2}{\pi}}G_4(\alpha_1,\alpha_2)+\sqrt{SNR_{2,\rho}}(Q(\alpha_1)+Q(\alpha_2))G_3(\alpha_1,\alpha_2)}, \end{aligned} \tag{18}$$

where $G_4(\alpha_1, \alpha_2) = Q(\alpha_1)e^{-\alpha_2^2/2} - Q(\alpha_2)e^{-\alpha_1^2/2}$ and $SNR_{2,\rho} = a_2(1-\rho^2)/\sigma$. This equation gives implicitly the dependence of the optimal threshold, t_{opt}, as a function of SNR_2 and ρ.

3.4 Adaptive Control Algorithm

The following two steepest-descent algorithms simultaneously control the weights w_{ij} and the gains $\lambda_{ij}, j = 1, 2, \ldots, K; j \neq k$ for K users by minimizing the energy $E\{y_i^2\}$. That is,

$$w_{ij}^{(k+1)}(\lambda_{ij}^k) = w_{ij}^k(\lambda_{ij}^k) + \mu \nabla_{w_{ij}} E\{y_i^2(\lambda_{ij}^k, w_{ij}^k)\} \tag{19}$$

$$\lambda_{ij}^{(k+1)}(w_{ij}^k) = \lambda_{ij}^k(w_{ij}^k) + \mu \nabla_{\lambda_{ij}} E\{y_i^2(\lambda_{ij}^k, w_{ij}^k)\}. \tag{20}$$

IV. PROBABILITY OF ERROR

For any setting of λ_2, the optimal weight, $w_{12,\text{opt}}(\lambda_2)$, is given by Eq. (10). With this weight,

$$\begin{aligned} P_{e_1} = \frac{1}{2}\{1 &+ [Q(\frac{\delta_1 + \sqrt{a_1}}{\sigma}) - Q(\frac{\delta_1 - \sqrt{a_1}}{\sigma})]Q(\alpha_1) \\ &+ [Q(\frac{\delta_2 + \sqrt{a_1}}{\sigma}) - Q(\frac{\delta_2 - \sqrt{a_1}}{\sigma})]Q(\alpha_2)\} \\ &+ \frac{1}{4}\{\frac{1}{\sqrt{2\pi}\sigma_{\eta_2}} \int_{-1}^{1} [Q(\frac{\gamma_1 + \sqrt{a_1}}{\sigma}) - Q(\frac{\gamma_1 - \sqrt{a_1}}{\sigma})] \\ &\cdot \exp(-\frac{(\eta_2 - \lambda_2\sqrt{a_2})^2}{2\sigma_{\eta_2}^2}) d\eta_2 \\ &+ \frac{1}{\sqrt{2\pi}\sigma_{\eta_2}} \int_{-1}^{1} [Q(\frac{\gamma_2 + \sqrt{a_1}}{\sigma}) - Q(\frac{\gamma_2 - \sqrt{a_1}}{\sigma})] \\ &\cdot \exp(-\frac{(\eta_2 + \lambda_2\sqrt{a_2})^2}{2\sigma_{\eta_2}^2}) d\eta_2\}, \end{aligned} \tag{21}$$

where

$$\begin{aligned} \delta_1 &= \rho\sqrt{a_2}(c-1), \quad \delta_2 = \rho\sqrt{a_2}(c+1), \\ \gamma_1 &= \rho\sqrt{a_2}(c\eta_2 - 1), \quad \gamma_2 = \rho\sqrt{a_2}(c\eta_2 + 1), \end{aligned}$$

and $c = w_{12}(t_2)/\rho\sqrt{a_2}$. Note that for $t_2 = t_{2,\text{opt}}$, using Eq. (16) we get

$$c = \frac{Q(\alpha_{1,\text{opt}}) - Q(\alpha_{2,\text{opt}})}{Q(\alpha_{1,\text{opt}}) + Q(\alpha_{2,\text{opt}})}. \tag{22}$$

V. NUMERICAL RESULTS

From (19) it is clear that the optimum threshold setting t_2 is independent of SNR_1. The solution of Eq. (20) numerically as a function of ρ is given in Fig. 4, with SNR_2 as a parameter. In Fig. 5, we depict $t_{2,\text{opt}}$ as a function of SNR_2 for $\rho = 0.7$. In Fig. 6 we compare the value of the output energy obtained with the hard limiter and with a threshold calculated according to the heuristic value of Eq. (1). The corresponding probability of error for these cases are given in Fig. 7. For comparison we add to this curve the probability of error at the output of the decorrelator. Fig. 8 depicts the same, except for $\rho = 0.3$.

Note, particularly in Fig. 7, that the error probability with the heuristic setting is better in some regions than with the optimum setting of threshold. This is due to the fact that the optimization was performed with respect to minimum energy, not error probability. In Fig. 8 the performance is almost the same. Nevertheless, the advantage of adaptive threshold setting is in disposing the need for measurement.

APPENDICES

1.)

$$\begin{aligned} E\{x_1 f(\eta_2)\} &= E\{(\sqrt{a_1}b_1 + \rho\sqrt{a_2}b_2 + n_1)f(\eta_2)\} \\ &= \rho\sqrt{a_2}E\{b_2 f(\eta_2)\}, \end{aligned} \tag{A-1}$$

where we used the fact that z_2 and b_1 are uncorrelated, and so is n_1 with z_2. It is easy to show that $E\{b_2 f(\eta_2)|b_2 = 1\} = E\{b_2 f(\eta_2)|b_2 = -1\}$. Therefore,

$$E\{b_2 f(\eta_2)\} = \frac{1}{\sqrt{2\pi}\sigma_{\eta_2}} \int_{-\infty}^{+\infty} f(\eta_2) \exp(-\frac{(\eta_2 - \overline{\eta}_2)^2}{2\sigma_{\eta_2}^2}) d\eta_2, \tag{A-2}$$

where with $b_2 = 1$, $\eta_2 = \lambda_2 z_2 = \lambda_2(\sqrt{a_2} + \xi_2)$, $\overline{\eta_2} = \lambda_2\sqrt{a_2}$. Separating the integral into its three regions, $(-\infty, -1)$, $[-1, 1]$ and $(1, \infty)$ with respect to η_2, then changing variable $x = (\eta_2 - \overline{\eta_2})/\sigma_{\eta_2}$, we get

$$\begin{aligned} E\{b_2 f(\eta_2)\} &= \frac{1}{\sqrt{2\pi}}[\int_{-\infty}^{-\alpha_2} e^{x^2/2} dx \\ &\quad + \int_{-\alpha_2}^{\alpha_1} (\sigma_{\eta_2} x + \lambda_2\sqrt{a_2}) e^{-x^2/2} dx] \\ &= \frac{\sigma_{\eta_2}}{\sqrt{2\pi}}(e^{-\alpha_2^2/2} - e^{-\alpha_1^2/2}) + \lambda_2\sqrt{a_2} \\ &\quad \cdot [1 - Q(\alpha_1) - Q(\alpha_2)] + Q(\alpha_1) - Q(\alpha_2), \end{aligned} \tag{A-3}$$

where α_1 and α_2 are defined in Eq. (10).

2.)

$$E\{f^2(\eta_2)\} = \frac{1}{2}[E\{f^2(\eta_2)|b_2 = 1\} + E\{f^2(\eta_2)|b_2 = -1\}]. \qquad \text{(A-4)}$$

It is easy to show that conditioned on $b_2 = 1$ and $b_2 = -1$ the two terms are equal. Therefore,

$$\begin{aligned} E\{f^2(\eta_2)\} &= E\{f^2(\eta_2)|b_2 = 1\} \\ &= \frac{1}{\sqrt{2\pi}\sigma_{\eta_2}} \int_{-\infty}^{+\infty} f^2(\eta) \exp(-\frac{(\eta_2 - \lambda_2\sqrt{a_2})^2}{2\sigma_{\eta_2}^2}) d\eta_2 \\ &= \frac{1}{\sqrt{2\pi}\sigma_{\eta_2}} [\int_0^{\infty} f^2(\eta_2) \exp(-\frac{(\eta_2 - \lambda_2\sqrt{a_2})^2}{2\sigma_{\eta_2}^2}) d\eta_2 \\ &\quad + \int_0^{\infty} f^2(\eta_2) \exp(-\frac{(\eta_2 + \lambda_2\sqrt{a_2})^2}{2\sigma_{\eta_2}^2}) d\eta_2. \end{aligned} \qquad \text{(A-5)}$$

Substituting $x = (\eta_2 - \lambda_2\sqrt{a_2})/\sigma_{\eta_2}$ in the first integral and $x = (\eta_2 + \sqrt{a_2})/\sigma_{\eta_2}$ in the second, after performing the integration we get

$$\begin{aligned} E\{f^2(\eta_2)\} &= \frac{\sigma_{\eta_2}^2}{\sqrt{2\pi}}[(2\alpha_0 - \alpha_2)e^{-\alpha_2^2/2} \\ &\quad - (2\alpha_0 + \alpha_1)e^{-\alpha_1^2/2}] + \sigma_{\eta_2}(1 + \alpha_0^2) \\ &\quad \cdot [1 - Q(\alpha_1) - Q(\alpha_2)] + Q(\alpha_1) + Q(\alpha_2), \end{aligned} \qquad \text{(A-6)}$$

where α_0, α_1 and α_2 are defined in Eq. (10).

3.)

$$\begin{aligned} E\{x_1 \frac{df(\lambda_2 z_2)}{d\lambda_2}\} &= E\{(\sqrt{a_1}b_1 + \rho\sqrt{a_2}b_2 + n_1)z_2 \frac{df(\eta)}{d\eta_2}\} \\ &= \rho\sqrt{a_2} E\{b_2 z_2 \frac{df(\eta_2)}{d\eta_2}\}, \end{aligned} \qquad \text{(A-7)}$$

where we used the fact that z_2 is uncorrelated with b_1 and n_1 and that $f(\eta_2)$ is a deterministic function. It is easy to show that the conditioned on both $b_2 = \pm 1$, $E\{b_2 z_2 df(\eta_2)/d\eta_2 | b_2\}$ has the same value. Therefore,

$$\begin{aligned} E\{b_2 z_2 \frac{df(\eta_2)}{d\eta_2} &= E\{b_2 z_2 \frac{df(\eta_2)}{d\eta_2} | b_2 = 1\} \\ &= \frac{1}{\sqrt{2\pi}\sigma_{\eta_2}} \int_{-1}^{1} \frac{\eta_2}{\lambda_2} \exp(-\frac{(\eta_2 - \lambda_2\sqrt{a_2})^2}{2\sigma_{\eta_2}^2}) d\eta_2 \end{aligned} \qquad \text{(A-8)}$$

Changing variable $x = (\eta_2 - \lambda_2\sqrt{a_2})/\sigma_{\eta_2}$, after integration, and using (A-7), we obtain

$$\begin{aligned} E\{x_1 \frac{df(\lambda_2 z_2)}{d\lambda_2}\} &= \frac{1}{\lambda_2}\{\frac{\sigma_{\eta_2}}{\sqrt{2\pi}}(e^{-\alpha_2^2/2} - e^{-\alpha_1^2/2}) \\ &\quad + \lambda_2\sqrt{a_2}[1 - Q(\alpha_2) - Q(\alpha_2)]\}, \end{aligned} \qquad \text{(A-9)}$$

where α_1 and α_2 are defined in (10).

4.)
$E\{f(\lambda_2 z_2)df(\lambda_2 z_2)/d\lambda_2\}$ again conditioned on $b_2 = \pm 1$, has the same value. Therefore,

$$\begin{aligned} E\{f(\lambda_2 z_2)\frac{df(\lambda_2 z_2)}{d\lambda_2}\} &= E\{f(\eta_2)z_2\frac{df(\eta_2)}{d\eta_2}\} \\ &= E\{f(\eta_2)z_2 df(\eta_2)/d\eta_2 | b_2 = 1\} \\ &= \frac{1}{\sqrt{2\pi}\sigma_{\eta_2}}\int_{-1}^{1}\frac{\eta_2}{\lambda_2}\exp(-\frac{(\eta_2 - \lambda_2\sqrt{a_2})^2}{2\sigma_{\eta_2}^2})d\eta_2. \end{aligned} \tag{A-10}$$

Changing variable $x = (\eta_2 - \lambda_2\sqrt{a_2})/\sigma_{\eta_2}$ and performing the integration gives

$$\begin{aligned} &E\{f(\lambda_2 z_2)\frac{df(\lambda_2 z_2)}{d\lambda_2}\} = \\ &\frac{1}{\lambda_2}\{\frac{\sigma_{\eta_2}^2}{\sqrt{2\pi}}[(2\alpha_0 - \alpha_2)e^{-\alpha_2^2/2} - (2\alpha_0 + \alpha_1)e^{-\alpha_1^2/2}] \\ &+ \sigma_{\eta_2}^2(1 + \alpha_0^2)[1 - Q(\alpha_1) - Q(\alpha_2)]\}. \end{aligned} \tag{A-11}$$

5.)

$$\begin{aligned} P_{e_1} = \frac{1}{2}[&Pr(n_1 < w_{12}(t_2)f(\eta_2) - \rho\sqrt{a_2}b_2 - \sqrt{a_1}) \\ &+ Pr(n_1 > w_{12}(t_2)f(\eta_2) - \rho\sqrt{a_2}b_2 + \sqrt{a_1})]. \end{aligned} \tag{A-12}$$

By using the fact that $Pr(\eta_2 < -1, b_2) = Pr(\eta_2 > 1, -b_2)$ we can write,

$$\begin{aligned} P_{e_1} = &[Pr(n_1 < w_{12}(t_2) - \rho\sqrt{a_2}b_2 - \sqrt{a_1}) \\ &+ Pr(n_1 > w_{12}(t_2) - \rho\sqrt{a_2}b_2 + \sqrt{a_1})]Pr(\eta_2 > 1|b_2) \\ &+ \frac{1}{2}[Pr(n_1 < w_{12}(t_2)\eta_2 - \rho\sqrt{a_2}b_2 - \sqrt{a_1},\ \eta_2 < |1|) \\ &+ Pr(n_1 > w_{12}(t_2)\eta_2 - \rho\sqrt{a_2}b_2 + \sqrt{a_1},\ \eta_2 < |1|)]. \end{aligned} \tag{A-13}$$

By letting

$$\begin{aligned} \delta_1 = \rho\sqrt{a_2}(c-1), \quad \delta_2 = \rho\sqrt{a_2}(c+1), \\ \gamma_1 = \rho\sqrt{a_2}(c\eta - 1), \quad \gamma_2 = \rho\sqrt{a_2}(c\eta + 1), \end{aligned}$$

where $c = w_{12}(t_2)/\rho\sqrt{a_2}$, we get

$$
\begin{aligned}
P_{e_1} &= \frac{1}{2}[Pr(n_1 < \delta_1 - \sqrt{a_1}) + Pr(n_1 > \delta_1 + \sqrt{a_1})] \\
&\quad \cdot Pr(\eta_2 > 1 | b_2 = 1) \\
&\quad + \frac{1}{2}[Pr(n_1 < \delta_2 - \sqrt{a_1}) + Pr(n_1 > \delta_2 + \sqrt{a_1})] \\
&\quad \cdot Pr(\eta_2 > 1 | b_2 = 1) \\
&\quad + \frac{1}{4}[Pr(n_1 < \gamma_1 - \sqrt{a_1},\ -1 < \eta_2 < 1 | b_2 = 1) \\
&\quad + Pr(n_1 > \gamma_1 + \sqrt{a_1},\ -1 < \eta_2 < 1 | b_2 = 1)] \\
&\quad + \frac{1}{4}[Pr(n_1 < \gamma_2 - \sqrt{a_1},\ -1 < \eta_2 < 1 | b_2 = -1) \\
&\quad + Pr(n_1 > \gamma_2 + \sqrt{a_1},\ -1 < \eta_2 < 1 | b_2 = -1)] \\
&= \frac{1}{2}[1 - Q(\frac{\delta_1 - \sqrt{a_1}}{\sigma}) + Q(\frac{\delta_1 + \sqrt{a_1}}{\sigma})]Q(\alpha_1) \\
&\quad + \frac{1}{2}[1 - Q(\frac{\delta_2 - \sqrt{a_1}}{\sigma}) + Q(\frac{\delta_2 + \sqrt{a_1}}{\sigma})]Q(\alpha_2) \\
&\quad + \frac{1}{2}[1 - Q(\alpha_1) - Q(\alpha_2)] \\
&\quad + \frac{1}{4}\{\frac{1}{\sqrt{2\pi}\sigma_{\eta_2}} \int_{-1}^{1} [Q(\frac{\gamma_1 + \sqrt{a_1}}{\sigma}) - Q(\frac{\gamma_1 - \sqrt{a_1}}{\sigma})] \\
&\quad \cdot \exp(-\frac{(\eta_2 - \lambda_2\sqrt{a_2})^2}{2\sigma_{\eta_2}^2}) d\eta_2\} \\
&\quad + \frac{1}{4}\{\frac{1}{\sqrt{2\pi}\sigma_{\eta_2}} \int_{-1}^{1} [Q(\frac{\gamma_2 + \sqrt{a_1}}{\sigma}) - Q(\frac{\gamma_2 - \sqrt{a_1}}{\sigma})] \\
&\quad \cdot \exp(-\frac{(\eta_2 + \lambda_2\sqrt{a_2})^2}{2\sigma_{\eta_2}^2}) d\eta_2\}. \qquad \text{(A-14)}
\end{aligned}
$$

References

[1] R. Lupas and S. Verdú, "Linear multiuser detector for synchronous code division multiple access channels," *IEEE Trans. on Info. Theory*, vol. IT-35, pp. 123–136, Jan. 1989.

[2] Z. Siveski, Y. Bar-Ness, and D. W. Chen, "Error performance of synchronous multiuser code division multiple access detector with multidimensional adaptive canceller," *European Trans. on Telecommunications and Related Technologies*, 1994.

[3] M. K. Varanasi and B. Aazhang, "Near optimum detector with synchronous code division multiple access system," *IEEE Trans. on Comm.*, vol. 39, pp. 725–736, May 1991.

[4] D. W. Chen, Z. Siveski, and Y. Bar-Ness, "Synchronous multiuser detector with soft decision adaptive canceller," in *28th Annual Conf. on Info. Sci. and Sys.*, (Princeton, NJ), March 1994.

[5] F. Viehofer, Z. Siveski, and Y. Bar-Ness, "Soft decision adaptive multiuser cdma detector for asynchronous awgn channel," in *The 32nd Annual Allerton Conference on Communication, Computing and Control*, (Urbana-Champaign, IL), Sept. 1994.

[6] S. Verdú, "Recent progress in multiuser detection," *Advances in Communication and Signal Processing*, 1989.

[7] X. Zhang and D. Brady, "Soft-decision multistage detection for asynchronous awgn channels," in *The 31st Annual Allerton Conference on Communication, Computing and Control*, (Monticello, IL), Sept. 1993.

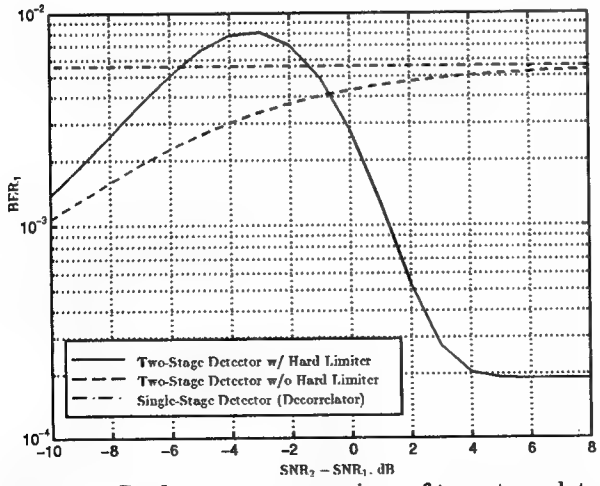

Figure 1: Performance comparison of two-stage detector, with Hard Limiter and without Hard Limiter; $SNR_1 = 8$ dB.

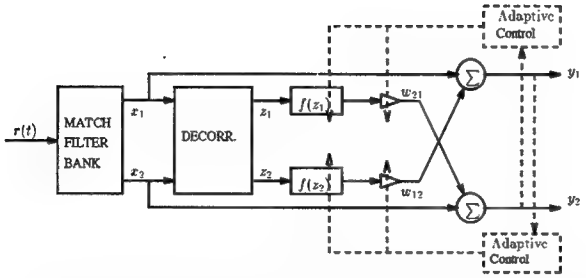

Figure 2: Two-stage (decorrelator/canceller) Detector with Adaptive Soft Limiter.

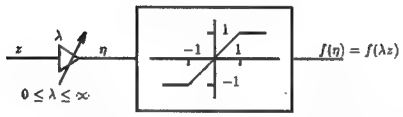

Figure 3: Soft Limiter with controlled threshold.

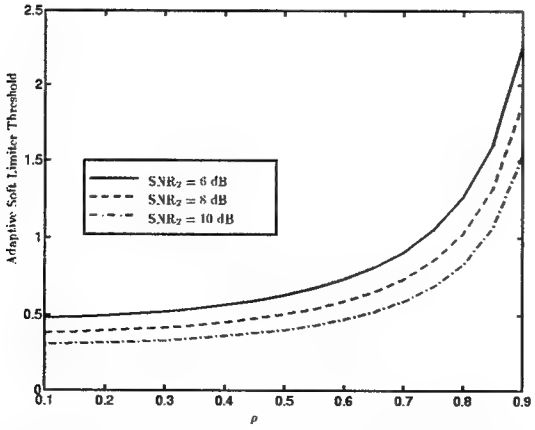

Figure 4: Optimal Threshold as a function of correlation coefficient, ρ, for $\mathrm{SNR}_1 = 8$ dB.

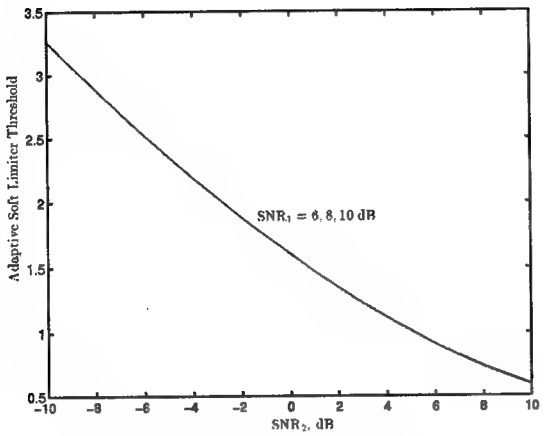

Figure 5: Optimal Threshold as a function of SNR_2, for $\rho = 0.7$.

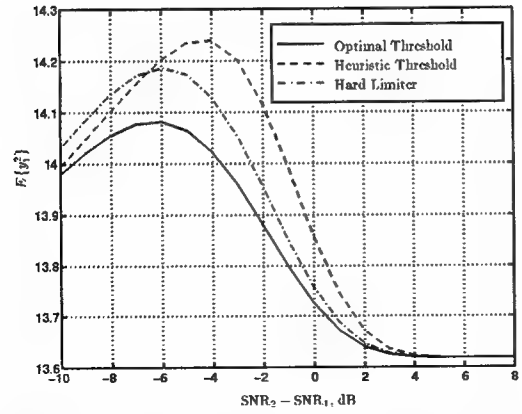

Figure 6: Output Energy of desired user, $E\{y_1^2\}$, with Hard Limiter, Heuristic Threshold and Optimal Threshold; $\mathrm{SNR}_1 = 8$ dB, $\rho = 0.7$.

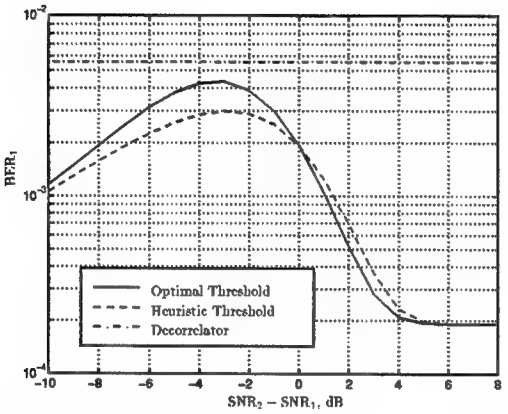

Figure 7: Bit Error Rate performance of desired user for Decorrelator, Heuristic Threshold and Optimal Threshold Detector; $\mathrm{SNR}_1 = 8$ dB, $\rho = 0.7$.

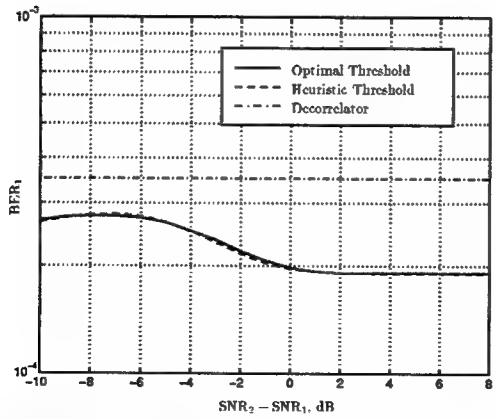

Figure 8: Bit Error Rate performance of desired user for Decorrelator, Heuristic Threshold and Optimal Threshold Detector; $\mathrm{SNR}_1 = 8$ dB, $\rho = 0.3$.

Appendix F

On the Performance of a Stochastic Gradient-Based Decorrelation Algorithm for Multiuser Multicarrier CDMA*

A. Haimovich and Y. Bar-Ness
Center for Communications and Signal Processing Research
Department of Electrical Engineering
New Jersey Institute of Technology
University Heights, Newark, NJ 07102
tel:(201)596-3534 fax:(201)596-8473

Abstract

A stochastic gradient-based decorrelation is suggested for separation of unknown linear mixture of signals. It is shown that while the decorrelation algorithm is similar in cost to the LMS algorithm, its rate of convergence is significantly faster making it more attractive for signal separation. Analysis of the decorrelator algorithm shows that the faster speed of convergence is a consequence of the eigenvalues spread associated with the decorrelation problem, which is smaller than the spread associated with the corresponding mean square problem. Operation of the algorithm is illustrated as an adaptive multiuser detector in a multiple carrier CDMA system.

1 Introduction

In this paper we address the problem of the recovery of unknown independent sources from observations of a linear mixture of the sources. We are concerned with a multiple input–multiple output system where each output is an unknown linear combination of the inputs. The following linear statistical model is assumed:

$$\mathbf{x} = \mathbf{A}\mathbf{b} + \mathbf{v} \tag{1}$$

where $\mathbf{x}$, $\mathbf{b}$, and $\mathbf{v}$ are random vectors with values in $\mathcal{R}^N$. The mixture matrix $\mathbf{A}$ is unknown but is invertible. The problem is to estimate realizations of

*This work was supported in part by a grant from ROME Air Development Center, AFSC, Griffiss Air Force Base, NY, under contract F30602-93-C-0118.

the vector $\mathbf{b}$ given observations of $\mathbf{x}$. This type of problem arises in numerous applications. The recovery of $\mathbf{b}$ when only the model's output observations $\mathbf{x}$ are available is referred to as *blind signal separation.* To find a solution to this problem it is necessary, in addition to the output observations, to have some information about the statistical properties of the components of $\mathbf{b}$. Examples of blind signal separation applications are the cancellation of cross-pol interference in dually polarized systems and multiuser detection in multiple access communications systems. The latter application will be used to illustrate the techniques considered in this paper.

One approach to signal separation is to view it as an interference cancellation problem, where at each channel output one signal is considered the signal of interest and the other signals are considered interferences. When a reference signal is available, the mean square error (MSE) between the output and the reference signal is minimized by the classical Wiener filter, which can be implemented using steepest descent algorithms such as the LMS and RLS. Such an example can be found in [1], where the LMS algorithm, operating as an interference canceler, is used as a separator of cross-polarized signals.

A different approach is to treat the separation problem in its own right. Notice that at high signal-to-noise ratio the separation problem is equivalent to the identification of the system $\mathbf{A}^{-1}$. Beginning with the early eighties a class of adaptive signal separators have been proposed that in effect estimates the inverse of the mixture matrix $\mathbf{A}^{-1}$, [2]. Their research was mainly aimed at communications applications, such as cross-pol separation in dually polarized links. It assumed that the signals to be separated are uncorrelated. This condition however, resulted in an indeterminate solution. Separation was shown, provided that "some knowledge" is available by which the signals can discriminated (for example slightly different spectral characteristics). Later, similar separator structures were suggested for implementation using neural networks [3]. They solved the indetermination problem by assuming that the signals to be recovered are independent. An independence test was approximated by way of decorrelation using non-linear functions [4].

In this paper we analyze the performance of a stochastic gradient-based decorrelation algorithm for blind signal separation. The algorithm has a computational complexity comparable with the LMS algorithm, but is shown to be faster than the latter. The main contribution of the paper is to prove, through an eigenvalue analysis, that the differences in the speed of convergence are a consequence of the different eigenvalue spreads associated with the implementation of the two algorithms. While the problem statement and proofs are quite general, the specific application considered is a synchronous multiuser multicarrier CDMA communication system in a fading environment. In this application the decorrelator is used as a multiuser detector. Multiuser detectors are a subject of continued research due to their promise of increased capacity for mobile communications, personal communications and other wireless networks. The decorrelator has been previously suggested as a low complexity near-far resis-

tant multiuser detector [5]. Other authors proposed non-adaptive and adaptive multiuser detectors incorporating the decorrelator [6], [7]. In this paper we focus on the transient response of the adaptive decorrelator.

The system model is presented in section 2. In section 3 we define separation criteria. Adaptive algorithms and the convergence analysis of the decorrelator are developed in section 4. Section 5 contains simulation results. Conclusions are provided in section 6.

2 System Model

The general system model is given in eq. (1) where the received signal consists of a linear transformation of the transmitted data and additive noise. To be more specific and to lend credibility to the model, we consider a synchronous multiuser multicarrier CDMA communication system such as depicted in [8]. The synchronous assumption is not necessary but it simplifies the notation. An asynchronous system can be made synchronous by oversampling provided all users' signals are have been acquired. The model presented below can be equally applicable to uplink or downlink communications. In multicarrier (MC)-CDMA an information symbol is transmitted on multiple subcarriers. The subcarrier waveforms are chosen mutually orthogonal (ex. rectangular RF-pulses with frequencies separated by an integer number of cycles). Each of N users is assigned a unique code expressed by a set of $0/\pi$ offsets of the subcarriers phase. The main advantage of this type of modulation over conventional direct sequence spread spectrum is that each subcarrier is subject to frequency-nonselective fading, thus eliminating the need for the complex RAKE receiver. The signal transmitted by the n-th user for the i-th bit is given by:

$$s_n(t) = \sqrt{\xi_n} b_n(i) \sum_{m=1}^{M} c_n(m) p(t) \cos\left(\omega_c t + \frac{m-1}{T}\Omega t\right) \tag{2}$$

where ξ_n is the waveform's energy. The information symbols are assumed binary $b_n(i) \in \{-1, 1\}$, independent and equiprobable. The signature code sequence for the n-th user is given by $c_n(m) = \pm 1/\sqrt{M}$, $m = 1, \ldots, M$, where M is the number of subcarriers. $p(t) = 2/\sqrt{T}$, $0 \leq t < T$ is the pulse shape and T is the symbol duration. To ensure orthogonality between waveforms, the frequency offset Ω is chosen to be an integer multiple of 2π.

The functional diagram of the multicarrier-multiuser CDMA receiver is shown in Figure 1. The n-th user signal, after coherent amplitude detection with each of the M subcarrier frequencies, is given by the M-dimensional vector:

$$\mathbf{r}_n(i) = \sqrt{\xi_n} b_n(i) \mathbf{H}_n \mathbf{c}_n \tag{3}$$

where the diagonal matrix $\mathbf{H}_n$ consists of the channel coefficients $h_{nm}, m = 1, \ldots, M$. The channel parameters h_{nm} are assumed to be Rayleigh distributed.

The paths of the individual subcarriers are assumed to be independent. Notice that under the coherent detection assumption, phase changes in the channel do not affect the output. The vector $\mathbf{c}_n^T = [c_n(1), \ldots, c_n(M)]$ is the n-th user code sequence vector. Henceforth, for brevity of notation explicit time dependency is dropped since the decision on $b_n(i)$ requires observation of signals only during that interval. Collecting the contributions of all the users and the additive noise, we have at the output of the coherent detectors:

$$\mathbf{q} = \overline{\mathbf{H}}\mathbf{E}\mathbf{b} + \eta_M \tag{4}$$

where $\mathbf{E}$ is a diagonal matrix, $\mathbf{E} = \text{diag}\left(\sqrt{\xi_n}\right)$, $n = 1, \ldots, N$, and $\overline{\mathbf{H}}$ is the matrix

$$\overline{\mathbf{H}} = [\mathbf{H}_1\mathbf{c}_1, \ldots, \mathbf{H}_N\mathbf{c}_N] \tag{5}$$

$\mathbf{b}$ is the vector of information bits, and the components of the noise vector η_M are assumed i.i.d. zero-mean Gaussian with variance σ^2. The signal after cross-correlation with the code of the j-th user can be written,

$$x_j = \mathbf{c}_j^T\overline{\mathbf{H}}\mathbf{E}\mathbf{b} + \mathbf{c}_j^T\eta_M \tag{6}$$

Finally, collecting the terms for all the users the received signal can be expressed in vector form,

$$\mathbf{x} = \mathbf{A}\mathbf{E}\mathbf{b} + \mathbf{v} \tag{7}$$

where $\mathbf{A} = \mathbf{C}^T\overline{\mathbf{H}}$ is the mixture matrix, and $\mathbf{v}(i)$ is the noise vector with the j-th component equal to $\mathbf{c}_j^T\eta_M$. Since the channel coefficients are unknown, the matrix $\mathbf{A}$ is unknown. It can be readily shown that the noise covariance matrix is given by,

$$E\left[\mathbf{v}\mathbf{v}^T\right] = \sigma^2\mathbf{C}^T\mathbf{C} \tag{8}$$

Notice that the MC-CDMA model in eq. (7) is the same as the general model assumed in (1). Multiuser detection has commonly been considered for uplink communications. With direct sequence CDMA, orthogonality between the signature waveforms is maintained in the synchronous uplink channel. However, the same does not hold for MC-CDMA, where subcarriers fade independently. Hence, decorrelation cannot be achieved by a simple inversion of the signature waveforms correlation matrix. Analysis of the convergence rate of adaptive decorrelation in the uplink channel is made very difficult by the fact that the matrix $\mathbf{AE}$ is not symmetric. Numerical examples in section 5 consider the uplink, however the analysis in section 4 assumes that $\mathbf{AE}$ is symmetric. This model represents the downlink of a MC-CDMA system. In this case, multiuser techniques could be useful to improve performance at the mobile. Systems requiring multiuser detection are expected to operate near capacity most of the time, thus the mobile could operate assuming all users are present. All signals transmitted by the base station and received at the mobile experience the same channel, i.e., $\mathbf{H}_n = \mathbf{H}$. With this condition, the mixture matrix is given by

$\mathbf{A} = \mathbf{C}^T\mathbf{H}\mathbf{C}$, and is clearly symmetric. Furthermore, it can be assumed that all signals are received at the mobile with equal energies , i.e., $\mathbf{E} = \mathbf{I}$, where $\mathbf{I}$ is the identity matrix (a constant gain common to all users can be incorporated in the matrix $\mathbf{A}$). The model for the received signal becomes,

$$\mathbf{x} = \mathbf{A}\mathbf{b} + \mathbf{v}$$

where the mixture matrix $\mathbf{A}$ is symmetric and unknown. Direct detection of the elements of vector $\mathbf{x}$ is impeded by the presence of the cochannel interference. Therefore, the goal is to add a receiver stage that provides signal separation through cochannel interference cancellation.

3 Signal Separation Criteria

Two signal separation criteria are considered: separation through minimization of the Mean Square Error (MSE) and separation through signal decorrelation. The criteria are used to develop control algorithms for the network weights. The network weights are represented by a matrix $\mathbf{W} = [\mathbf{w}_1, \ldots, \mathbf{w}_N]$, where $\mathbf{w}_n$ is the $N \times 1$ weight vector applied to the network input vector $\mathbf{x}$ to obtain the output for the n-th user, $y_n = \mathbf{w}_n^T\mathbf{x}$. An estimate of the data bits is then obtained from $\widehat{\mathbf{b}} = \text{sgn}\mathbf{y}$, where $\mathbf{y} = \mathbf{W}^T\mathbf{x}$. The following conditions are assumed to hold for the data and the channel: (1) the components of the data vector $\mathbf{b}$ are assumed independent, binary, and equiprobable, (2) the mixture matrix is symmetric, (3) the mixture matrix $\mathbf{A}$ is strictly diagonally dominant, i.e., $a_{ii} > \sum_{j \neq i} |a_{ij}|$ for $i = 1, \ldots, N$. The latter condition ensures that in the absence of noise, a correct decision is made with respect to each of the desired users with probability one. This condition also implies that the matrix $\mathbf{A}$ is invertible [9, p.349].

3.1 MSE Separation

The MSE signal separator minimizes the mean squared error between its output and a reference signal. Typically the reference is initially supplied by a training signal. When the adaptive weights converged and the errors with respect to the training signal are small, the detector is switched to operate in decision directed mode, and the reference signal is supplied by the estimated symbol. The MSE signal separator is the optimal linear receiver. The network weights are given by,

$$\begin{aligned} \mathbf{W}_{mse} &= \arg\min_{w} E\left[\left\|\widehat{\mathbf{b}} - \mathbf{W}^T\mathbf{x}\right\|^2\right] \\ &= \mathbf{R}_x^{-1}\mathbf{R}_{\widehat{bx}} \end{aligned} \tag{9}$$

where $\mathbf{R}_x = E\left[\mathbf{x}\mathbf{x}^T\right]$ is the correlation matrix of the inputs, and $\mathbf{R}_{\widehat{bx}} = E\left[\mathbf{x}\widehat{\mathbf{b}}^T\right]$ is the cross-correlation matrix between the estimated bits and the input. We

will show that the application of this weights matrix leads to signal separation in the high SNR case. Neglecting the noise contribution we have:

$$\begin{aligned} \mathbf{R}_x &\simeq \mathbf{A}E\left[\mathbf{b}\mathbf{b}^T\right]\mathbf{A}^T \\ &= \mathbf{A}^2 \end{aligned} \tag{10}$$

where we used $E\left[\mathbf{b}\mathbf{b}^T\right] = \mathbf{I}$, since the signals are assumed independent between users. The cross-correlation matrix is:

$$\begin{aligned} \mathbf{R}_{\widehat{b}x} &= E\left[(\mathbf{A}\mathbf{b}+\mathbf{v})\widehat{\mathbf{b}}^T\right] \\ &= \mathbf{A}\mathbf{P} \end{aligned} \tag{11}$$

where $\mathbf{P}$ is a diagonal matrix, $\{\mathbf{P}\}_{ii} = 1 - 2\Pr\left[\widehat{b}_i \neq b_i\right] = 1 - 2P_{ei}$, and it is shown in the appendix that:

$$E\left[\widehat{b}_i b_j\right] = \begin{cases} 1-2P_{ei} & i=j \\ 0 & i \neq j \end{cases} \tag{12}$$

The weights are given by $\mathbf{W}_{mse} = \mathbf{A}^{-1}\mathbf{P}$. When the effect of the noise can be neglected, this linear transformation applied to the input vector, recovers the transmitted signals vis., $\mathbf{y} = \mathbf{W}_{mse}^T\mathbf{x} = \mathbf{P}\mathbf{b} + \mathbf{W}_{mse}^T\mathbf{v} \simeq \mathbf{P}\mathbf{b}$.

3.2 Signal Separation by Decorrelation

The decorrelator seeks to decorrelate each output y_n from all the other users bit estimate. This criterion can be expressed as:

$$\mathbf{W}_d = \arg\left\{E\left[\widehat{\mathbf{b}}\mathbf{y}^T\right] = \mathbf{\Lambda}\right\} \tag{13}$$

where $\mathbf{\Lambda}$ is a diagonal matrix. We now develop an expression for the weight matrix solution to the decorrelation criterion of eq. (13) and then show that this weight vector indeed performs signal separation. Again assuming negligible noise and using the results of the appendix, we have:

$$\begin{aligned} E\left[\widehat{\mathbf{b}}\mathbf{y}^T\right] &\simeq E\left[\widehat{\mathbf{b}}\mathbf{b}^T\mathbf{A}\mathbf{W}\right] \\ &= \mathbf{P}\mathbf{A}\mathbf{W} \end{aligned} \tag{14}$$

and from eq. (13) the decorrelation criterion is equivalent to the condition $\mathbf{P}\mathbf{A}\mathbf{W} = \mathbf{\Lambda}$. It results that the decorrelation weight matrix solution is given by:

$$\mathbf{W}_d = \mathbf{A}^{-1}\mathbf{\Lambda}_1 \tag{15}$$

where $\mathbf{\Lambda}_1 = \mathbf{\Lambda}\mathbf{P}$ is a diagonal matrix. Indeed when this weight matrix is applied to the noiseless input vector $\mathbf{x}$ it results in signal separation vis., $\mathbf{y} = \mathbf{W}_d^T\mathbf{x} \simeq \mathbf{W}_d^T\mathbf{A}\mathbf{b} = \mathbf{\Lambda}_1\mathbf{b}$. Note that while the amplitude of the separated signals cannot be determined by this procedure, the bit detection is not affected by this indetermination since $\mathrm{sign}\mathbf{\Lambda}_1\mathbf{b} = \mathrm{sign}\mathbf{b}$.

4 Adaptive Decorrelation

Adaptive signal separation algorithms can be directly derived from the MSE and decorrelation criteria formulated in eqs. (9) and (13), respectively. The MSE criterion can be implemented using the well known LMS adaptation. In this section we formulate, analyze and compare the decorrelation algorithm with the LMS algorithm. LMS update of the signal separation network weights is expressed by the relations:

$$\begin{aligned} \mathbf{W}(k+1) &= \mathbf{W}(k) + \mu \mathbf{x}(k) \mathbf{e}^T(k) \\ \mathbf{e}(k) &= \widehat{\mathbf{b}}(k) - \mathbf{W}^T(k) \mathbf{x}(k) \\ \widehat{\mathbf{b}}(k) &= \text{sign}\mathbf{b}(k) \end{aligned} \tag{16}$$

The convergence analysis of the LMS algorithm is well known. Under a set of assumptions often referred to as independence assumptions , a necessary and sufficient condition for convergence is that the step size parameter meets the condition $0 < \mu < 2/\lambda_{\max}(\mathbf{R}_x)$, where $\lambda_{\max}(\mathbf{R}_x)$ is the largest eigenvalue of the covariance matrix $\mathbf{R}_x$. It is also well known that the convergence speed of the LMS algorithm is determined by eigenvalue spread $\chi = \lambda_{\max}(\mathbf{R}_x)/\lambda_{\min}(\mathbf{R}_x)$.

A stochastic gradient-based decorrelation algorithm can be formulated directly from eq. (13). It seeks to null the instantaneous cross-correlation between the outputs of the signal separation networks and the detected symbols:

$$\begin{aligned} \widetilde{\mathbf{W}}(k+1) &= \widetilde{\mathbf{W}}(k) - \mu \left[\widehat{\mathbf{b}}(k) \mathbf{y}^T(k) - \text{diag}\left(\widehat{\mathbf{b}}(k) \mathbf{y}^T(k) \right) \right] \\ \text{diag}(\mathbf{W}(k+1)) &= \mathbf{I} \\ \widehat{\mathbf{b}}(k) &= \text{sign}\mathbf{b}(k) \end{aligned} \tag{17}$$

where the operator diag generates a diagonal matrix of the elements on the main diagonal of the argument, and $\widetilde{\mathbf{W}}(k) = \mathbf{W}(k) - \text{diag}(\mathbf{W}(k))$. Note that the adaptive decorrelator has a computational complexity similar to the LMS. Signal separation by decorrelation is different from the MSE separator. The MSE weight vector for any user is derived using previous symbol estimates of that user as a reference signal. In contrast, the decorrelator can be interpreted as using reference signals derived from all other users bit estimates. Suggesting an operation where processing for each user is helped by the other users, this structure has been referred to as *bootstrapped,* [10]

4.1 Analysis of the Adaptive Decorrelator

The LMS decorrelator have been observed to converge faster than the conventional LMS error algorithm [10]. We prove that the eigenvalue spread for the adaptive decorrelator is smaller than for the LMS, thereby providing the reasoning for the faster convergence speed of the former.

To simplify the notation and without loss of generality, consider the weight vector $\mathbf{w}_1$ which decorrelates the output for the first user y_1 from the other users detected symbols $\widehat{b}_2, \ldots, \widehat{b}_N$. Define the vector $\widehat{\mathbf{B}} = \left[0, \widehat{b}_2, \ldots, \widehat{b}_N\right]^T = \mathbf{U}_1 \widehat{\mathbf{b}}$, where $\mathbf{U}_1$ is a unity matrix with its first element zeroed. We can rewrite eq. (18) for $\mathbf{w}_1$:

$$\begin{aligned} \mathbf{w}_1(k+1) &= \mathbf{w}_1(k) - \mu y_1(k) \widehat{\mathbf{B}}(k) \\ &= \left[\mathbf{I} - \mu \widehat{\mathbf{B}}(k) \mathbf{x}^T(k)\right] \mathbf{w}_1(k) \end{aligned} \tag{18}$$

We assume that the independence assumptions hold as they do for the LMS algorithm. We can write:

$$\begin{aligned} \mathrm{E}\left[\mathbf{w}_1(k+1)\right] &= \left[\mathbf{I} - \mu \mathbf{R}_{\widehat{B}x}\right] \mathrm{E}\left[\mathbf{w}_1(k)\right] \\ &= \left[\mathbf{I} - \mu \mathbf{U}_1 \mathbf{A}\right] \mathrm{E}\left[\mathbf{w}_1(k)\right] \end{aligned} \tag{19}$$

where $\mathbf{R}_{\widehat{B}x} = E\left[\widehat{\mathbf{B}}(k) \mathbf{x}^T(k)\right] = \mathbf{U}_1 \mathbf{R}_{\widehat{b}x}$ and we used the relation,

$$\begin{aligned} \mathbf{U}_1 \mathbf{R}_{\widehat{b}x} &= \mathbf{U}_1 E\left[(\mathbf{A}\mathbf{b} + \mathbf{v}) \mathbf{b}^T\right] \\ &= \mathbf{U}_1 \mathbf{A} \end{aligned} \tag{20}$$

Define the following matrix and vector partitions: $\mathbf{w}_1^T = \left[\begin{array}{c|c} w_1 & \overline{\mathbf{w}}^T \end{array}\right]$, $\mathbf{I} = \left(\begin{array}{c|c} 1 & 0 \\ \hline 0 & \overline{\mathbf{I}} \end{array}\right)$, $\widehat{\mathbf{B}}^T = \left(\begin{array}{c|c} 0 & \overline{\mathbf{B}}^T \end{array}\right)$, $\mathbf{x}^T = \left(\begin{array}{c|c} x_1 & \overline{\mathbf{x}}^T \end{array}\right)$. Then the adaptive decorrelator in eq. (18) can be rewritten as follows:

$$E\left[\overline{\mathbf{w}}(k+1)\right] = \left[\overline{\mathbf{I}} - \mu \mathbf{R}_{\overline{B}\overline{x}}\right] E\left[\overline{\mathbf{w}}(k)\right] - \mu E\left[\overline{\mathbf{B}}(k) x_1(k) w_1(k)\right] \tag{21}$$

where $\mathbf{R}_{\overline{\mathbf{B}}\overline{\mathbf{x}}} = E\left[\overline{\mathbf{B}}\overline{\mathbf{x}}^T\right]$. Form this relation we deduce that the convergence properties of the adaptive decorrelator are controlled by the eigenvalues of $\mathbf{R}_{\overline{B}\overline{x}}$.

Proposition 1. *For convergence of the decorrelation algorithm the following condition has to be satisfied:*

$$0 < \mu < 2 \;/\; \lambda_{\max}\left(\mathbf{R}_{\overline{B}\overline{x}}\right) \tag{22}$$

Proof. The proof follows from the well known convergence condition of the LMS algorithm [11], and the analogy of the LMS and decorrelator algorithms.

Proposition 2. *The following relation exists between the largest eigenvalues of* $\mathbf{R}_{\overline{B}x}$ *and* $\mathbf{R}_{\widehat{b}x}$*:*

$$\lambda_{\max}\left(\mathbf{R}_{\widehat{b}x}\right) \geq \lambda_{\max}\left(\mathbf{R}_{\overline{B}\overline{x}}\right) \tag{23}$$

Proof. The matrix $\mathbf{R}_{\overline{Bx}}$ can be expressed as a partition of the matrix $\mathbf{R}_{\widehat{bx}}$:

$$\mathbf{R}_{\widehat{bx}} = \begin{pmatrix} r_1 & \vdots & \mathbf{r}_1^T \\ \cdots & \vdots & \cdots \\ \mathbf{r}_1 & \vdots & \mathbf{R}_{\overline{Bx}} \end{pmatrix} \tag{24}$$

Define the ratio

$$\rho(z) = \frac{\mathbf{z}^T \mathbf{R}_{\widehat{bx}} \mathbf{z}}{\mathbf{z}^T \mathbf{z}} \tag{25}$$

Applying the Courant-Fisher Minimax theorem [12], $\lambda_{\max}\left(\mathbf{R}_{\widehat{bx}}\right) = \max_{w} \rho(z)$. Using the matrix partition in eq. 24 and maximizing $\rho(z)$ over the restriction $z_1 = 0$, where z_1 is the first component of the vector $\mathbf{z}$, we get

$$\lambda_{\max}\left(\mathbf{R}_{\widehat{bx}}\right) \geq \max_{\substack{z \\ z_1=0}} \rho(z) = \lambda_{\max}\left(\mathbf{R}_{\overline{Bx}}\right) \tag{26}$$

Proposition 3. *The following relation exists between the smallest eigenvalues of* $\mathbf{R}_{\overline{Bx}}$ *and* $\mathbf{R}_{\widehat{bx}}$*:*

$$\lambda_{\min}\left(\mathbf{R}_{\widehat{bx}}\right) \leq \lambda_{\min}\left(\mathbf{R}_{\overline{Bx}}\right) \tag{27}$$

Proof. According to the Interlacing property which follows from the Courant-Fisher Minimax theorem [12], and noting that $\mathbf{R}_{\overline{Bx}}$ is the $(N-1) \times (N-1)$ leading principal submatrix of $\mathbf{R}_{\widehat{bx}}$, we have:

$$\lambda_{\min}\left(\mathbf{R}_{\widehat{bx}}\right) \leq \lambda_{N-1}\left(\mathbf{R}_{\overline{Bx}}\right) = \lambda_{\min}\left(\mathbf{R}_{\overline{Bx}}\right) \tag{28}$$

Proposition 4. *If the noise is negligible then the eigenvalues of* $\mathbf{R}_x$ *are equal to the square of the eigenvalues of* $\mathbf{R}_{\widehat{bx}}$*.*

Proof. We have the relation $\mathbf{R}_{\widehat{bx}} = \mathbf{PA} \simeq \mathbf{A}$, and for negligible noise we have $\mathbf{R}_x \simeq \mathbf{AEEA}^T$. Consequently, $\mathbf{R}_x \simeq \mathbf{R}_{\widehat{bx}}^T \mathbf{R}_{\widehat{bx}}$. Since $\mathbf{R}_{\widehat{bx}}$ (with the approximation $\mathbf{P} \simeq \mathbf{I}$, is symmetric, it follows that $\lambda_i(\mathbf{R}_x) = \lambda_i^2\left(\mathbf{R}_{\widehat{bx}}\right)$ for $1 \leq i \leq N$. In particular, we have for the eigenvalue spread,

$$\chi(\mathbf{R}_x) = \frac{\lambda_{\max}(\mathbf{R}_x)}{\lambda_{\min}(\mathbf{R}_x)} = \left(\frac{\lambda_{\max}\left(\mathbf{R}_{\widehat{bx}}\right)}{\lambda_{\min}\left(\mathbf{R}_{\widehat{bx}}\right)}\right)^2 = \chi^2\left(\mathbf{R}_{\widehat{bx}}\right) \tag{29}$$

Proposition 5. *The eigenvalue spread $\chi(\mathbf{R}_x)$ associated with the LMS algorithm, is larger than the spread $\chi\left(\mathbf{R}_{\overline{Bx}}\right)$ associated with the decorrelator algorithm.*

Proof. From Propositions 2,3 and 4 we have:

$$\chi(\mathbf{R}_x) = \chi^2\left(\mathbf{R}_{\widehat{bx}}\right) \geq \chi^2\left(\mathbf{R}_{\overline{Bx}}\right) \tag{30}$$

Proposition 5 provides the explanation why the decorrelator algorithm is faster than the LMS algorithm.

Proposition 6. *The following relation exists between the largest step size parameters of the decorrelator and LMS algorithms:*

$$\mu_{\max}\left(\mathbf{R}_{\overline{Bx}}\right) \geq \sqrt{2\mu_{\max}(\mathbf{R}_x)} \tag{31}$$

Proof. From Propositions 2 and 4 we have,

$$\begin{aligned} \mu_{\max}\left(\mathbf{R}_{\overline{Bx}}\right) &= 2\lambda_{\max}^{-1}\left(\mathbf{R}_{\overline{Bx}}\right) \\ &\geq 2\lambda_{\max}^{-1}\left(\mathbf{R}_{\widehat{bx}}\right) \\ &= \sqrt{2\mu_{\max}(\mathbf{R}_x)} \end{aligned} \tag{32}$$

5 Numerical Results

The LMS and the decorrelator algorithms were compared in terms of the probability of error for detecting the transmitted data. Consider the probability of bit error for the i-th user. Since the data bit can take on one of two equiprobable values the total probability of error is equal to the conditional probability $P\left(\widehat{b}_i \neq b_i \mid b_i\right)$. The probability of error at the output of the separator can be computed as a function of the weight vector $\mathbf{w}_i^T$:

$$\begin{aligned} P_{ei} &= P\left(\widehat{b}_i \neq b_i \mid b_i\right) \\ &= P\left(\mathbf{w}_i^T\mathbf{x} > 0 \mid b_i = -1\right) \\ &= E_{\substack{b\in\{1,-1\}^N \\ b_i=-1}}\left[P\left(\mathbf{w}_i^T\mathbf{x} > 0 \mid b_i = -1\right)\right] \\ &= 2^{1-N}\sum_{\substack{b\in\{-1,1\}^N \\ b_i=-1}} Q\left(\frac{t_{ii} - \sum_{j\neq i} t_{ij}b_j}{\sigma\sqrt{\mathbf{w}_i^T\mathbf{w}_i}}\right) \end{aligned} \tag{33}$$

where $Q(z) = \frac{1}{\sqrt{2\pi}}\int_z^\infty e^{-\frac{y^2}{2}}dy$, t_{nj} is the j-th element of the vector $\mathbf{t}_i = \mathbf{w}_i^T\mathbf{AE}$.

The convergence of the algorithms was studied by simulations. The simulations consisted of a $N = 4$ users system each using an $M = 15$ chip Gold code

spreading sequence. The multipath fading channel was modeled as Rayleigh random variables independent between carriers. The fading characteristics were assumed fixed through each simulation run and independent between runs. The probability of error was evaluated with respect to the first user. The SNR is defiend with respect to the first user. The signal-to-interference ratio (SIR) is defined as the power ratio of the designated user to each of the other users (assumed to have equal power). Figure 2 shows the average learning curves of the probability of error for SNR = 12 dB and SIR = -3 dB. Shown is the average of 20 runs (20 independent channels). The channel was held fixed during each run. This simulation represents the uplink channel model. Signals are received through independent channels, and the mixture matrix is asymmetric and given by $\mathbf{A} = \mathbf{C}^T\overline{\mathbf{H}}$, where $\overline{\mathbf{H}}$ is given by eq. (5). The faster convergence speed of the decorrelator is strikingly evident. To evaluate the steady state response of the algorithms, the following error probability benchmarks are shown in Figure 3: (1) decorrelation with $\left(\mathbf{C}^T\mathbf{C}\right)^{-1}$ (channel effects ignored), (2) decorrelation with $\mathbf{A}^{-1}$ (known channel), and (3) single user (no multiuser interference). The scenario was the same as in the previous figure, except that Figure 3 represents a single run generated with the same channel as the one used to compute benchmark (2). The mixture matrix $\mathbf{A}$ for this run is given by:

$$\mathbf{A} = \begin{bmatrix} .0.8605 & -0.2215 & 0.0943 & -0.0832 \\ -0.1324 & 0.8381 & -0.1215 & -0.2926 \\ 0.0472 & -0.2651 & 0.9173 & 0.1691 \\ -0.1690 & -0.0150 & 0.0035 & 0.9999 \end{bmatrix}$$

Notice that decorrelation using the inverse of the signature waveforms correlation matrix (curve #1), results in considerable performance degradation. The simulation results clearly show that the adaptive decorrelator has a higher rate of convergence than the LMS algorithm, as well as converging closer to the error for known channel (curve #2). Figure 4 shows the average of 20 runs for the case of symmetric mixture matrix. This is the downlink case with SIR = 0 dB and all users experiencing the same channel. The decorrelator has faster convergence rate than the LMS, but the difference is smaller than in the asymmetric case. This is due to the fact that negative SIR actually helps the decorrelator which is using decisions of the other users.

To estimate the convergence region of each algorithm we took the approach suggested in [13]. A figure of merit γ is defined that relates the initial and final probabilities of error, P_{ei}, and P_{ef}, as follows:

$$\gamma = 1 - \frac{P_{ef}}{P_{ein}} \tag{34}$$

when $P_{ef} \ll P_{ein}$, $\gamma \approx 1$. Note that $\gamma = 0$ corresponds to no convergence is indicated by $P_{ef} = P_{ein}$. Figure 5 shows the convergence curves when SIR = -3 dB, and the SNR is varied from -6 dB to +14 dB, to result in the initial

probabilities of error indicated on the abscissa. The figure shows that not only is the decorrelator faster, but it also has a wider region of convergence than the LMS.

6 Conclusions

In this paper we analyzed the transient response of a stochastic gradient-based decorrelation algorithm and showed that it has a faster convergence rate than due to a lesser eigenvalue spread. Furthermore, the algorithm was shown to have wider regions of convergence than the LMS. The decorrelation and the LMS algorithms are of the same complexity. The application of the adaptive decorrelator was suggested as a multiuser detector for a synchronous multiple carrier CDMA system in a fading environment.

A Evaluation of $E\left[\widehat{b}_i b_i\right]$

This appendix contains the evaluation of $E\left[\widehat{b}_i b_i\right]$. From the definition we have,

$$\begin{aligned} E\left[\widehat{b}_i b_i\right] &= \sum_{\widehat{b}_i, b_i} \widehat{b}_i b_i P\left(\widehat{b}_i b_i\right) \\ &= \sum_{\widehat{b}_i, b_i} \widehat{b}_i b_i P\left(\widehat{b}_i / b_i\right) P\left(b_i\right) \end{aligned} \tag{35}$$

The sum over $\widehat{b}_i$ can be separated into correct and erroneous decisions,

$$\begin{aligned} E\left[\widehat{b}_i b_i\right] &= 0.5\left(\sum_{\widehat{b}_i = b_i} P\left(\widehat{b}_i = b_i \mid b_i\right) + \sum_{\widehat{b}_i \neq b_i} P\left(\widehat{b}_i \neq b_i \mid b_i\right)\right) \\ &= 0.5 \times 2\left(P\left(\widehat{b}_i = b_i \mid b_i\right) + P\left(\widehat{b}_i \neq b_i \mid b_i\right)\right) \\ &= 1 - 2P_{ei} \end{aligned} \tag{36}$$

where $P(e_i)$ is the probability of error for the i-th user.

B Evaluation of $E\left[\widehat{b}_i b_j\right]$

From the definition we have,

$$E\left[\widehat{b}_i b_j\right] = \sum_{\widehat{b}_i, b_j} \widehat{b}_i b_i P\left(\widehat{b}_i b_j\right) \tag{37}$$

The joint probability of $\widehat{b}_i$ and b_j can be developed as follows:

$$\begin{aligned} P\left(\widehat{b}_i b_j\right) &= P\left(\widehat{b}_i \mid b_j\right) P\left(b_j\right) \\ &= \sum_{b_i} P\left(\widehat{b}_i \mid b_i, b_j\right) P\left(b_i\right) P\left(b_j\right) \\ &= 0.25\left(P\left(\widehat{b}_i = b_i \mid b_j\right) + P\left(\widehat{b}_i \neq b_i \mid b_j\right)\right) \\ &= 0.25\left(1 - 2P_{ei}\right) \end{aligned} \tag{38}$$

Thus we get,

$$E\left[\widehat{b}_i b_j\right] = 0.25\,(1-2P_{ei})\sum_{\widehat{b}_i,b_j}\widehat{b}_i b_i = 0 \qquad (39)$$

The results in eqs. (36) and (39) are combined and shown in eq. (12).

References

[1] M. Kavehrad, "Performance of cross-polarized QAM signals over non-dispersive fading channels," *AT&T Bell Lab. Technical Journal*, vol. 63, pp. 499–521, Mar. 1984.

[2] M. S. J.W.Carlin Y. Bar-Ness, S. Gross and W. Studdiford, "An if cross-pol canceler for microwave radio," *Journal on Selected Areas in Communications - Advances in Digital Comm. by Radio*, vol. SAC-3, pp. 502–514, Apr. 1987.

[3] C. Jutten and J. Herault, "Blind separation of sources, Part I: An adaptive algorithm based on neuromimetric architecture," *Signal Processing, Elsevier*, vol. 24, pp. 1–10, July 1991.

[4] C. Jutten and J. Herault, "Blind separation of sources, Part II: Problems statement," *Signal Processing, Elsevier*, vol. 24, pp. 11–20, July 1991.

[5] R. Lupas and S. Verdu, "Linear multiuser detectors for synchronous code-division multiple-access channels," *IEEE Trans. Information Theory*, vol. IT-35, pp. 123–136, Jan. 1989.

[6] M. K. Varanasi and B. Aazhang, "Near-optimum detection in synchronous code-division multiple-access systems," *IEEE Trans. Communications*, vol. 39, pp. 725–736, May 1991.

[7] Z. Siveski, Y. Bar-Ness, and D. W. Chen, "Error performance of synchronous multi-user code division multiple acess detector with multidimensional adaptive canceler," *European Transaction on Telecommunication and Related Technologies*, vol. 5, pp. 719–724, Nov-Dec 1994.

[8] Y. Bar-Ness, J. Linnartz, and X. Liu, "Synchronous multi-user multi-carrier CDMA communication system with decorrelating interference canceler," in *Proceedings of the 1994 IEEE Personal Indoor and Mobile Radio Communications (PIMRC)*, pp. 184–188, 1994.

[9] R. A. Horn and C. R. Johnson, *Matrix Analysis*, Cambridge University Press, Cambridge, UK, 1992.

[10] A. Dinc and Y. Bar-Ness, "Bootstrap: A fast adaptive signal separator," in *Proceedings of the 1992 International Conference on Acoustics, Speech and Signal Processing*, pp. II.325–II.328, 1992.

[11] S. Haykin, *Adaptive Filter Theory*, Prentice Hall, Englwood Cliffs, NJ, 2-nd ed., 1991.

[12] G. H. Golub and C. F. V. Loan, *Matrix Computations*, The Johns Hopkins University Press, Baltimore, MD, 2-nd ed., 1983.

[13] S. J. Nowlan and G. E. Hinton, "A soft decision-directed LMS algorithm for blind equalization," *IEEE Trans. Communications*, vol. 41, pp. 275–279, Feb. 1993.

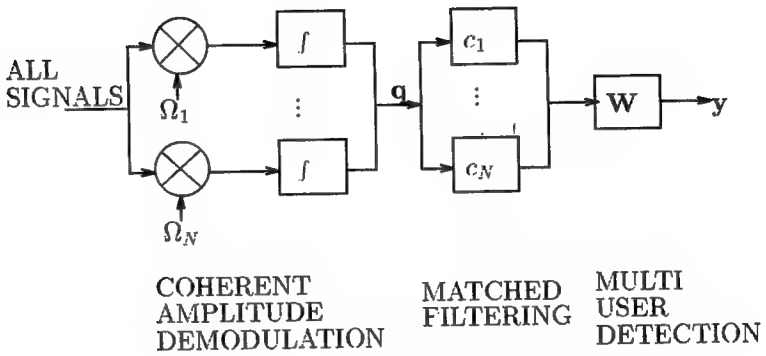

Figure 1: Multicarrier-multiuser CDMA receiver.

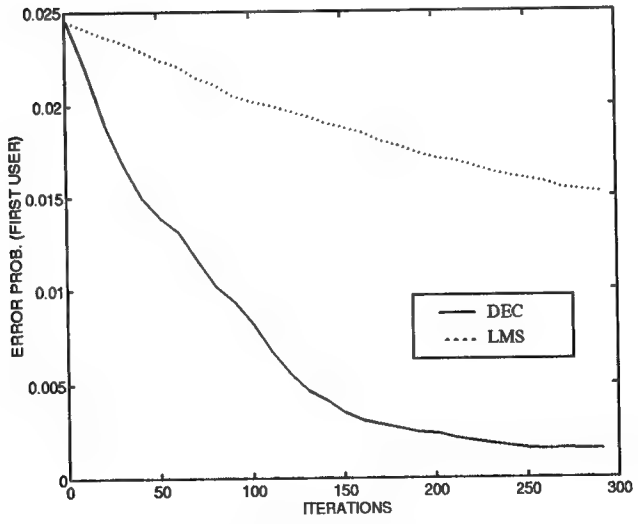

Figure 2: Learning curve of the average probability of error of the first user. Asymmetric mixture matrix. SNR = 12dB, SIR = -3dB.

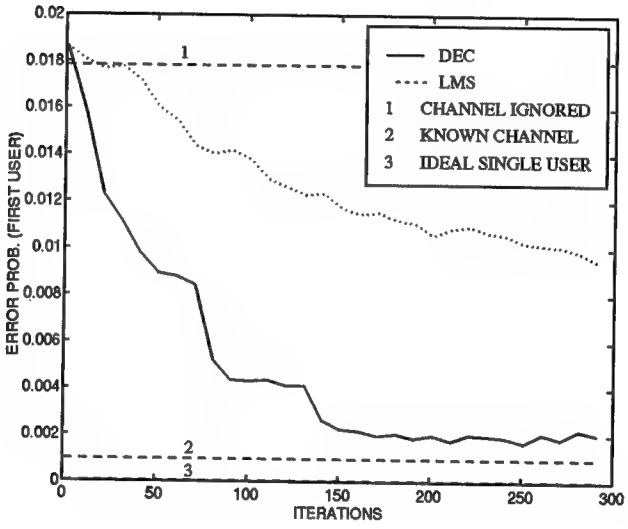

Figure 3: Learning curve of the average probability of error for a single run. Asymmetric mixture matrix. SNR = 12dB, SIR = -3dB.

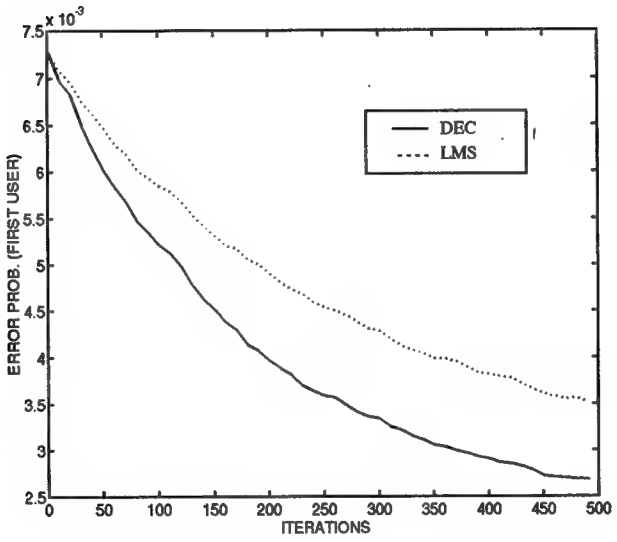

Figure 4: Learning curve of the average probability of error. Symmetric mixture matrix. SNR = 12dB, SIR = 0 dB.

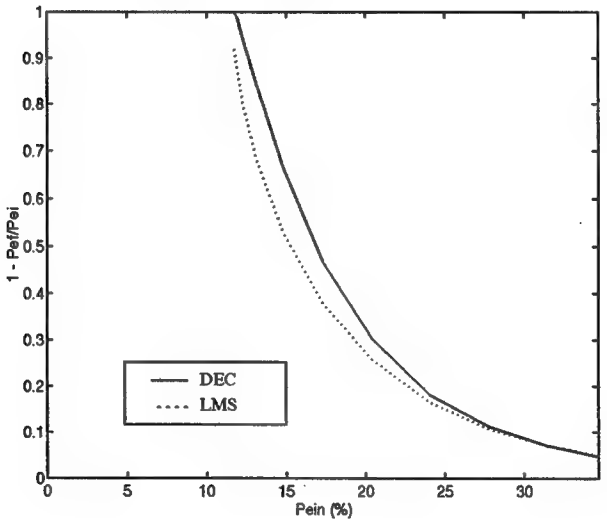

Figure 5: Convergence regions after 100 iterations for the probability of error of the first user. Asymmetric mixture matrix SNR = 12dB, SIR = -3 dB.

Appendix G

Multi-Shot Approaches to Multiuser Separation and Interference Suppression in Asynchronous CDMA †

Hongya Ge Y. Bar-Ness
hongya@shannon.njit.edu barness@hertz.njit.edu
Tel: (201) 642-4990 Fax: (201) 596-5680
Center for Communications and Signal Processing Research
Department of Electrical and Computer Engineering
New Jersey Institute of Technology
University Heights, Newark, NJ 07102

August 29, 1996

Abstract

In this work, we present a new, computationally simple scheme (termed the multi-shot approach) to separate and detect multiuser signals in asynchronous CDMA communication systems. By exploring the structure inherent in the matrix decomposition of properly arranged data, obtained from multi-shot matched filtering, we propose a near-far resistant multiuser detector. The proposed multiuser detector combines the multi-shot matched filter outputs through a matrix filtering and de-biasing processing, suggested by the inherent structure in data. Simulation results support the newly proposed detection scheme.

I Introduction

Code Division Multiple Access (CDMA) is an accepted scheme for future high capacity digital wireless/cellular communications. The need for a large number of users within a finited bandwidth dictates the implementation of a semi-orthogonal set of signature waveforms, such as Gold or Kasami codes. The cross correlation between the user's code will cause Multiuser Interference (MI). A conventional digital receiver that ignores the existence of other users will degrade quickly with the increase of interference. Further, the existence of many users will heavily interfere with the desired weak user. This is referred to as the 'near-far problem' in CDMA systems. Hence a multiuser detector is necessary for multiple access (MA) communication systems. Many near-far resistant multiuser detectors have been proposed and analyzed for synchronous CDMA systems [1, 2, 3]. For the asynchronous

†This work was supported in part by Rome Air Force Lab under contract F30602-94-C-0135, and by the Office of Sponsored Research, NJIT.

case, that is, when the received users' signals are not synchronized in time such as in uplink (from mobiles to base station) wireless communications [4, 5], the idea of a 'one-shot decorrelator' was proposed, where a bank of filters is matched to one of the users' code, while the others are matched to the left and right parts of other users' code. This merely increases the dimension of the matched filtering output vector and the cross-correlation matrix. Except for the large dimension, the near-far resistant multiuser detector for an asynchronous channel is similar to the synchronous case. It was recently demonstrated, however, that for some relative delays between the user codes, the correlation matrix becomes singular, so that the above-mentioned linear transformation-based method failed.

Instead, in this work, we present a new multi-shot approach to separate and detect multiuser signals in asynchronous CDMA communication systems. The proposed method first explores the structure inherent in the matrix decomposition of the properly arranged data, obtained from multi-shot matched filtering. Then we make a matrix approximation to make the tentative multiuser information bit estimation trackable and simple. After analyzing the bias intorduced by matrix approximation, we further proposed a matrix filtering and debiasing scheme to improve the overall detection performance. Simulation results support the newly proposed detection scheme.

II Problem Formulation

In CDMA communication systems, the data $r(t)$ at the receiver is actually a mixture of K multiuser signals, that is,

$$r(t) = \sum_{k=1}^{K} \sqrt{a_k} \sum_{i} b_k(i)\, s_k(t - iT - \tau_k) + w(t)\,, \tag{1}$$

where K is the total number of users. $\sqrt{a_k}$, τ_k, $s_k(t)$, and $b_k(i)$ are the amplitude, transmission delay, signature waveform (of duration T), and information bit (at the ith symbol interval) of the kth user, respectively. $w(t)$ is an additive white Gaussian noise process with zero mean and a two-sided power spectral density (PSD) of σ^2.

For the synchronous transmission channel, the transmission delays associated with all the users, τ_k's, are equal and can be treated as zeros. We showed in [6] that the outputs of a bank of K matched filters, sampled at the end of the ith sybmol interval ($t = iT$) form the sufficient statistic of all the users' information bit, $\{b_k(i)\}_{k=1}^{K}$, within the ith symbol interval. Hence, the one-shot approach is an appropriate way to detect and separate multiuser information bits [1, 2, 3]. However, for an asynchronous transmission channel, situation becomes more complicated, since delays of all the users, τ_k's, are not the same in general. In the following sections, we propose a multi-shot approach and associated signal processing techniques to get a near-far resistant multiuser detector through matrix decomposition, approximation, and debisaing processing.

Without loss of generality, we make the assumption that delays of all the K users satisfy the relationship $0 \le \tau_1 \le \tau_2 \le \cdots \le \tau_K < T$. Recall that the signature waveforms of all the users, $s_k(t)$'s, are of duration T, therefore, any delay values larger than the symbol interval T can be treated into another bit. We then consider

the output of the kth matched filter, sampled at the $t = iT$ $(i = 0, 1, \ldots)$ instant,

$$\begin{aligned} x_k(i) &= \int_{iT+\tau_k}^{(i+1)T+\tau_k} r(t)\, s_k(t - iT - \tau_k)\, dt\,, \qquad (k = 1, 2, \ldots, K) \\ &= \sum_{l=1}^{K} \sqrt{a_l}\, b_l(i)\, \rho_{k\,l} + \sum_{l=k+1}^{K} \sqrt{a_l}\, b_l(i-1)\, \rho_{l\,k}^{(+)} + \sum_{l=1}^{k-1} \sqrt{a_l}\, b_l(i+1)\, \rho_{l\,k}^{(-)} + n_k(i)\,, \end{aligned} \tag{2}$$

where $\{\, n_k(i) \,\}_{k=1}^{K}$ is a sequence of *colored* Gaussian noise due to the multi-shot matched filtering; and

$$\rho_{k\,l} \triangleq \int_0^T s_k(t)\, s_l(t - \tau_l + \tau_k)\, dt\,;$$

$$\rho_{l\,k}^{(+)} \triangleq \begin{cases} \displaystyle\int_0^T s_l(t + T - \tau_l + \tau_k)\, s_k(t)\, dt\,, & l > k \\ 0\,, & l \le k \end{cases};$$

$$\rho_{l\,k}^{(-)} \triangleq \begin{cases} \displaystyle\int_0^T s_k(t)\, s_l(t - T - \tau_l + \tau_k)\, dt\,, & k > l \\ 0\,, & k \le l \end{cases}$$

After stacking the outputs of a bank of K multi-shot matched filters into a $K \times 1$ vector $\mathbf{x}(i) \triangleq \left[\, x_1(i) \quad x_2(i) \quad \cdots \quad x_K(i) \,\right]^T$, we obtain the following matrix decomposition notation for the ith bit multi-shot matched filter outputs,

$$\begin{aligned} \mathbf{x}(i) &= \mathbf{P}\,\mathbf{A}\,\mathbf{b}(i) + \mathbf{P}_U\,\mathbf{A}\,\mathbf{b}(i-1) + \mathbf{P}_L\,\mathbf{A}\,\mathbf{b}(i+1) + \mathbf{n}(i)\,, \\ &= \begin{bmatrix} \mathbf{z}(i-1) \\ \mathbf{z}(i) \\ \mathbf{z}(i+1) \end{bmatrix} + \mathbf{n}(i)\,, \end{aligned} \tag{3}$$

where $\mathbf{z}(i) \triangleq \mathbf{A}\,\mathbf{b}(i)$; $\mathbf{n}(i) \sim \mathcal{N}(\mathbf{0},\, \sigma^2\,\mathbf{P})$ is a colored Gaussian noise vector; $\mathbf{P}$ is a symmetric and positive definite matrix defined by $\mathbf{P}(k,\, l) = \rho_{k\,l}$; $\mathbf{P}_U$ is an upper triangle matrix defined by $\mathbf{P}_U(k,\, l) = \rho_{l\,k}^{(+)}$; and $\mathbf{P}_L$ is a lower triangle matrix defined by $\mathbf{P}_L(k,\, l) = \rho_{l\,k}^{(-)}$. We can even show that $\mathbf{P}_U = \mathbf{P}_L^T$.

Since the matrix $\mathbf{A}$ in (3), defined as $\mathbf{A} = \mathrm{diag}\left\{\, \sqrt{a_1},\, \sqrt{a_2},\, \cdots,\, \sqrt{a_K} \,\right\}$, is a positive definite diagonal matrix, as long as the sequence of vector $\{\mathbf{z}(i)\}$ can be estimated properly, the multiuser information bit sequence $\{\mathbf{b}(i)\}$ can then be obtained from the following decision rule,

$$\mathbf{b}(i) = \mathrm{sign}\,\{\mathbf{z}(i)\}\,,$$

where we assumed the multiuser information sequence $\{\mathbf{b}(i)\}$ is generated by BPSK source.

Note from (3) that for the special case of synchronous channel, where the delays of all K users are equal, the matrices $\mathbf{P}_U$ and $\mathbf{P}_L$ vanish. Hence, for the case of synchronous channel, only the multiuser interferences appear in the signal term of data $\mathbf{x}(i)$. But for the more gerenal case of asynchronous channel, besides the multiuser interferences, intersymbol interferences (ISI) also exist due to the additional terms in (3). Our problem is to design a near-far resistant multiuser detector of reduced computational complexity (linear in the number of users K) so that we can detect and separate multiuser information bit sequence $\{\mathbf{b}(i)\}$ from the data sequence $\{\mathbf{x}(i)\}$.

In the next section, we further analyze the structure inherent in the properly arranged multi-shot matched filtering data, the statistics of the noise component, and the bias introduced by matrix approximation. We then propose a computationally simple approach to design a near-far resistant multiuser detector for asychronous CDMA system.

III Proposed Multiuser Separation Approaches

Based on the multi-shot matched filtering output data model in (3), we further arrange the available N-bit data sequence $\{\mathbf{x}(i)\}_i^{i+N-1}$ into a $NK \times 1$ vector as follows,

$$\underbrace{\begin{bmatrix} \mathbf{x}(i) \\ \mathbf{x}(i+1) \\ \mathbf{x}(i+2) \\ \vdots \\ \mathbf{x}(i+N-1) \end{bmatrix}}_{\mathbf{X}(:,\,i)} = \underbrace{\begin{bmatrix} \mathbf{P}_U & \mathbf{P} & \mathbf{P}_L & \mathbf{0} & \mathbf{0} & \cdots & \mathbf{0} \\ \mathbf{0} & \mathbf{P}_U & \mathbf{P} & \mathbf{P}_L & \mathbf{0} & \cdots & \mathbf{0} \\ \mathbf{0} & \mathbf{0} & \mathbf{P}_U & \mathbf{P} & \mathbf{P}_L & \cdots & \mathbf{0} \\ \vdots & \vdots & \vdots & \ddots & \ddots & \ddots & \vdots \\ \mathbf{0} & \mathbf{0} & \mathbf{0} & \cdots & \mathbf{P}_U & \mathbf{P} & \mathbf{P}_L \end{bmatrix}}_{NK\times(N+2)K} \begin{bmatrix} \mathbf{z}(i-1) \\ \mathbf{z}(i) \\ \mathbf{z}(i+1) \\ \mathbf{z}(i+2) \\ \vdots \\ \mathbf{z}(i+N) \end{bmatrix} + \begin{bmatrix} \mathbf{n}(i) \\ \mathbf{n}(i+1) \\ \mathbf{n}(i+2) \\ \vdots \\ \mathbf{n}(i+N-1) \end{bmatrix} \tag{4}$$

$$= \underbrace{\begin{bmatrix} \mathbf{P} & \mathbf{P}_L & \mathbf{0} & \cdots & \mathbf{0} \\ \mathbf{P}_U & \mathbf{P} & \mathbf{P}_L & \cdots & \mathbf{0} \\ \mathbf{0} & \mathbf{P}_U & \mathbf{P} & \ddots & \vdots \\ \vdots & \vdots & \ddots & \ddots & \mathbf{P}_L \\ \mathbf{0} & \mathbf{0} & \cdots & \mathbf{P}_U & \mathbf{P} \end{bmatrix}}_{\mathcal{P}} \underbrace{\begin{bmatrix} \mathbf{z}(i) \\ \mathbf{z}(i+1) \\ \mathbf{z}(i+2) \\ \vdots \\ \mathbf{z}(i+N-1) \end{bmatrix}}_{\mathbf{Z}(:,\,i)} + \underbrace{\begin{bmatrix} \mathbf{P}_U\,\mathbf{z}(i-1) \\ \mathbf{0} \\ \vdots \\ \mathbf{0} \\ \mathbf{P}_L\,\mathbf{z}(i+N) \end{bmatrix}}_{\text{bias}} + \underbrace{\begin{bmatrix} \mathbf{n}(i) \\ \mathbf{n}(i+1) \\ \mathbf{n}(i+2) \\ \vdots \\ \mathbf{n}(i+N-1) \end{bmatrix}}_{\text{noise } \mathbf{N}(:,\,i)} \tag{5}$$

Note that the first term in (5) is an approximation of the first term in (4). We have proven that the matrix $\mathcal{P}$ in (5) is an $(NK \times NK)$ symmetric, positive definite, block-tridiagonal, and full-rank matrix. If we neglect the bias term in (5), the approximation, a simple truncation, makes estimation easy. Even further, we have shown that the noise vector in (5) is *colored* Gaussian with a probability density function (PDF) of $\mathcal{N}(\mathbf{0}, \mathcal{R})$, and $\mathcal{R} = \sigma^2\,\mathcal{P}$. Hence, the *Unconstrained* Maximum Likelihood Estimate (MLE) of N-bit multiuser information $\mathbf{Z}(:,\,i)$ and $\mathbf{B}(:,\,i)$ are obtained from,

$$\begin{aligned} &\hat{\mathbf{Z}}(:,\,i) = \left(\mathcal{P}^T\,\mathbf{R}^{-1}\,\mathcal{P}\right)^{-1}\mathcal{P}^T\,\mathbf{R}^{-1}\,\mathbf{X}(:,\,i) = \mathcal{P}^{-1}\,\mathbf{X}(:,\,i)\,, \\ &\hat{\mathbf{B}}(:,\,i) = \operatorname{sign}\left\{\hat{\mathbf{Z}}(:,\,i)\right\}\,. \end{aligned} \qquad (i = 1,\,2,\,3,\,\ldots) \tag{6}$$

It should be pointed out that from (3) we can see the ISI due to the asynchronous transmission comes from the neighboring two bits. That is, each bit of multiuser information is present at most in three bits of multi-shot matched filtering data. In order to use (6) to detect and separate multiuser information bits, we need to jointly process N-bits of data $\mathbf{x}(i)$, and the minimum value of N should be equal to three. We further notice that there exists a nice structure in the properly arranged N-bit multiuser information $\left\{\hat{\mathbf{Z}}(:,\,i)\right\}_1^N$, which can be used to

further improve the overall detection performance. We can arrange the estimates in (6) into a square matrix, i. e.

$$\hat{\mathbf{Z}} = \left[\begin{array}{cccc} \hat{\mathbf{Z}}(:,1) & \hat{\mathbf{Z}}(:,2) & \cdots & \hat{\mathbf{Z}}(:,N) \end{array} \right] = \left[\begin{array}{cccc} \hat{\mathbf{z}}(1) & \hat{\mathbf{z}}(2) & \cdots & \hat{\mathbf{z}}(N) \\ \hat{\mathbf{z}}(2) & \hat{\mathbf{z}}(3) & \cdots & \hat{\mathbf{z}}(N+1) \\ \vdots & \vdots & \cdots & \vdots \\ \hat{\mathbf{z}}(N) & \hat{\mathbf{z}}(N+1) & \cdots & \hat{\mathbf{z}}(2N) \end{array} \right]. \tag{7}$$

The structure of $\hat{\mathbf{Z}}$ in (7) suggests that the improved estimate of the multiuser information bit $\mathbf{b}(i)$ can be obtained via an anti-diagonal averaging processing. Or,

$$\hat{\mathbf{b}}(i) = \text{sign}\left\{ \frac{1}{N} \sum_{i=1}^{N} \hat{\mathbf{Z}}\left((N-i)K + 1 : (N-i+1)K,\, i \right) \right\}. \tag{8}$$

The simulation results in figure 1 of next section show the improvement in the detection performance (in terms of error probability) obtained via anti-diagonal averaging.

Note that the above results in (6), (7), and (8) are obtained by neglecting the bias term (caused by truncation approximation) in (5). Certainly, the effect of this truncation will be small when we jointly process a large number of multiple bits of multi-shot data (using a large value of N). Our simulation results in figure 2 indeed show the performance improvement by incresing N. But incresing the data dimension N will unavoidably increase the computations involved. From figure 2 we also observe that there exits a limit, which is near-far resistant, on the performance even though we can keep increasing the value of N. And this limit is due to the existence of noise term in (5). Our observation is that with the help of the inherent structure in matrix $\mathcal{P}$, we can handle the bias term properly, and *still* achieve the near-far resistant performance limit *without increasing* the value of N and computations involved. Specifically, matrix $\mathcal{P}$ in (5) has a block-tridiagonal structure. Since $\mathbf{P}$ is a symmetric positive definite matrix, $\mathbf{P}_L$ is a lower triangle matrix, and $\mathbf{P}_U$ is an upper triangle matrix with $\mathbf{P}_U = \mathbf{P}_L^T$. We can show that the above matrix $\mathcal{P}$ is a symmetric positive definite matrix of full rank. Of most importance is the fact that this matrix $\mathcal{P}$ is also a *diagonal dominant* matrix. Therefore, its inverse $\mathcal{P}^{-1}$ is also a *diagonal dominant* matrix (see figure 4). We also notice the fact that the bias vector in (5) is almost a zero vector, except for the first sub-block and the last sub-block. With the inverse matrix filtering of (6), the estimate of N-bit multiuser information has the form of,

$$\hat{\mathbf{Z}}(:,i) = \mathcal{P}^{-1}\mathbf{X}(:,i) = \underbrace{\left[\begin{array}{c} \mathbf{z}(i) \\ \mathbf{z}(i+1) \\ \vdots \\ \mathbf{z}(i+N-2) \\ \mathbf{z}(i+N-1) \end{array} \right]}_{\text{true value}} + \underbrace{\mathcal{P}^{-1} \left[\begin{array}{c} \mathbf{P}_U\,\mathbf{z}(i-1) \\ \mathbf{0} \\ \vdots \\ \mathbf{0} \\ \mathbf{P}_L\,\mathbf{z}(i+N) \end{array} \right]}_{\text{bias}} + \underbrace{\mathcal{P}^{-1}\mathbf{N}(:,i)}_{\text{noise}}. \tag{9}$$

Due to the *diagonal dominant* feature of matrix $\mathcal{P}^{-1}$, the estimates of the first bit multiuser information, $\hat{\mathbf{z}}(i)$, and the last bit multiuser information, $\hat{\mathbf{z}}(i+N-1)$, will be mostly affected by the truncation bias. While the estimate of multiuser information bit in the middle sub-block of the N-bit vector $\hat{\mathbf{Z}}(:,i)$ will be least affected by the truncation bias. Therefore, we can simply use the minimum value of $N = 3$, and only estimate the middle

bit of multiuser information with reduced computation as follows. We denote the inverse of $\mathcal{P}$ as,

$$\mathcal{P}^{-1} = \begin{bmatrix} \mathbf{P} & \mathbf{P}_L & \mathbf{0} \\ \mathbf{P}_U & \mathbf{P} & \mathbf{P}_L \\ \mathbf{0} & \mathbf{P}_U & \mathbf{P} \end{bmatrix}^{-1} = \begin{bmatrix} \triangle_{11} & \triangle_{12} & \triangle_{13} \\ \triangle_{21} & \triangle_{22} & \triangle_{23} \\ \triangle_{31} & \triangle_{32} & \triangle_{33} \end{bmatrix}. \tag{10}$$

Since we need only to estimate the middle bit of multiuser information $\mathbf{z}(i+1)$ by joint processing of 3-bit multi-shot matched filtered data vector $\mathbf{x}(i)$, $\mathbf{x}(i+1)$, $\mathbf{x}(i+2)$, i. e.

$$\hat{\mathbf{z}}(i+1) = \underbrace{\begin{bmatrix} \triangle_{21} & \triangle_{22} & \triangle_{23} \end{bmatrix}}_{\mathbf{W}} \begin{bmatrix} \mathbf{x}(i) \\ \mathbf{x}(i+1) \\ \mathbf{x}(i+2) \end{bmatrix}. \tag{11}$$

In general, the $K \times NK$ matrix $\mathbf{W}$ can be calculated in advance by iteratively using the results of block matrix (of less dimension) inversion and the nice structure of matrix $\mathcal{P}$ in (5). For the case of $N = 3$, we calculated $K \times 3K$ matrix $\mathbf{W}$ as follows,

$$\mathbf{W} = -(\mathbf{P} - \mathbf{P}_L \mathbf{P}^{-1} \mathbf{P}_U - \mathbf{P}_U \mathbf{P}^{-1} \mathbf{P}_L)^{-1} \begin{bmatrix} \mathbf{P}_U \mathbf{P}^{-1} & -\mathbf{I} & \mathbf{P}_L \mathbf{P}^{-1} \end{bmatrix}. \tag{12}$$

In figure 5, we demonstrate the system structure of the signal processing parts, base on (11) and the matrix $\mathbf{W}$ in (12). It can be seen that when the transmission delay changes, instead of re-inverting the whole $(NK \times NK)$ matrix $\mathcal{P}$, we only need to update the sub-matrices $\mathbf{P}$, $\mathbf{P}_U$, $\mathbf{P}_L$ of less dimension with much less computations. Simulation results in figure 3 also show the near-far resistant performance achieved by the proposed computationally simple multiuser detector with debiasing technique of (11).

IV Simulation Results

Simulation results using the proposed multi-shot approaches are shown in the figures 1 through 3. In these figures, we compare the detection performance of the proposed detector with that of the conventional detector. We also investigate the potential improvement in performance with further anti-diagonal averaging processing; the effects of increasing the matrix dimention (value of N); and the effects of debiasing the approximation error to get a near-far resistant dectector. In our simulations, we choose normalized Gold code of length seven as the normalized signature waveforms for the case of three users,

$$s_1 = \frac{1}{\sqrt{7}} \begin{bmatrix} 1 & -1 & -1 & 1 & 1 & 1 & -1 \end{bmatrix};$$
$$s_2 = \frac{1}{\sqrt{7}} \begin{bmatrix} 1 & 1 & -1 & -1 & -1 & -1 & -1 \end{bmatrix};$$
$$s_3 = \frac{1}{\sqrt{7}} \begin{bmatrix} -1 & 1 & -1 & 1 & 1 & 1 & -1 \end{bmatrix}.$$

The transmission delays associated with all three users are chosen as,

$$\tau_1 = 0,\ \tau_2 = T_c,\ \tau_3 = 2T_c,$$

where T_c stands for the chip interval, and the symbol interval $T = 7T_c$ for our simulations.
Note that the SNR of each user is defined as the ratio of bit energy to noise density, or,

$$SNR(k) = \frac{a_k}{2\sigma^2}, \qquad (k = 1, 2, 3)$$

where we assumed the symbol interval T is normalized.
In each example, 100,000 independent trials are run for obtaining the error probability of the desired user. Shown in figure 1 through figure 3 are the error probability of the desired user (with fixed SNR) versus the SNRs of each interferencing user, with various multiuser processor. Also shown in these figures are the detection performance of the conventional single user detector for comparision. The near-far resistant feature of the proposed multiuser with reduced computation detector can be easily seen from figure 3.

V Conclusions

In this paper, we proposed a computationally simpe multiuser detection and separation scheme for asynchronous CDMA communication applications. The proposed detector achieves the near-far resistant performance with a very simple debiasing signal processing technique. The possible simplification in system implementation is also demonstrated by incorporating the block-tridiagonal structure of the matrix $\mathcal{P}$ into our debiasing technique.

Acknowledgment

The first author would like to thank Profs. Donald W. Tufts and Ramdas Kumaresan for their helpful discussions on this work.

References

[1] R. Lupas and S. Verdú, "Linear Multiuser Detector for synchronous code division multiple access channels," *IEEE Trans. on Information Theory*, vol. IT-35, no. 1, pp. 123-136, Jan. 1989.

[2] M. K. Varanasi and B. Aazhang, "Near-Optimum Detection in Synchronous Code-Division Multiple-Access Systems," *IEEE Trans. on Commun.*, vol. 39, no. 5, pp. 725–736, May. 1991.

[3] Z. Siveski, Y. Bar-Ness, and D. W. Chen, "Error Performance of Synchronous Multiuser Code Division Multiple Access Detector with Multidimensional Adaptive Canceler," *European Trans on Telecommun. and related Technologies*, vol. 5, no. 6, pp719–724, Nov.-Dec., 1994.

[4] S. Verdu, "Minimum Probability of Error for Asynchronous Gaussian Multiple-Access Channel," *IEEE Trans. on Inform. Theory*, vol. IT-32, no. 1, pp. 85–96, Jan. 1986.

[5] Z. Siveski, L. Zhong, and Y. Bar-Ness, "Adaptive Multiuser Detector for Asynchronous AWGN channels," *PRIME-94*, The Hague, The Netherlands, pp. 416–419, Sep. 21-23, 1994.

[6] H. Ge, and Y. Bar-Ness, "Bayesian Approach of Multiuser Separation and Interference Suppression in CDMA Communication Systems," *Proceedings of the 29th Asilomar Conference on Signals, Systems, and Computers*, Oct., 1995.

[7] J. Proakis, *Digital Communications*, third edition, McGraw-Hill, Inc., NY, 1995.

[8] Z. Xie, C. K. Rushforth, and R. T. Short, "Multiuser Signal Detection using Sequential Decoding," *IEEE Trans. Communications*, vol. COM-38, pp. 578–583, May, 1990.

[9] Z. Xie, C. K. Rushforth, and R. T. Short, "A Family of Suboptimum Detectors for Coherent Multiuser Communications," *IEEE J. Selected Areas Commun.*, vol. SAC-8, pp. 683–690, May, 1990.

[10] S. Verdu, "Recent Progress in Multiuser Detection," *Advances in Communications and Signal Processing*, Spring-Verlag, Berlin, 1989.

[11] H. Poor, and S. Verdu, "Single-User Detectors for Multiuser Channels," *IEEE Trans. on Communications*, vol. 36, pp. 50-60, Jan., 1988.

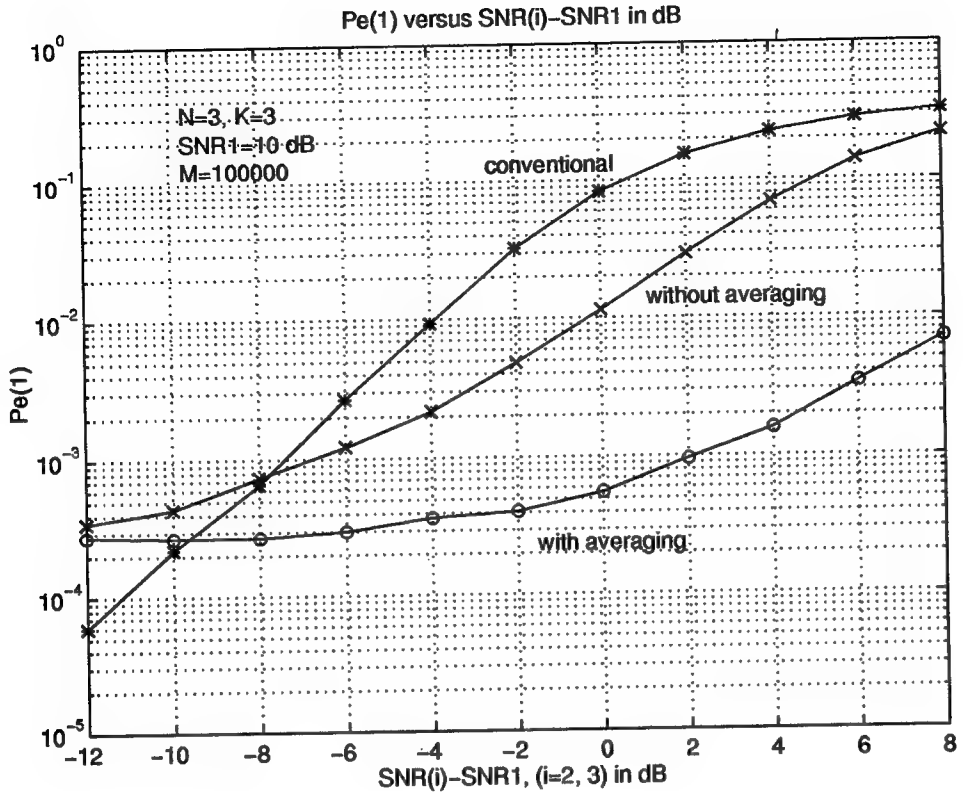

Figure 1: Performance comparison of various detectors in asynchronous multiuser CDMA communication systems. The performance improvement obtained by anti-diagonal averaging processing is also shown in this figure.

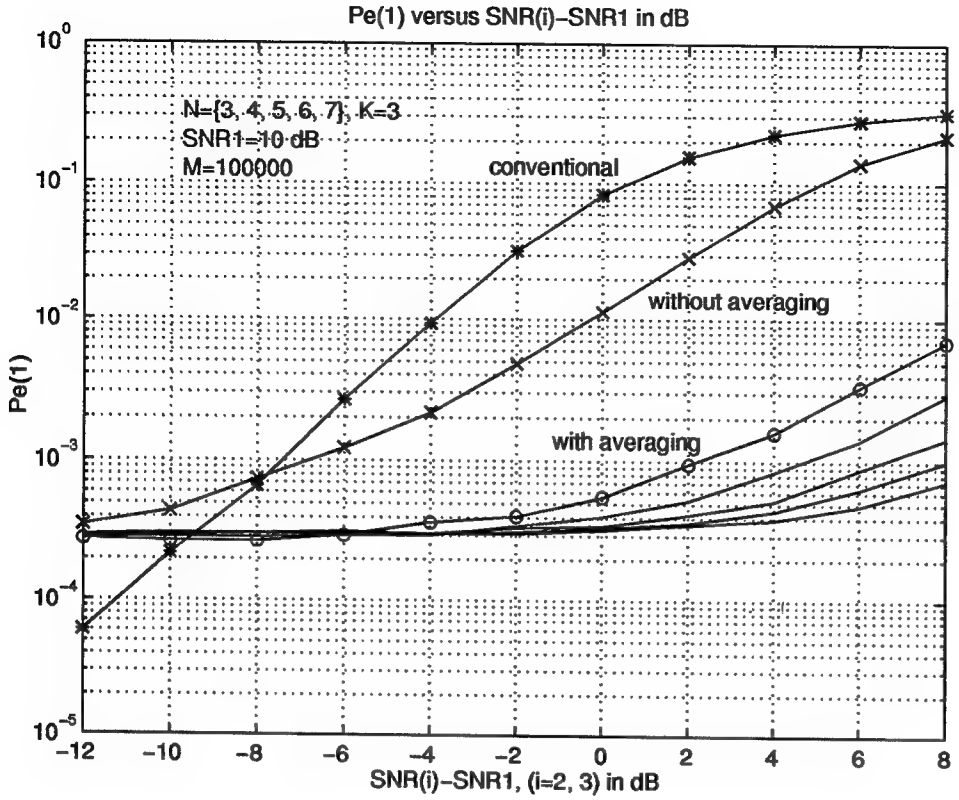

Figure 2: Performance comparison of various detectors in asynchronous multiuser CDMA communication systems. The performance improvement obtained by increasing the data dimension N is shown in this figure.

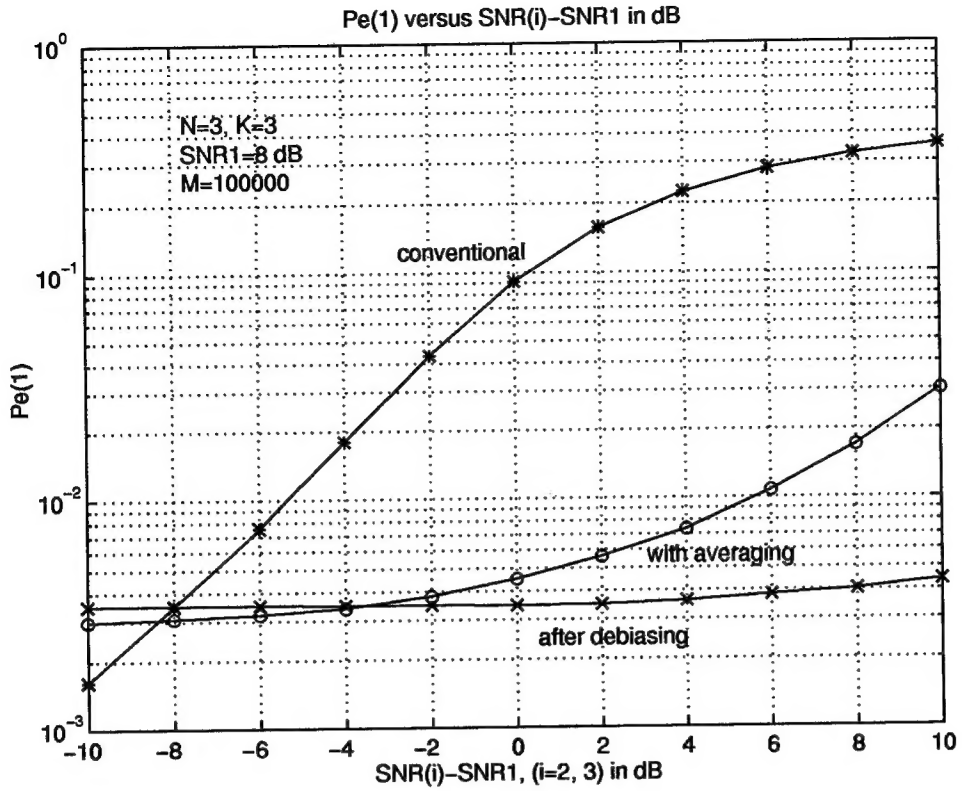

Figure 3: Performance comparison of various detectors in asynchronous multi-user CDMA communication systems. The performance improvement obtained by debiasing processing is shown in this figure.

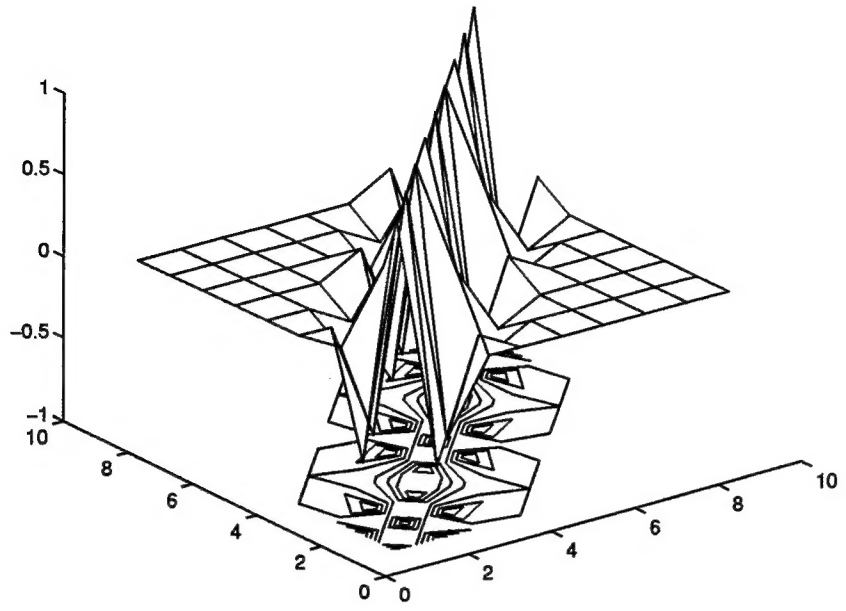

(a). structure of matrix $\mathcal{P}$.

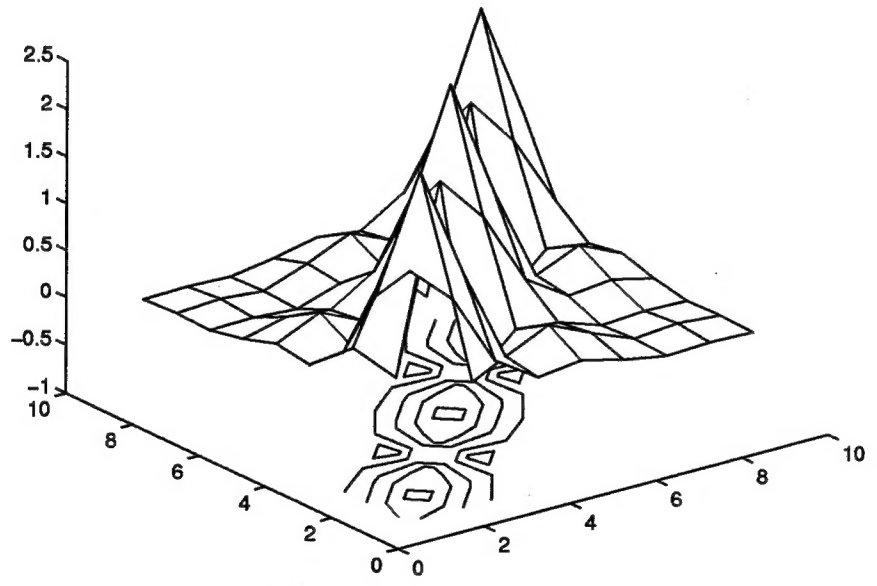

(b). structure of matrix $\mathcal{P}^{-1}$

Figure 4: Structure of matrix $\mathcal{P}$ and matrix $\mathcal{P}^{-1}$ shown by mesh and contour plots. Parameters used are the same as that used in figure 1. Note that the diagonal-dominant feature appears in both $\mathcal{P}$ and $\mathcal{P}^{-1}$.

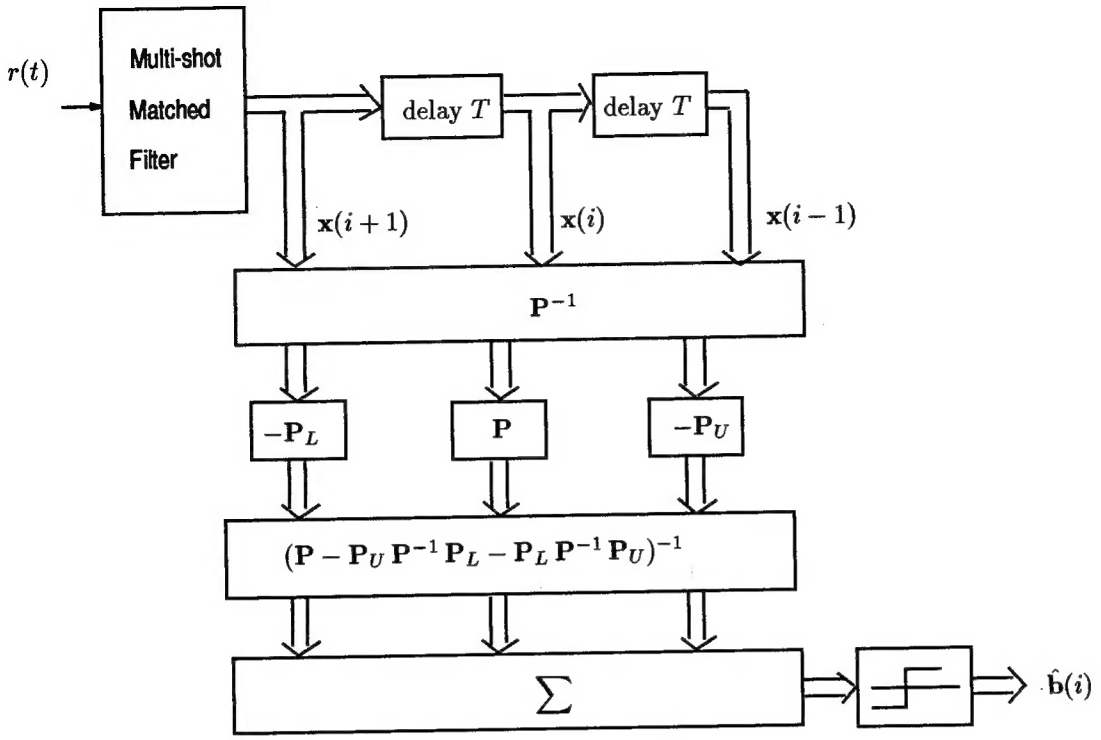

Figure 5: System implementation of the signal processing part of the proposed multiuser detection and separation scheme.

☆U.S. GOVERNMENT PRINTING OFFICE: 1997-509-127-47098

MISSION

OF

ROME LABORATORY

Mission. The mission of Rome Laboratory is to advance the science and technologies of command, control, communications and intelligence and to transition them into systems to meet customer needs. To achieve this, Rome Lab:

a. Conducts vigorous research, development and test programs in all applicable technologies;

b. Transitions technology to current and future systems to improve operational capability, readiness, and supportability;

c. Provides a full range of technical support to Air Force Materiel Command product centers and other Air Force organizations;

d. Promotes transfer of technology to the private sector;

e. Maintains leading edge technological expertise in the areas of surveillance, communications, command and control, intelligence, reliability science, electro-magnetic technology, photonics, signal processing, and computational science.

The thrust areas of technical competence include: Surveillance, Communications, Command and Control, Intelligence, Signal Processing, Computer Science and Technology, Electromagnetic Technology, Photonics and Reliability Sciences.